1992-09-01

Development and Application of Ultrastructural in Situ Hybridization to Visualize the Spatial Organization of mRNA: a Dissertation

Gary J. Bassell
University of Massachusetts Medical School

DEVELOPMENT AND APPLICATION OF ULTRASTRUCTURAL IN SITU HYBRIDIZATION TO VISUALIZE THE SPATIAL ORGANIZATION OF mRNA

A Dissertation Presented

by

GARY J. BASSELL

Submitted to the Graduate School of Biomedical Sciences
of the University of Massachusetts Medical Center
in partial fulfillment of the requirements for the degree of

DOCTOR OF PHILOSOPHY

May 1992

Department of Cell Biology

DEVELOPMENT AND APPLICATION OF ULTRASTRUCTURAL

IN SITU HYBRIDIZATION TO VISUALIZE THE

SPATIAL ORGANIZATION OF mRNA

A Dissertation Presented

by

GARY J. BASSELL

Approved as to style and content by:

_____
Dr. Susan Gagliardi, Chairperson of Committee

_____
Dr. Gary Stein, Member

_____
Dr. Jeannie Lawrence, Member

_____
Dr. Frederick Fay, Member

_____
Dr. Sheldon Penman, Member

_____
Dr. Robert Singer, Advisor

_____
Dr. Thomas Miller, Dean

ACKNOWLEDGEMENT

I would like to express my sincere thanks to my mentor, Dr. Robert Singer. I was fortunate to join his laboratory at a most exciting time; the work on spatial organization of nucleic acids had just begun and there existed a unique spirit and comradery between the small group of people who became involved in this research. My scientific training was obtained in an environment rich in intellectual curiosity, discussion and debate. As a graduate student in Rob's lab for over six years, I am now quite anxious to enter the next phase of my scientific career. However, I will miss being a part of Rob's lab. For anyone that has ever worked with Rob for any length of time, you know what I am talking about. It is difficult to summarize this experience in one paragraph. Perhaps the best way to thank him for his commitment, confidence and friendship is to say; "that if I could go back in time, I would be his student all over again."

I would also like to take this opportunity to thank the many members of the laboratory whose contribution and assistance were greatly valued. To Jeanne Lawrence who initially served as my co-advisor, and has always been there to offer valuable suggestions and discussion. To Christine Powers for training me in electron microscopy and providing consummate technical assistance. To Krishan Taneja for many helpful discussions, and whose expertise with oligonucleotide probes was appreciated. To the research fellows in the lab for their discussions, expertise and valuable advice on how I might "finish" my thesis: Cyndi Sundell, Rifaat Bashir, Ed Kislauskis, Tony Ross.

I would also like to thank: Sherwin Pockwinse for electron microscopy assistance and trouble shooting; Chris Dunshee for excellent photographic work; Cindy Beaudry for secretarial

assistance; and Lars Beatty for computer graphics assistance. I'd also like to thank John McNeil for his friendship and for fixing things after I broke them.

I would like to thank the members of my research advisory committee for their suggestions and discussion: Susan Gagliardi, Jeanne Lawrence, Edward Fey, Janet Stein and Gary Stein. With special thanks to Susan Gagliardi for her involvement, support and encouragement.

DEDICATION

TO MY WIFE HELEN

Thank you for your love, faith and humor

ABSTRACT

It has been well documented that mRNA is associated with the cytoskeleton, and that this relationship is involved in translation and mRNA sorting. The molecular components involved in the attachment of mRNA to the cytoskeleton are only poorly understood. The objective of this thesis was to directly visualize the interaction of mRNA with the cytoskeleton, with sufficient resolution to identify the filament systems and structures involved. This work required the development of novel in situ hybridization methods for use with electron microscopy. This allowed resolution to visualize single mRNA molecules and individual filaments.

The development of a silver enhancement methodology for both the light and electron microscopic detection of biotinated oligo-dT probes permitted a synoptic view of the intracellular distribution of poly(A) mRNA. At the light microscope, the distribution of poly(A) mRNA did not resemble the individual distribution patterns of microfilaments, intermediate filaments or microtubules. Ultrastructural examination revealed that poly(A) mRNA was not uniformly distributed along cytoskeletal filaments, but clustered at their intersections. The composition of these mRNA containing structures was investigated by both morphologic and in situ hybridization analysis using antibodies to cytoskeletal proteins. In thin sections, polysomes were observed attached to both microfilaments and intermediate filaments. To permit the simultaneous detection of oligo-dT hybridization and specific cytoskeletal proteins, a double labelling method using colloidal gold conjugated antibodies was developed. The majority of poly(A) mRNA was associated with the actin cytoskeleton, with 72% of the hybridization localized within 5nm of a labelled microfilament. Within the actin cytoskeleton, poly(A) mRNA was localized to intersections of orthogonal networks. Greater than

50% of poly(A) colocalized with the actin crosslinking proteins, filamin and α-actinin, but not vinculin.

A significant amount of poly(A) mRNA was found to be associated with intermediate filaments. The double label gold analysis demonstrated that 33% of the hybridization signal localized within 5nm of labelled vimentin filaments. Prior disorganization of the actin cytoskeleton using cytochalasin did not disrupt the association of mRNA with vimentin. These observations are consistent with our morphologic results of polysome-intermediate filament associations, and indicate that microfilaments are not the only filament system to which mRNA is bound. Furthermore, a small amount of hybridization signal (12%) consistently was observed along microtubules, providing an additional cytoskeletal network to distribute mRNA.

To further characterize the spatial organization of mRNA within the cytoskeleton, ultrastructural methods were developed to directly visualize individual mRNA molecules. First, oligonucleotide probes chemically modified with a single hapten and directly conjugated primary reagents were used to permit detection of an individual hybridized probe molecule by a single gold particle. Second, biotin and digoxigenin labelled oligonucleotide probes were used to simultaneously visualize the intermolecular and intramolecular relationships of two nucleic acid sequences. Third, reverse transcriptase was used to extend hybridized primers in situ which permitted visualization of the poly(A) sequence concomittant with the conformation of an mRNA molecule. These methods have permitted analysis of how single mRNA molecules may be positioned with respect to each other within the cytoskeleton.

The ultrastructural visualization of mRNA within its structural environment has demonstrated heterogeneous interactions with the cytoskeleton. Future work will be needed to further characterize the mechanism of mRNA attachment. The proteins which bridge nucleic acid sequences to specific

intersections can be identified. It will be interesting to learn how the identified mRNA-cytoskeletal interactions might be involved in the regulation of both mRNA translation and intracellular location. Lastly, and perhaps the most challenging goal, is to investigate whether the identified mRNA-cytoskeletal interactions are used by the cell to influence its own shape, polarity and architecture.

TABLE OF CONTENTS

LIST OF FIGURES

Figure

LIST OF TABLES

Table

The more one looks, the more one sees.

Teilhard de Chardin

CHAPTER I

INTRODUCTION

Many cell types are defined by their unique shape, polarity and complex organization of internal structure. A skeletal muscle fiber is characterized by the parallel and highly registered arrays of myofibrils. Most neuronal types can be described by the unique shape of two morphologically and functionally distinct processes; axons and dendrites. A major challenge of modern cell biology is to identify the organizational principles which make possible these specific characteristics of cellular assembly. Our understanding of how this macromolecular organization becomes achieved is limited.

To approach this basic biological question, considerable biochemical research has been devoted to the identification of mechanisms involved in protein sorting. Signal peptide sequences have been identified which allow the nascent chains of membrane and secretory proteins to be cotranslationally translocated into the rough endoplasmic reticulum for further modification and transport (Blobel and Sabatini, 1971; Blobel and Dobberstein, 1975). Similarly, other sequences have been identified which permit proteins to be targeted to mitochondria, lysosomes and nuclei (reviewed in Silhavy, 1989).

More recently, evidence has been provided which indicate that specific mRNAs are not simply diffuse throughout the cytoplasm, but are localized to distinct subcellular regions. For example, actin mRNA was localized to fibroblast lamellae, yet vimentin mRNA was localized to the perinuclear cytoplasm (Lawrence and Singer,1986). Microtubule associated protein-2 mRNA was localized to neuronal dendrites, whereas tubulin mRNAs localized to cell bodies (Garner et al 1988). The mechanisms involved in localizing mRNAs within the cell are unknown. The sorting of mRNAs could play an important role in establishing localized synthesis of proteins at their sites of function or assembly, and hence may directly influence cellular organization. The technology used to study the above intracellular distributions of mRNAs has been in situ hybridization followed by **light microscopy**, permitting definition of only broad cellular regions in which a specific mRNA is concentrated i.e. peripheral, perinuclear. The actual compartments within a cell to which these mRNAs are targetted are probably more specific, and the spatial location of mRNA defined by specific internal structures which are not resolved by light microscopy.

From the work of Penman, it is known that mRNA is associated with the cytoskeleton (Lenk et al, 1977). This relationship has now been studied in several laboratories using a biochemical approach to demonstrate that a variety of mRNA species are enriched in cytoskeletal fractions (reviewed in

Hesketh, 1991). The mRNA-cyoskeletal interaction might be involved in promoting the synthesis of proteins at specific intracellular locations. The possibility of a relationship between mRNA attachment to the cytoskeleton and mRNA localization within the cell has not been previously studied since this investigation requires a level of visual resolution not provided by light microscopy. An in situ hybridization technology for use with **electron microscopy** would be ideally suited for this purpose, as the high resolution provided would permit simultaneous visualization of mRNA and the **cytoskeleton. With this technology it will be possible to describe the components involved in the attachment of mRNA to the cytoskeleton.** These observations are essential for understanding mechanisms involved in the spatial organization of mRNA.

The objective of this thesis was to investigate the spatial organization of mRNA with resolution sufficient to determine how mRNA is compartmentalized within the cell. The term **compartmentalization** is defined as the high resolution organization of mRNA in contrast to low resolution distributions of specific mRNAs localized to gross topographical regions within the cytoplasm of individual cells. **This thesis is directed toward the development and application of ultrastructural in situ hybridization methods to permit identification of the cytoskeletal components involved in the spatial**

compartmentalization of mRNA. In order to derive general mechanisms for the cellular distribution of mRNA, we have focussed on the poly(A) sequence, a marker for the 3' end of most mRNAs. Therefore, this work will determine whether nonuniform intracellular positioning of mRNA is a general phenomenon and not just observable for the few specific mRNAs which have been studied in any single system. For example, when total poly-A mRNA is visualized at the light microscope it appears distributed throughout the cytoplasm and not grossly localized to any particular topological region. When the intracellular distribution of poly(A) mRNA is viewed with ultrastructural resolution, the distribution of poly-(A) mRNA may exhibit heterogeneous interactions with the cytoskeleton. **One hypothesis which will be tested is that more than one filament system is involved in the attachment of mRNP to the cytoskeleton. A second hypothesis is that mRNPs are localized to subdomains within a single filament system.**

These ultrastructural investigations are directed toward elucidating mechanisms by which the cell could sort numerous mRNAs and thereby influence wherein a cell proteins are synthesized. The direct visualization of poly(A) mRNA simultaneously with cytoskeletal components will reveal how close mRNA molecules are positioned with respect to each other and what are the specific cytoskeletal components involved. Further application of this technology will be essential to

investigate how the identified components are involved in sorting specific mRNAs. For example, are different filament systems utilized to segregate mRNAs to distinct topographical locations? In addition, these studies could also be extended to ask whether cytoskeletal subdomains are organized to provide sites for the synthesis of functionally related proteins at common locations.

High resolution description of mRNA-cytoskeletal interactions would have further significance for understanding how this association is involved in translation (reviewed in Hesketh, 1991). Several reports demonstrated that the association of mRNA with the cytoskeleton may be required for translation. Preferential synthesis of viral proteins was achieved through the displacement of host mRNAs from the cytoskeleton (Cervera et al, 1981, Bonneau et al, 1985). However, it is not known how the cytoskeleton is structurally involved in the mechanism of protein synthesis since it has not been possible to visualize the mRNA-cytoskeletal interaction. When intact cells were analyzed by high voltage electron microscopy, polysomes were visualized at junctions of microtrabeculae (Wolosewick and Porter, 1979). It is as yet undefined whether these findings represent specific sites of translation. Our investigation of the ultrastructural localization of mRNA could reveal such domains within the cytoskeleton.

The development and application of ultrastructural in situ hybridization methods to study the spatial compartmentalization of mRNA is organized into four chapters. The second chapter

contains early work on the intracellular distribution of histone mRNAs. Through these research efforts evolved the compartmentalization hypothesis and the motivation for improved ultrastructural in situ hybridization methods. The third chapter is a review of current EM in situ hybridization approaches. The rationale for continued methodology development for this thesis begins with a discussion on the need for correlative light and electron microscopy. The methodology development of silver enhanced colloidal gold labelled antibodies provides a continuum of magnification and resolution, and hence a synoptic view of the cell. This approach serves as the methodological foundation for the thesis. The fourth chapter continues the development of EM in situ hybridization technology and demonstrates that poly-A mRNA is compartmentalized within the cytoskeleton, and is localized to multiple filament systems and their subdomains. The fifth chapter involves the development of single molecule detection methods: in situ transcription and double label in situ hybridization to visualize two nucleic acid sequences simultaneously. This novel technology is utilized here to visualize the cytoskeletal attachment sites of mRNA molecules.

CHAPTER II

INTRACELLULAR DISTRIBUTION OF HISTONE mRNA

INTRODUCTION

Cell cycle regulated histone mRNAs are destabilized in the cytoplasm at the termination of S-phase (1-6). The mechanism whereby mRNA stability is coupled to DNA synthesis is unknown. It has been speculated that an accumulation of unbound histone protein in the nucleus might promote their transport into the cytoplasm, and autogenously affect the stability of histone mRNA (7-9). Histone mRNAs need to be translated (3,10) and to contain a stem loop structure at a precise location within the 3' UTR (10) in order to serve as substrates for degradation.

To investigate whether the degradation of histone mRNA within the cytoplasm was localized intracellularly, cell cycle regulated histone mRNAs were targetted to RER membranes through the expression of a chimeric signal peptide-histone gene (11). The translocation of histone mRNAs to an inappropriate subcellular region resulted in their inability to become destabilized during DNA synthesis inhibition. The subcellular location where histone mRNAs normally reside was further investigated by in situ hybridization. Since histone mRNA stability is dependent on the status of DNA replication and histone proteins are rapidly transported into the nucleus following their synthesis,

it was first hypothesized that histone mRNAs were localized near the nucleus. However, initial autoradiographic in situ studies indicated that the perinuclear region exhibited decreased amounts of histone mRNA, with the majority distributed throughout the rest of the cytoplasm (12). Moreover, the autoradiographic grain distribution exhibited a patchy appearance and suggested that histone mRNAs might be clustered at focal sites throughout the cytoplasm (12).

The objective of this study is to investigate whether histone mRNAs are clustered in the cytoplasm, and if this localization plays a role in histone mRNA stability. This work is organized into three sections based on the in situ hybridization approaches which were utilized to investigate this phenomenon: autoradiographic and nonisotopic light microscopic detection, and ultrastructural detection.

RESULTS

Autoradiography

The first goal was to investigate if the autoradiographic grain clustering observation was real or artifactual. Figure 1A illustrates hybridization of an H3/H4 probe to a primary chick muscle culture. As observed previously in WI38 cells (12), the intracellular distribution of autoradiographic grains exhibited a patchy appearance throughout the cytoplasm, with the

FIGURE 1

Intracellular Histone mRNA Distribution-Autoradiographic Detection. A). Hybridization of ^{3}H-labelled H3/H4 DNA probe to two day chick muscle culture. Strongly labelled and unlabelled single cells are present within each field. Myotubes are unlabelled. Cells were counterstained with Toluidine Blue. B). Hybridization of tubulin cDNA probe. C). Hybridization of β-actin cDNA probe. D). Histone mRNA label after 10' hydroxyurea incubation. E). 20' hydroxyurea treatment. Histone mRNA label is significantly reduced. F). 60' hydroxyurea treatment results in elimination of hybridization signal.

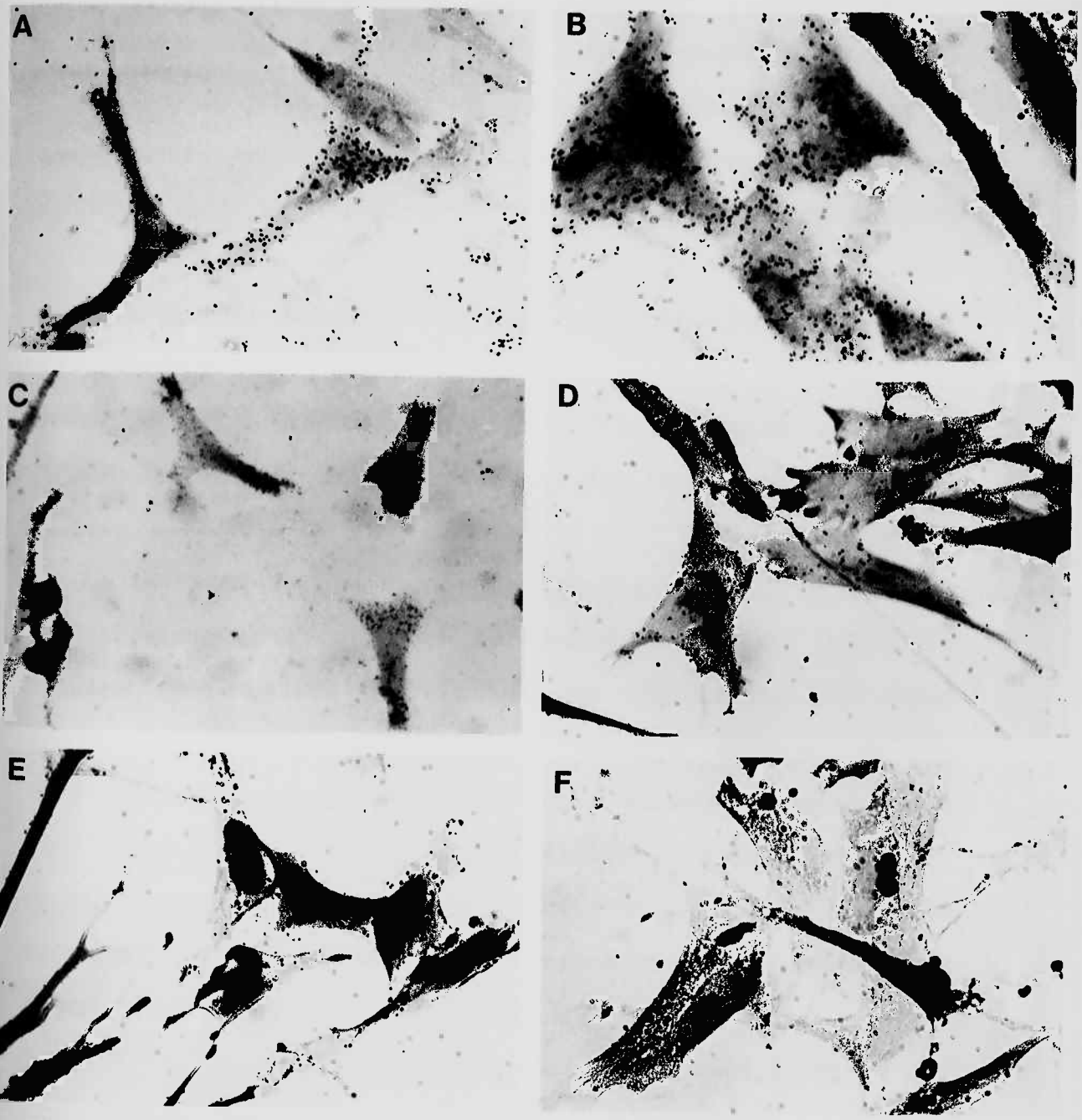
A
B
C
D
E
F

perinuclear cytoplasm having significantly less label. 53% of the mononucleated cells within the population exhibited intense hybridization with the H3/H4 probe. The remainder of single cells only exhibited background level of grains. Myotubes, which do not express cell cycle regulated histone genes, were not hybridized with the histone probe. The presence of mitotic cells outside of S-phase and differentiated cells within the population provided an effective internal control for the system.

To evaluate whether the intracellular clustering of autoradiographic grains was a phenomenon unique to histone mRNA, parallel coverslips were hybridized with actin and tubulin probes. In Figure 1C, hybridization to actin mRNA was localized to the fibroblast lamella as observed previously (13). Within this region it appeared that the distribution of grains was more uniform than histone mRNA, and did not exhibit high focal concentrations surrounded by unlabeled areas. However, it was very difficult to make observations about local variations in actin mRNA levels, owing to the large percentage of actin mRNA which is concentrated peripherally (>90%). In Figure 1B, hybridization to tubulin mRNA is distributed throughout the cytoplasm and not grossly localized to any particular morphologic region. The amount of tubulin mRNA hybridization over nuclei was considerably greater than observed with the histone or actin probes. The intracellular distribution of tubulin mRNA did exhibit a clustery appearance, with tightly linked groups of

autoradiographic grains dispersed through the cytoplasm. Therefore, grain clustering was not a unique phenomenon for histone mRNA.

It was of interest to evaluate the effects of DNA synthesis inhibition on the cellular distribution of histone mRNA. If histone mRNA degradation is localized intracellularly, it might be possible to visualize this process by inducing the rapid degradation of histone mRNA. For example, if degradation occurs by an autogeneous mechanism dependent on elevated histone levels in the cytoplasm, it is possible that histone mRNAs in the perinuclear cytoplasm would be degraded first. Degradation might occur in a perinuclear to peripheral direction. Alternatively, the intracellular distribution of histone mRNA might become spatially reorganized in order to promote the accessibility of histone mRNAs to appropriate nucleases i.e. more clustered.

Figure 2 illustrates the results of DNA synthesis inhibition on the intracellular distribution of histone mRNA. Cells were treated with hydroxyurea for 10, 20 and 60 minutes prior to fixation. The amount of histone mRNA per cell was inversely proportional to the time of DNA synthesis inhibition. There were no observable changes to the intracellular distribution of histone mRNA at the 10 and 20 minute time points (Figure 1D-E). Although the hybridization signal per cell is reduced, there was no evidence of mRNA redistribution by autoradiography. At 60 minutes in hydroxyurea, histone mRNA was no longer detectable

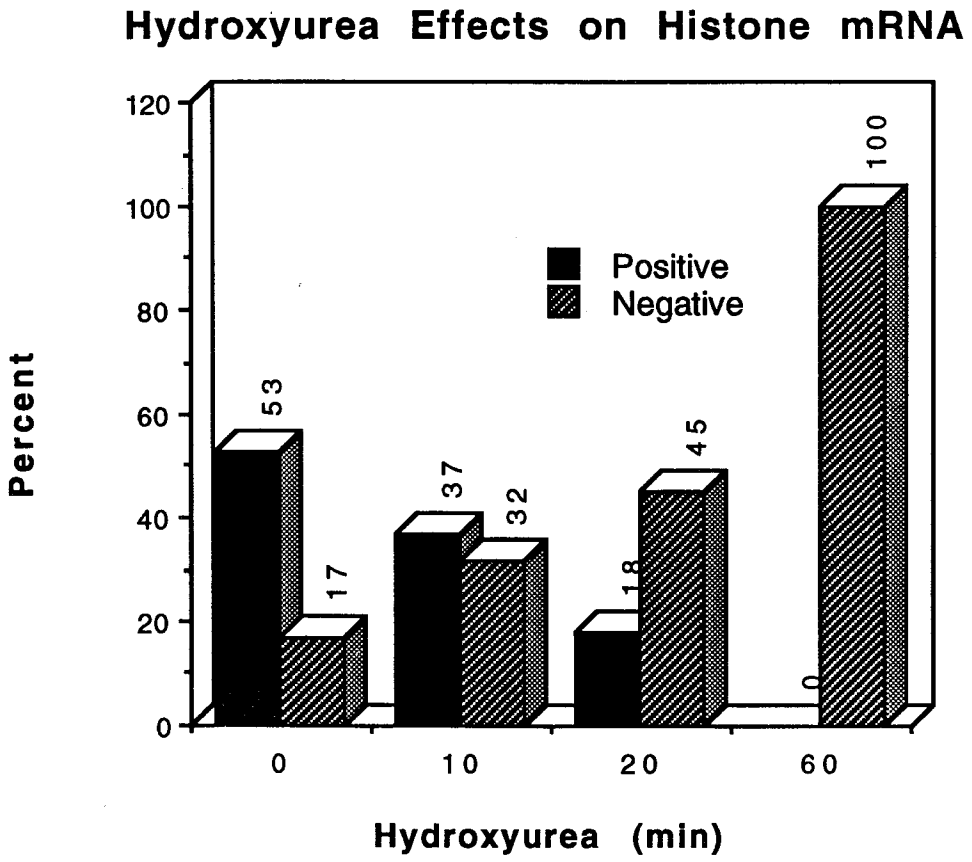

FIGURE 2. Chick fibroblast cultures were incubated with 10mM hydroxyurea at the above time points prior to fixation. Following hybridization with a ^{3}H-labelled H3/H4 DNA probe cells were processed for autoradiography. 75 cells were photographed at each time point (40X objective) and scored as follows: Positive (> ten fold grain density above noise), Intermediate (> three fold grain density above noise), or Negative (> three fold grain density above noise).

(Fig. 1F).

From this microscopic study, it can also be investigated how degradation of histone mRNA occurs at the single cell level. Following DNA synthesis inhibition, the half life of histone mRNA is approximately ten minutes and 50% of the histone mRNA is degraded after a 10 minute hydroxyurea treatment (4,5,14). Is 50% of the histone mRNA degraded in each cell, or is 100% of the mRNA degraded in only half of the cells?

With each hydroxyurea time point, 75 cells were scored for their relative amounts of hybridization. Cells having >10 times the number of grains over background levels were scored as positive (53%, 0 min). Approximately 30% of the cells exhibited intermediate levels of histone mRNA, and were clearly at least three fold above background levels. Cells indistinguishable from background grain levels were scored as negative (17%). The ratio of positive to negative cells decreased with increasing time in hydroxyurea (Fig.2). There was no evidence that histone mRNA degradation was nonhomogeneous within the population. If 100% of the histone mRNA was degraded from half of the cells, one would predict that the percent of negative cells would increase by 41% (26+30/2). By contrast, the fraction of negative cells was observed to increase by only 15%. This is likely explained by homogeneous degradation i.e. 50% per cell, with most of the cells (37%) still having >10:1 hybridization signals and scored as positive. The 15% increase in negative cells is likely

attributed to degradation in cells containing intermediate levels of histone mRNA.

Nonisotopic Detection

From the autoradiographic detection of tritiated probes, we observed that the grain clustering pattern was not specific for histone mRNAs. There are a few possible explanations: (1) The clustering phenomenon is an artifact and not representative of the intracellular mRNA distribution. (2) Clustering of mRNAs is a general process utilized by cells for specific functions i.e. mRNA degradation, oligomeric protein assembly . (3) Histone mRNAs are clustered in the cytoplasm in a manner distinct from other mRNAs, but these differences can not be detected autoradiographically. In order to investigate these possibilities, it was essential to determine whether histone mRNA clustering could be observed by another detection method. It was also important to compare the intracellular distribution of histone mRNA with other mRNAs.

At this time in the laboratory, I attempted to develop a nonisotopic detection methodology for use with light microscopy. Using current methods, only lytic viral infections could be reproducibly detected by nonisotopic methods. The commercial availability of biotin labelled nucleotides made possible the evaluation of a variety of cytochemical techniques i.e. fluorescence, colorimetric. These methods could potentially provide approximately ten fold greater resolution than

autoradiography, and would be ideally suited for intracellular localization analysis. Unfortunately, these nonisotopic methods were less sensitive than autoradiography.

Considerable time was devoted to developing a more sensitive nonisotopic method for detection of histone mRNAs. For fluorescence detection of biotinated probes, antibiotin antibodies from several sources gave hybridization independent staining of vacuolar structures suggesting binding to endogenous biotin. High background was also obtained from several sources of avidin i.e. streptavidin, avidin-DH. This could not be competed by preincubation of cells with unlabeled biotin/avidin, or by preadsorption with biotin and suggested that sites in addition to endogenous biotin were causing noise. Hybridizations on other cell lines i.e. WI38 also presented similar high background staining. The above background problems precluded the sensitive detection of probe. For colorimetric detection of biotinated probes, streptavidin incubation followed by biotinated alkaline phosphatase produced high background staining. In addition to the two step procedure (above), avidin-alkaline phosphatase conjugates can be synthesized by mixing avidin at various stoichiometric ratios with the biotinated alkaline phosphatase. Despite picogram sensitivity on a filter, these multimeric conjugates made with biotin-avidin bonds were too large and had poor penetrability characteristics in unextracted cells.

The best results came from a collaboration with Novo Laboratories who synthesized a low molecular weight covalently linked streptavidin- alkaline phosphatase conjugate. The background staining in this experiment was comparatively low, and permitted detection of histone and actin mRNA (see Figure 3). Actin mRNA was localized to the fibroblast lamella as observed previously (13). Within this region, the distribution exhibited a clustery appearance (Figure 3A-B). Hybridization to histone mRNA (mixture of H1,H3 and H4 probes) exhibited a clustered appearance throughout the cytoplasm (Fig. 3C-D). This experiment confirmed previous autoradiographic observations that histone mRNA appears clustered throughout the cytoplasm. The increased resolution of the nonisotopic method suggested that although histone mRNA and actin mRNA exhibited distinct regionalization patterns, their distributions were similarly clustered.

FIGURE 3. Intracellular Histone mRNA Distribution-Nonisotopic Detection (A,B). Hybridization of biotinated actin DNA probes followed by detection with Streptavidin alkaline phosphatase conjugate (Novo Laboratories). Label is localized to fibroblast lamella (arrowheads), and exhibits a clustery distribution within this region. (C,D). Hybridization to histone mRNA exhibited a clustery distribution throughout the cell, but was not grossly localized to any morphologic region (arrowheads). Unlabelled fibroblast within field (arrow). Bar, 25μ

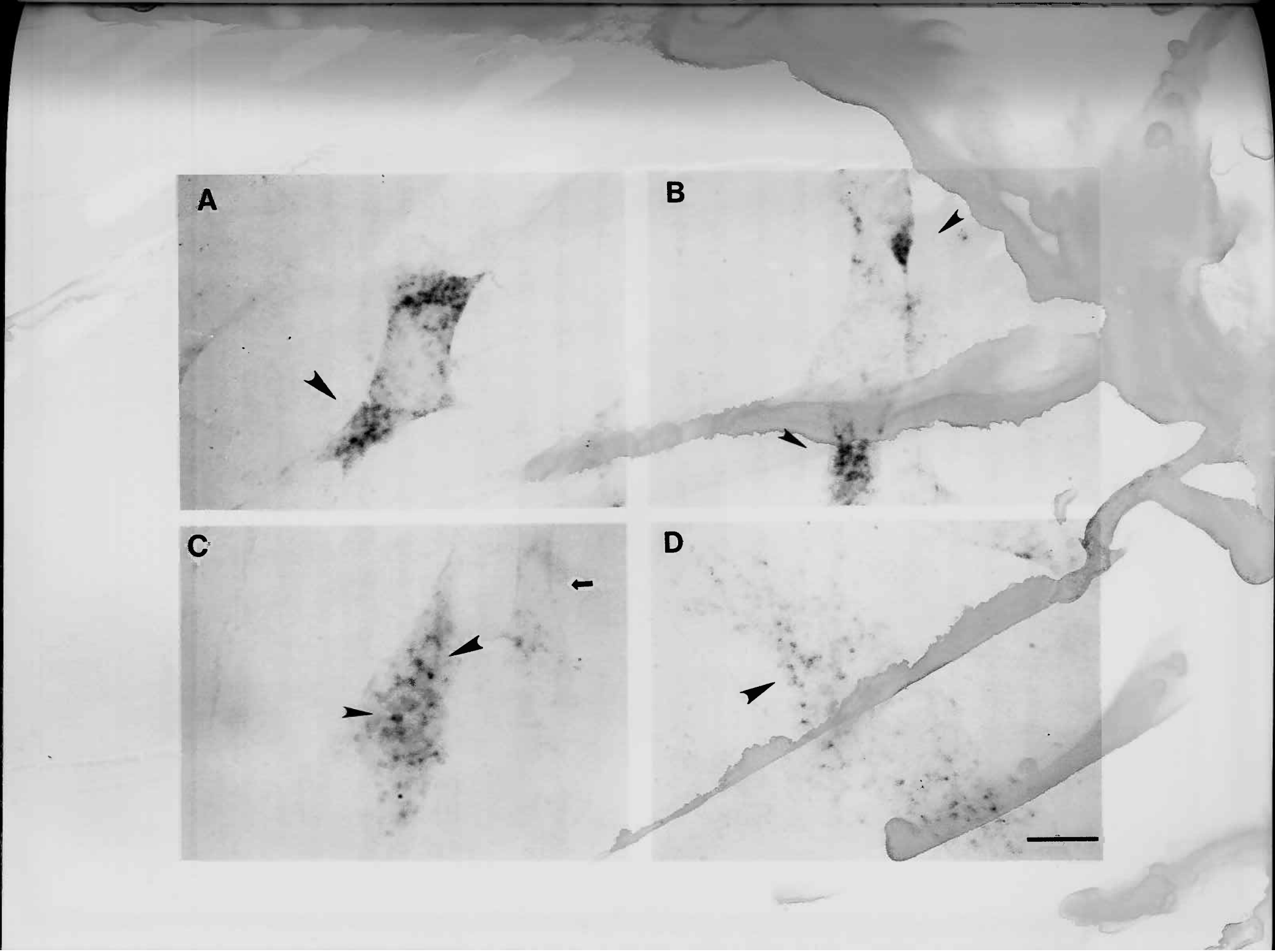
A
B
C
D

At this juncture, I decided that the additional development required in fluorescence and enzymatic detection technology might not provide the appropriate techniques to accomplish long term research objectives. The initial goal was to investigate whether histone mRNAs were clustered in the cytoplasm by a non-autoradiographic detection methodology. With development of a reproducible nonisotopic method, the resolution of the light microscope could be utilized to confirm the clustering pattern. However, it is impossible to understand these spatial relationships at a molecular level by light microscopy.

Light microscopy has been useful in the identification of gross patterns of mRNA localization i.e. peripheral. The intracellular clustering pattern of histone mRNA is quite distinct from these reports which demonstrate mRNA localization to distinct topographical regions i.e. lamella, dendrite. The undefined cellular locations which contain histone mRNA are considerably smaller and cannot be characterized with respect to the above large morphologic regions. From cell fractionation analysis, histone mRNAs have been shown to be associated with the cytoskeleton (15). It is possible that the cytoskeleton is involved in conferring the observed grain clustering phenomenon. To study this possibility requires the development of in situ hybridization at the ultrastructural level. This technology would have the needed resolution to study mRNA localization at the molecular level and their interaction with the cytoskeleton.

Ultrastructural Detection

To investigate whether the cytoplasmic clustering of histone mRNA is a real distribution and distinguishable from other mRNAs, I continued the electron microscopic in situ hybridization research in the laboratory. A whole mount methodology had recently been reported in which hybridization to actin, vimentin and tubulin mRNAs were detected by antibiotin antibodies and colloidal gold conjugated secondary antibodies. This methodology allowed the first direct visualization of the association of mRNA with the cytoskeleton. Figure 4 is a schematic of what one would expect to visualize if biotin labeled actin probe molecules were hybridized along the length of a 2Kb actin mRNA molecule. The biotin groups are detected by the immunogold method, resulting in a tightly linked array of gold particles. By this approach, sequence specific hybridization could be both qualitatively and quantitatively distinguishable from background noise, since non specific sticking of probe or detection components would be independent events and not expected to produce an iterative pattern of gold particles.

In fact, this is what was observed experimentally. Clusters of gold particles were observed in curvilinear arrays with relatively constant spacing, and proportional to the size of the target mRNA. The size of these gold particle clusters (GPC) was

FIGURE 4.

THE BASIS OF SIGNAL TO NOISE ENHANCEMENT FOR THE DETECTION FOR HYBRIDS BY ELECTRON MICROSCOPY

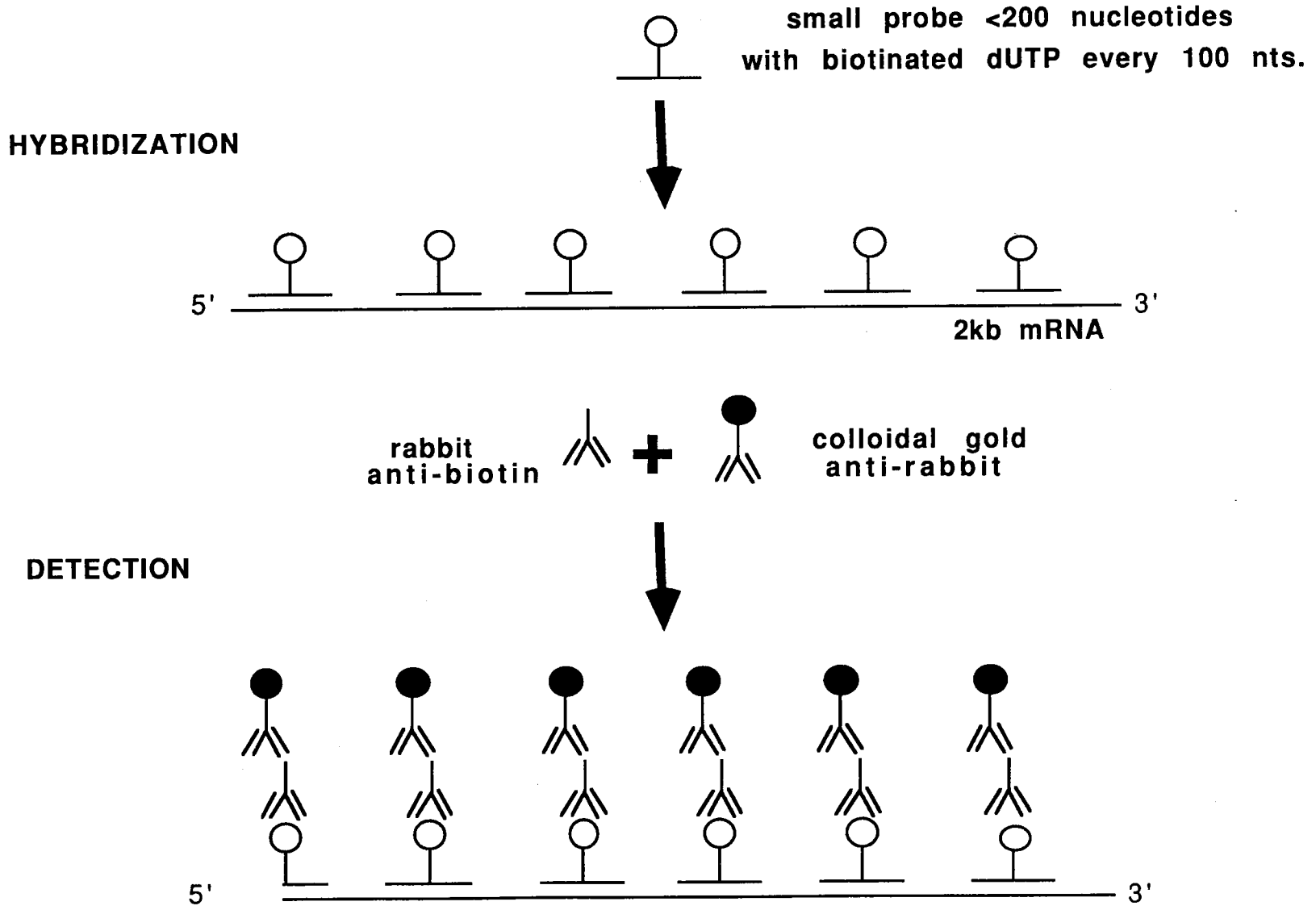

quantitated and demonstrated that the signal to noise ratio increased logarithmically, proportional to the number of gold particles within a cluster. When as many as eight particles were observed together, the signal to noise ratio was 30:1, indicating with a probability of 97% that the cluster represented hybridization to actin mRNA.

The ultrastructural localization of histone mRNA was compared to actin mRNA using the above whole mount methodology. Biotin labelled histone (H3/H4 chick clone obtained from the Stein laboratory) and β-actin (full length chick cDNA) (16) probes were hybridized on parallel samples. Probe fragment size was between 150-300 bases determined by agarose gel electrophoresis. It is important to have probe molecules of this size in order to prevent large GPC's from occuring in a hybridization independent manner. As a hybridization control, cells were digested with RNAase A prior to hybridization.

After immunogold detection, ten cells were examined for each sample at 25,000X magnification. Within each field of view, the number of gold particles in each GPC size category was quantitated i.e. 1's,2's,3's. Between 25-50 fields were evaluated per cell. The quantitative results of two hybridizations is shown in Figure 5A-C. Hybridizations to actin and histone mRNA were quantitatively distinguishable from background. In the actin samples, a signal to noise ratio of 3:1 was observed for single

FIGURE 5. Histogram showing the relationship between colloidal gold particles per unit area (375 fields) and the number of particles per cluster. A). β-actin DNA probe hybridization in untreated and RNAase A digested cells. B). Histone (H3/H4) DNA probe hybridization in undigested and RNAase A digested fibroblasts. C). Comparison of histone and actin gold particle cluster sizes.

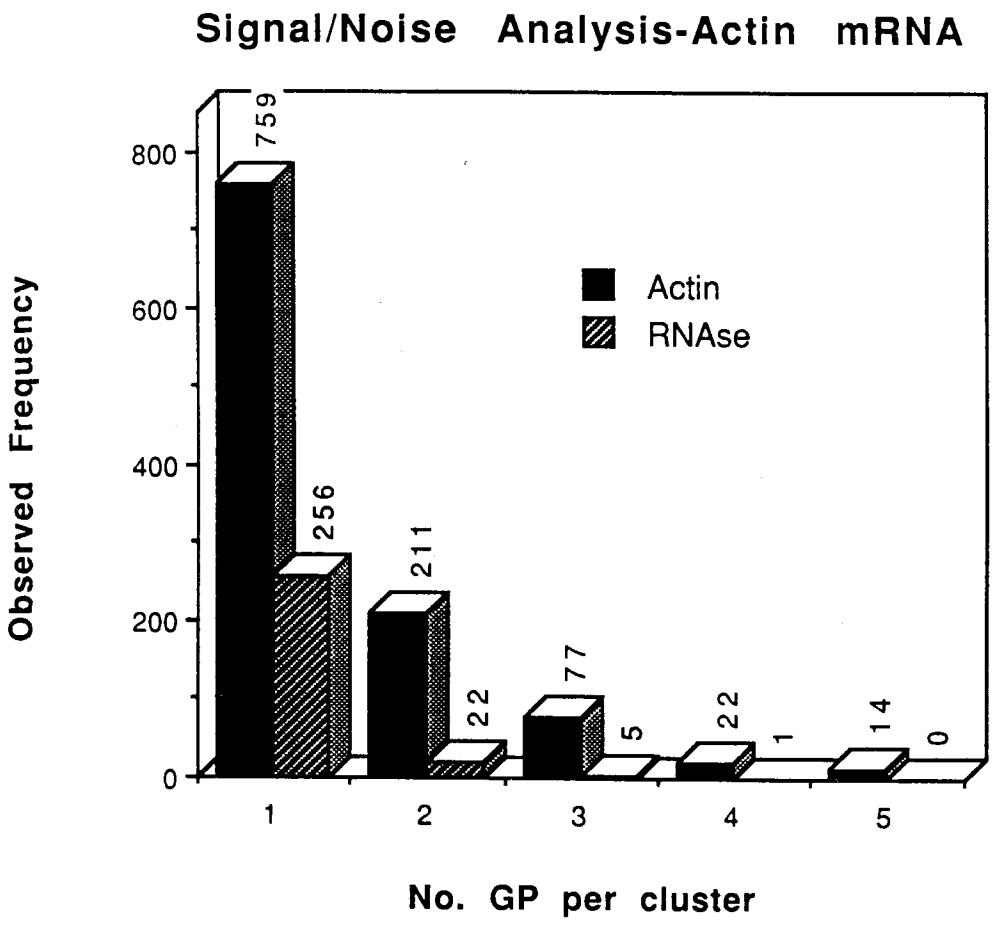
Signal/Noise Analysis-Actin mRNA
Observed Frequency
800
600
400
200
0
759
256
211
22
77
5
22
1
14
0
Actin
RNAse
1
2
3
4
5
No. GP per cluster

Signal/Noise Analysis-Histone mRNA

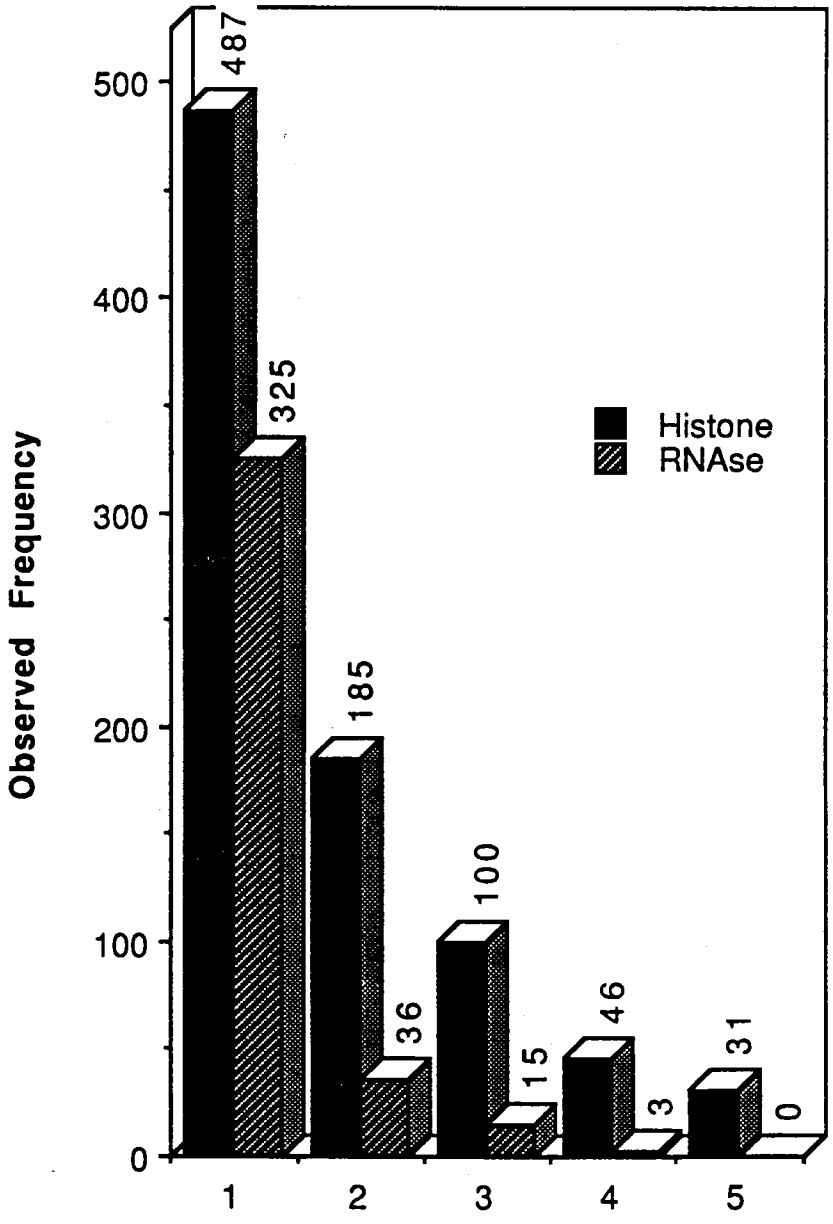

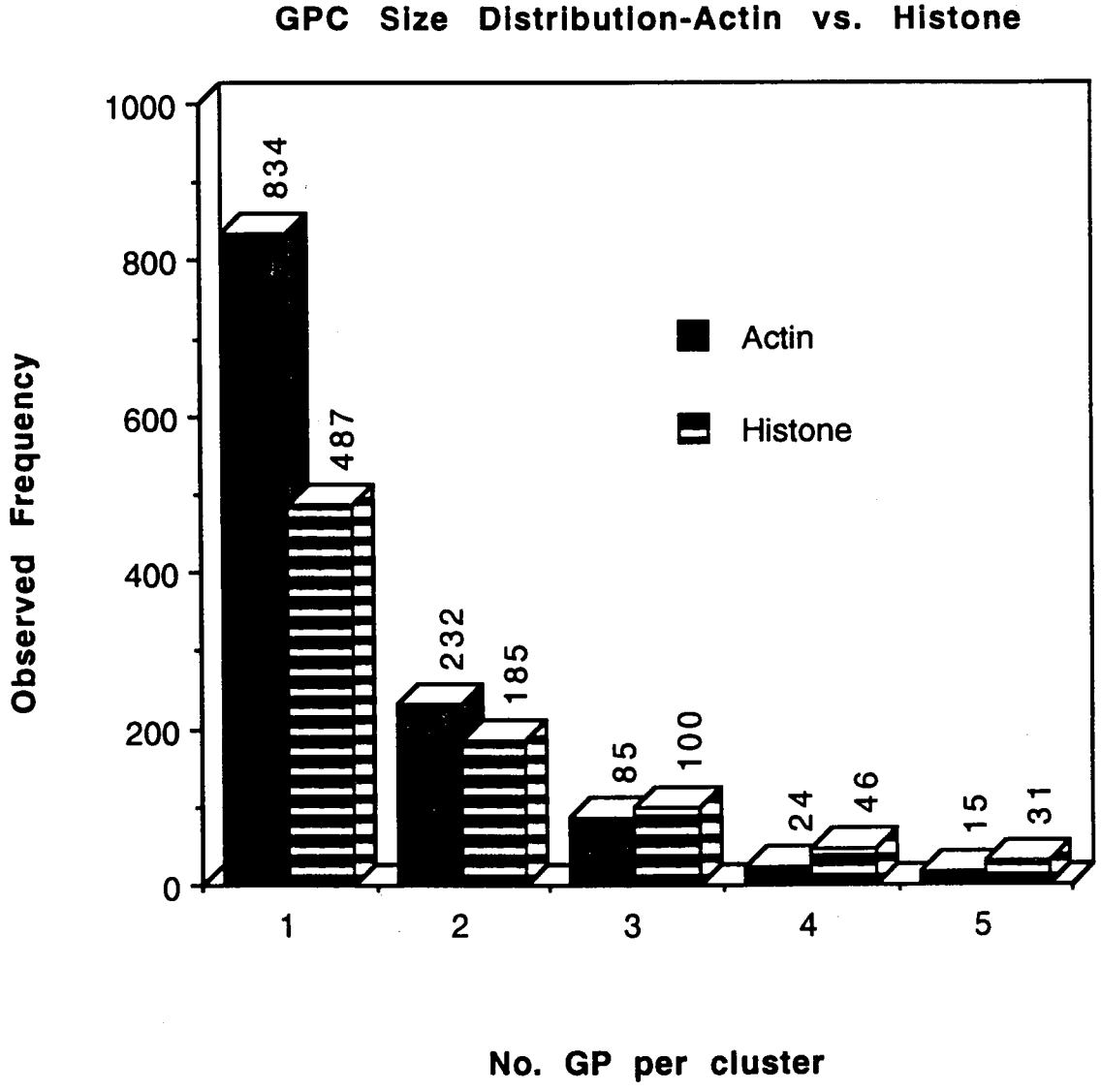
GPC Size Distribution-Actin vs. Histone
Observed Frequency
1000
800
600
400
200
0
834
487
232
185
85
100
24
46
15
31
Actin
Histone
1
2
3
4
5
No. GP per cluster

particles and increased to 22:1 for GPC's containing four particles. In the histone samples, single gold particles gave a S/N ratio of 1.5:1 and increased to 15:1 at four particles. In both samples, with GPC's larger than five particles the probability approaches 100% that the signal represented hybridization. In Figure 5C, a reciprocal relationship is observed in the comparison of GPC sizes for actin and histone mRNAs. Histone mRNAs were characterized by larger sizes of gold particle clusters than actin mRNA. The amount of total gold was higher for actin mRNA (1190 GPC) than histone mRNA (849 GPC). Consistent with this general relationship, higher frequencies for actin mRNA were observed in the single and paired gold particle categories. By contrast, as the size of the GPC increased, histone mRNAs contained larger percentages of the total signal. With GPC's containing more than four particles, histone mRNA contributes twice the signal. For histone mRNA, 9% of the signal is from GPC's with more than three particles, whereas only 3% is observed for actin mRNA.

It is unclear why histone mRNA would produce larger sized gold particle clusters than actin mRNA, since histone mRNAs are considerably smaller. The histone probe was made from a plasmid containing both an H3 and H4 gene. H4 mRNAs range from 400-500 bases, and H3 mRNAs are between 500-600 bases (17,18). The actin probe was made from a full length cDNA of 2Kb. Based on the size differences between actin and histone mRNA, one would predict that the gold particle clusters for actin

mRNA would be approximately four times as large. One possible explanation for the unexpected large histone gold particle clusters, could be that histone mRNAs are grouped together. This is an interesting possibility as it would suggest that functionally related mRNA molecules could be colocalized within nanometers on the cytoskeleton.

To further evaluate histone mRNA clustering, it was investigated if large GPC's could be observed with hybridizations using either an H3 or an H4 probe by itself. The previous experiments utilized a histone probe derived from a clone with both H3 and H4 genes. The objective of the next experiments was to compare GPC sizes of specific histone mRNA species with significantly larger mRNAs.

The results of a comparison of an H3 probe (clone pST519D, 0.5Kb mRNA) (19) to a neu oncogene probe (clone pABT7005, 4.4Kb mRNA) in a human epithelial cell line, derived from human breast tumor, are shown in Figure 6. Although the target histone mRNA species is one tenth the size of neu mRNA, histone hybridizations were characterized by larger GPC's. In this analysis the total histone signal is 1.6 times greater than neu, whereas in the previous experiment, the total actin signal was greater than histone. Therefore, it is important to consider in this analysis that the relative abundance of histone mRNA might account for higher frequencies (1-4 fold) in each GPC category. However, based on

FIGURE 6. Frequency distribution of gold particle cluster sizes (154 fields). H3 DNA probe hybridization to SKBR3 human cell line (epithelial). Neu oncogene DNA probe hybridization.

GPC Size Distribution: Histone vs. Neu

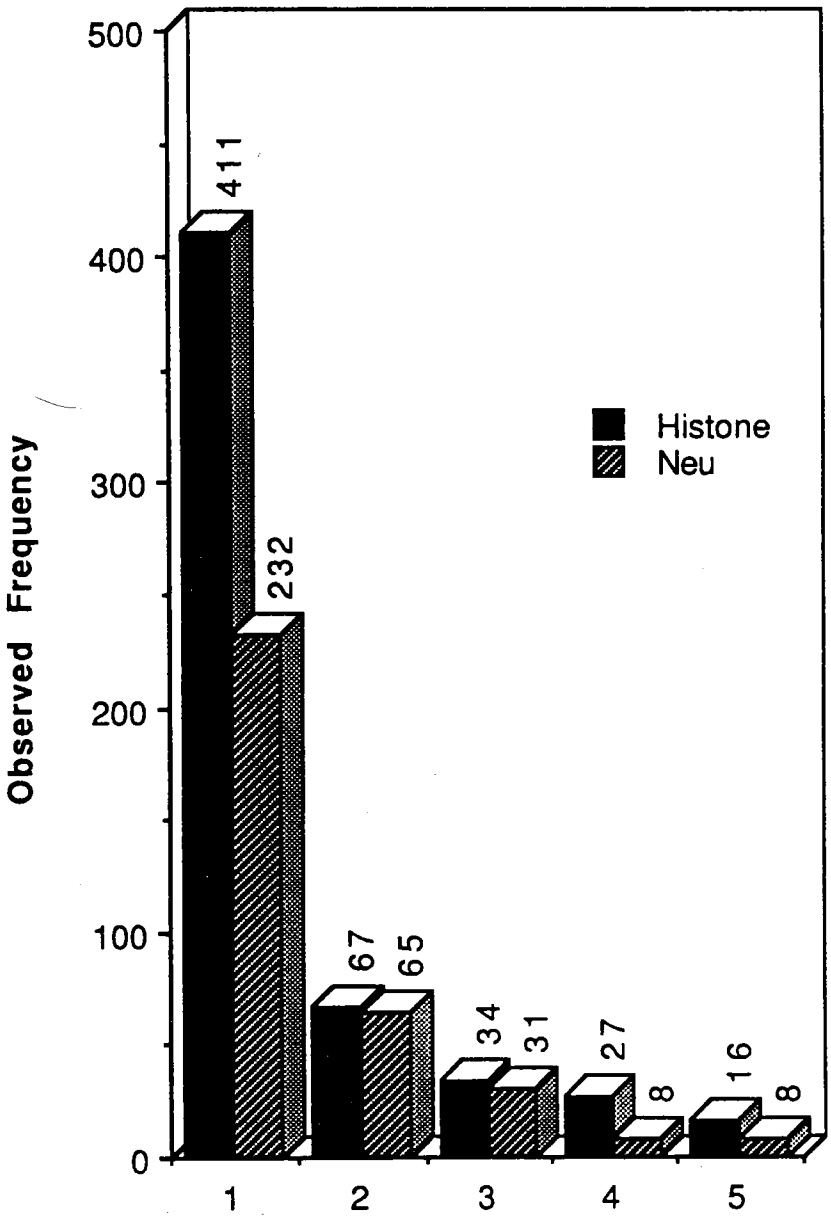

the mRNA size differences it was expected that neu mRNA would excede histone in the larger size categories. Within each sample, if the data is expressed as the percentage of total signal contributed by large GPC's, this will provide for comparison independent of mRNA abundance. For the H3 sample, 7.7% of the signal is from GPC's >3 particles, whereas 4.6% of the neu GPC's were large.

The above experiments demonstrate that the size of gold particle clusters resulting from detection of histone mRNA are larger than observed for larger nonhistone mRNAs. This suggests that histone mRNAs may be localized in groups, whereas other mRNAs are not. Therefore, it should be possible to demonstrate differences in gold particle cluster sizes for histone mRNA species of different sizes. An experiment which showed a difference in cluster size was a comparison of an H4 probe (clone pFO108A, 400 bases mRNA) (20,21) to an H1 probe (clone pFNC16A, appx. 850 base mRNA) (22). The results of this experiment (Figure 7) indicated that H1 GPC's were larger than H3, which is an expected relationship based on their mRNA size differences. For the H4 probe, 6.4% of the signal is from GPC's >4, and 18% are this size with the H1 probe.

It was of interest to investigate how histone mRNAs might be grouped together on the cytoskeleton in a manner distinct from other mRNAs. This would be important toward the precise characterization of mechanisms involved in the posttranscriptional

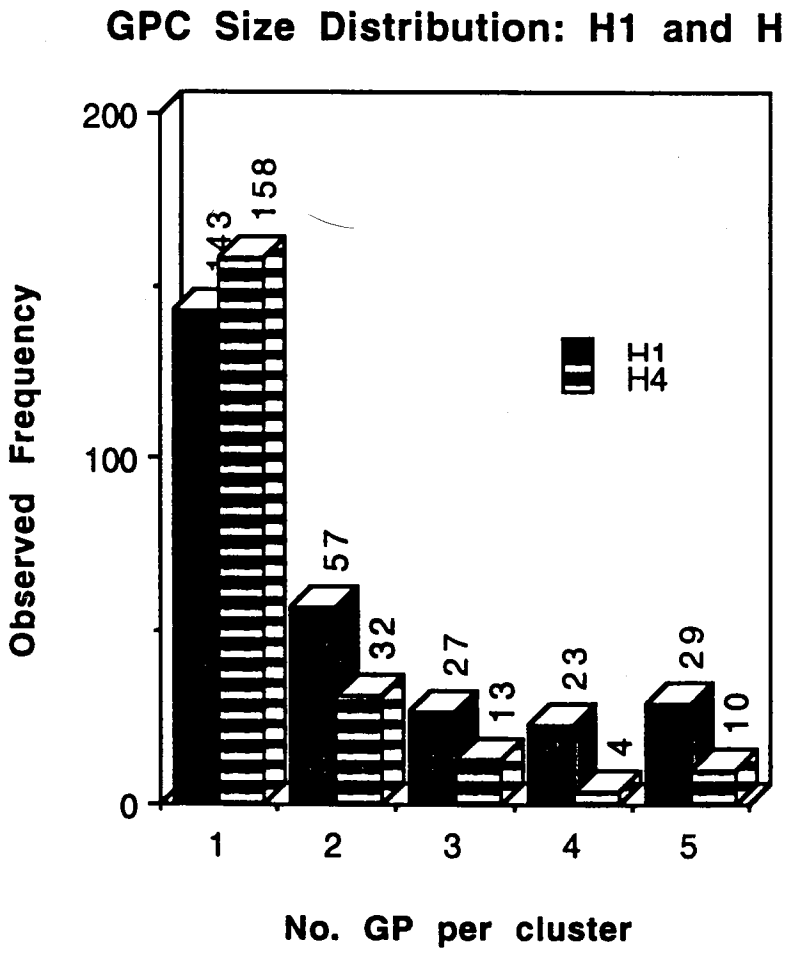

FIGURE 7. Frequency distribution of gold particle cluster sizes (246 fields). H1 DNA probe hybridization to human dipoid fibroblasts. H4 DNA probe hybridization.

regulation of histone mRNA. For example, are H3 mRNA molecules clustered with H4 mRNAs or just with other H3 mRNAs? Having demonstrated that an individual histone species exhibits large GPC's, it was then investigated if cluster sizes could be experimentally increased by combination of H3 and H4 probes. This approach might reveal whether H3 and H4 mRNAs are colocalized. However, these experiments did not show that the sizes of gold particle clusters could be increased by combining the two probes. A visual sampler of the large histone GPCs obtained in the above experiments is shown in Figure 8.

These results suggested that mRNA clustering may be homotypic, however double label techniques would be needed to confirm this. For example, if a biotin labeled H3 probe was hybridized simultaneously with an H4 probe labeled with another hapten, it would be possible to directly visualize the localization of both species. Boehringer Mannheim had just introduced digoxigenin labeled nucleotides and fluorochrome labeled antidigoxigenin FAB fragments for in situ hybridization. Unfortunately, commercially available gold labeled FAB or light chain specific secondary antibodies exhibited poor binding. However, monoclonal antibodies to digoxin (digoxigenin plus sugar residue) were utilized with some success. In one experiment, a signal to noise ratio of 6:1 was obtained for GPC's >3 particles. H3 and H4 probes could not be colocalized within a string of gold

FIGURE 8. Ultrastructural Detection of Histone mRNA Using Immunogold.

A-C. Examples of large gold particle clusters.

A. H3/H4 DNA probe hybridization to chicken fibroblast.

B. H3 DNA probe hybridization to human epithelial cell.

C. H4 DNA probe hybridization to human fibroblast.

D. Double label detection of H3 (5nm gold) and H4 (10nm gold) using biotin and digoxigenin DNA probes.

Bar, 100nm.

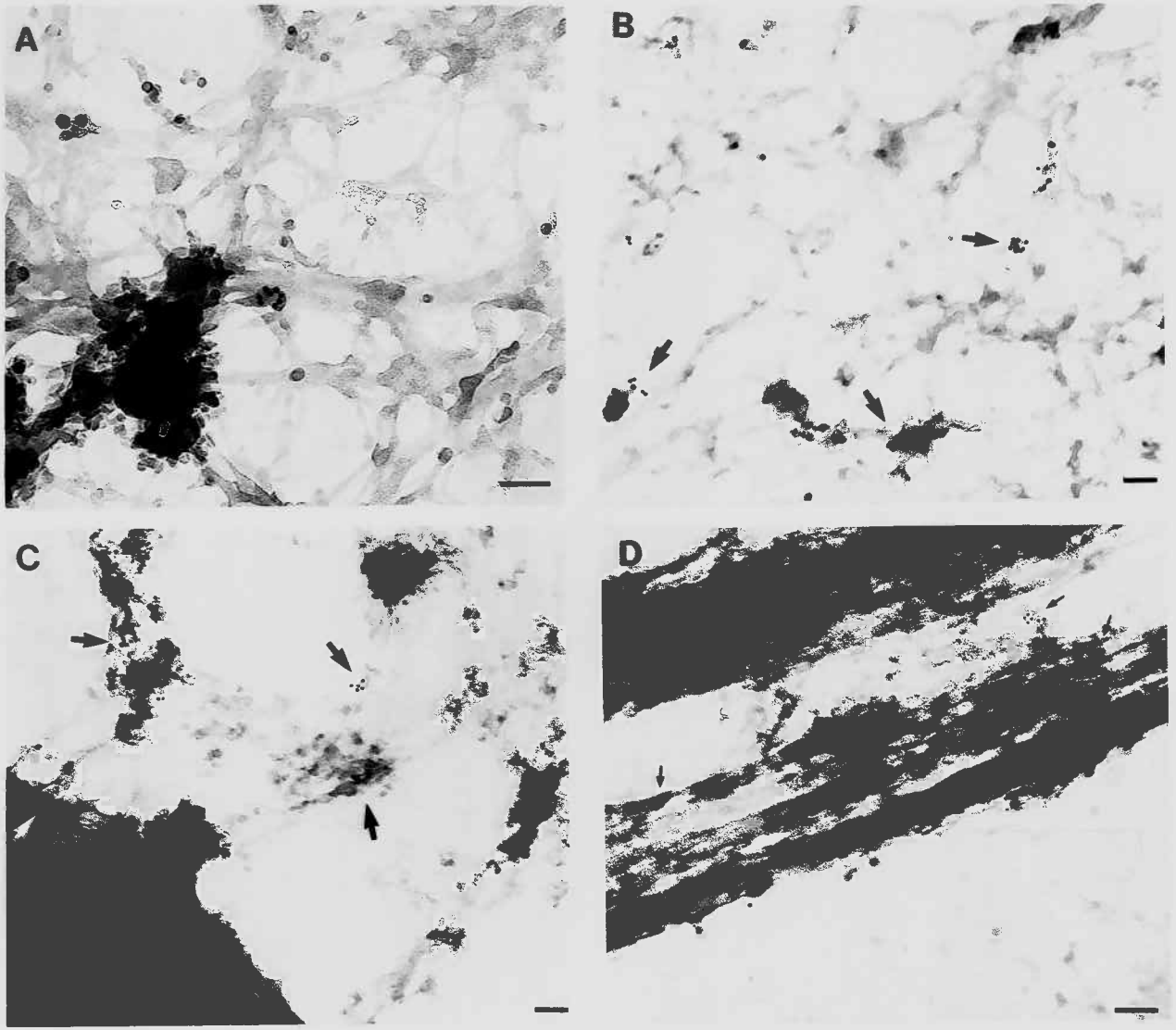
A
B
C
D

particles. Figure 8D is illustrative of the homotypic gold particle clusters obtained i.e. 5nm particle clusters, 10 nm particle clusters. This preliminary experiment would suggest that the large GPC's observed with histone probes are more likely attributed to clusters of a specific mRNA species. Although the respective H3 and H4 mRNAs were not colocalized within a single cluster, they are localized near each other i.e. within 0.1 um. Future development of a double label technology would provide an important tool to address these issues.

DISCUSSION

The objective of this study was to investigate if histone mRNAs are clustered in the cytoplasm, and study the functional significance of this localization. The in situ hybridization techniques used to address this distribution began with autoradiographic detection where the phenomenon was initially described (12). The grain clustering phenomenon was confirmed, but was not restricted to histone mRNA. It was determined that higher resolution techniques were needed to evaluate whether this phenomenon was real or artifactual. The application of an electron microscopic method demonstrated unique differences between the ultrastructural localization of histone mRNAs with other mRNAs. The observed size of gold particle clusters obtained from detection of biotinated histone probes did not correlate with

the size of the hybridized histone mRNAs. This work suggested that histone mRNAs might be localized in groups of molecules. In order to test this hypothesis the continued development of double label in situ hybridization methods will be essential. The utilization of specific oligonucleotide probes might also prove valuable. For example, biotin and digoxigenin labeled oligonucleotide could be synthesized to a specific sequence, and hybridized simultaneously in competition. If H3 mRNA molecules are localized in clusters, it should be possible to colocalize two sizes of gold particles within a single GPC. Similar experiments could be performed to evaluate whether H3 an H4 mRNA molecules are grouped.

The evaluation of the subcellular localization of histone mRNA has thus far been descriptive and phenomenologic. The objective of the research however was to investigate the role of spatial organization in the function of histone mRNA regulation. The ultrastructural technology will in the future reveal these relationships. The intracellular sites on the cytoskeleton which contain histone mRNA remain undefined. It is possible that the cytoskeleton might be involved in spatially colocalizing histone mRNAs. However, the cytoskeletal components involved in the attachment and distribution of mRNA in general are only poorly understood. Moreover, it is not known how closely individual mRNA molecules are positioned with respect to one another on the cytoskeleton. At this point, the evaluation of functional mRNA

compartmentalization had to begin with the study of mechanisms involved in the interactions of mRNA with the cytoskeleton. Through the identification of these mechanisms, it should then be possible to investigate if a cell can position functionally related mRNA molecules at common locations.. Another limitation to the histone study can be attributed to the paucity of EM ISH methods. The technology is in its infancy and much development needs to be done before the full potential becomes realized. The need for high resolution double label and/or oligonucleotide methods has been discussed. However, there is even a more urgent need to develop lower resolution ultrastructural methodology. A common criticism of EM research is that microscopic observations at a molecular level make it difficult to relate the "trees to the forest". For example, it is difficult to extrapolate the autoradiographic grain clustering distribution to the colloidal gold particle clusters. The data are obtained from separate detection methods, and there is no continuum of observation at intermediate magnifications. In consideration of the importance to understand the interaction of mRNA with the cytoskeleton through the continued development of an ultrastructural approach, I have directed subsequent work toward these goals.

REFERENCES

1. Plumb, M.A., Stein, G. Stein, J. (1983). Nucleic Acids Res. 11, 2391-2410.
2. Plumb, M.A., Stein, G. Stein, J. (1983). Nucleic Acids Res. 11, 7927-7945.
3. Baumbach, L., Marashi, F., Plumb, M., Stein, G., Stein, J. (1984). Biochemistry 23, 1618-1625.
4. Baumbach, L.L., Stein, G. Stein, J. (1987). Biochemistry 26, 6178-6187.
5. DeLisle, A. J., Graves, R.A., Marzluff, W.F., Johnson, L.F. (1983). Mol. Cell. Biol. 3, 1920-1929.
6. Graves, R.A., Marzluff, W.F. (1984). Mol. Cell. Biol. 4, 351-357.
7. Stein, G., Stein, J. (1984). Mol. Cell. Biochem. 64, 105-110.
8. Peltz, S.W., Ross, J. (1987). Mol. Cell. Biol. 7, 4345-4356.
9. Sariban, E., Wu, R., Erickson, L., Bonner,W. (1985). Mol. Cell. Biol. 5,1279-1286.
10. Graves, R.A., Pandey, N., Chodchoy, N., Marzluff, W. (1987), Cell 48, 615-626.
11. Zambetti, G., Stein, J., Stein, G. (1987). Proc. Natl. Acad. Sci. 84, 2683-2687.
12. Lawrence, J.B., Singer, R., Villnave, C., Stein, J., Stein, G. (1988). Proc. Natl. Acad. Sci. 85, 463-467.
13. Lawrence, J.B., Singer, R. (1986). Cell 45, 407-415

14. Sittman, D.B., Graves, R.A., Marzluff, W.F. (1983). Proc. Natl. Acad. Sci. 80,1849-1853.

15. Zambetti, G., Schmidt, W., Stein, G., Stein, J. (1985) J. Cell. Phys. 125, 345-353.

16. Cleveland, D.W., Lopata, M.A., MacDonald, R.J., Cowan, N.J., Rutter, W.J. Kirschner, M.W. (1980). Cell 20, 95-105.

17. Lichtler, A.C., Detke, S., Phillips, I.R., Stein, G., Stein, J. (1980) Proc. Natl. Acad. Sci. 77, 1942-1946.

18. Lichtler, A.C., Sierra, F., Clark, S., Wells, J., Stein, J., Stein, G. (1982). Nature 298,195-198.

19. Marashi, F., Helms, S., Shiels, A., Silverstein, S., Greenspan, D., Stein, G., Stein J. (1986). Biochem. Cell Biol. 64, 277-289.

20. Sierra, F., Lichtler, A., Marashi, F., Rickles, R., Van Dyke, T., Clark, S., Wells, J., Stein, G., Stein, J. (1982). Proc. Natl. Acad. Sci. 79, 1795-1799.

21. Plumb, M., Stein, J., Stein, G. (1983). Nucleic Acids Res. 11, 2391-2410.

22. Carozzi, N., Marashi, F., Plumb, M., Zimmerman, S., Zimmerman, A., Coles, L., Wells, J., Stein, G., Stein, J. (1984). Science 228, 1115-1116.

CHAPTER III

ULTRASTRUCTURAL IN SITU HYBRIDIZATION USING IMMUNOGOLD

INTRODUCTION

Overview

The electron microscopic detection of nonisotopic probes hybridized in situ can provide high resolution information on the spatial localization of nucleic acids within a morphological context. This review is intended to provide an update of the current progress in nonisotopic in situ hybridization at the ultrastructural level with emphasis on colloidal gold markers for high resolution. Although the technique is not widespread, the applications so far have been quite diverse: for instance identification of genes on chromosomes (1-11), rRNA in chloroplasts (12-14) and in mitochondria (15), messenger RNA in cultured cells (16-18), viral nucleic acids in infected cells (19-20). It should be emphasized that much more development is needed before the full potential of this technology becomes realized.

In situ hybridization using immunogold reagents followed by electron microscopy was reported by Wu and Davidson (1) who described a method for gene mapping to Drosophila polytene chromosomes. Poly-dT coated colloidal gold particles were used to detect Poly-dA tailed DNA probes. The development of biotin-

labelled DNA probes by Langer and Ward (21) led to their use with light microscopic in situ hybridization to DNA (22) and mRNA (23), and eventually for use with electron microscopy. Immunogold (2) and immunoperoxidase (3) procedures were described in 1982 using antibiotin primary antibodies followed by labelled secondary antibodies to detect biotinated DNA probes hybridized to mouse satellite DNA. Several other applications to gene mapping followed (4-11), with most laboratories using the colloidal gold technology because of the enhanced resolution obtained using electron dense markers of constant size and diameter which are directly bound to the primary antibodies.

Detection of RNA by electron microscopy was reported by Binder (15) who described the localization of mitochondrial rRNA and small nuclear RNAs in Drosophila ovaries using an immunogold technique. Subsequent reports included the detection of Po mRNA in myelin forming Schwann cells (24), and work done in our laboratory on the association of actin, vimentin and tubulin mRNAs with the cytoskeleton as well as the localization of myosin heavy chain mRNA in developing muscle sarcomeres (16-18,25). McFadden has investigated nuclear and chloroplast encoded rRNA distributions (12-14) in plant cells. Thiry studied the spatial localization of rDNA and its transcripts (26).

Specific Application to the Study of the Spatial Organization of Nucleic Acids

An individual cell maintains a highly organized and asymmetric architecture. Understanding how newly synthesized proteins are sorted and targetted to their proper locations has been an active area of research in modern cell biology. We are interested in the spatial organization of nucleic acid molecules within individual cells. A number of reports have demonstrated that specific mRNAs can be localized to distinct cellular regions. We demonstrated that α-actin mRNA was localized to the leading lamellae in motile fibroblasts, whereas vimentin mRNA exhibited a perinuclear distribution (27-29). Figure 9 is illustrative of this finding. Additionally, myelin basic protein mRNA has been shown to be regionalized to oligodendrocyte processes (30-31). Microtubule associated protein-2 mRNA was found concentrated to neuronal dendrites, whereas tubulin mRNA was localized to cell bodies (32). Acetylcholine receptor mRNA was shown to be localized to the neuromuscular junction (33). Earlier studies with nontranslated maternal mRNAs have demonstrated non-random distributions in Ascidian eggs (34,35), Xenopus oocytes (36), and Drosophila embryos (37). It is likely that the position of a message within a cell plays an important role in establishing localized synthesis of proteins near their site of function.

FIGURE 9: Detection and localization of β-actin mRNA. Biotin-labelled oligonucleotide probes were hybridized to cultures of chicken embryo fibroblasts, and the hybridized probe was detected using a streptavidin-alkaline phosphatase conjugate (BRL). β-actin mRNA was highly localized to the leading edge of the fibroblast. Details of the actin oligonucleotide probe methodology have been published (28). Bar, 10 μm.

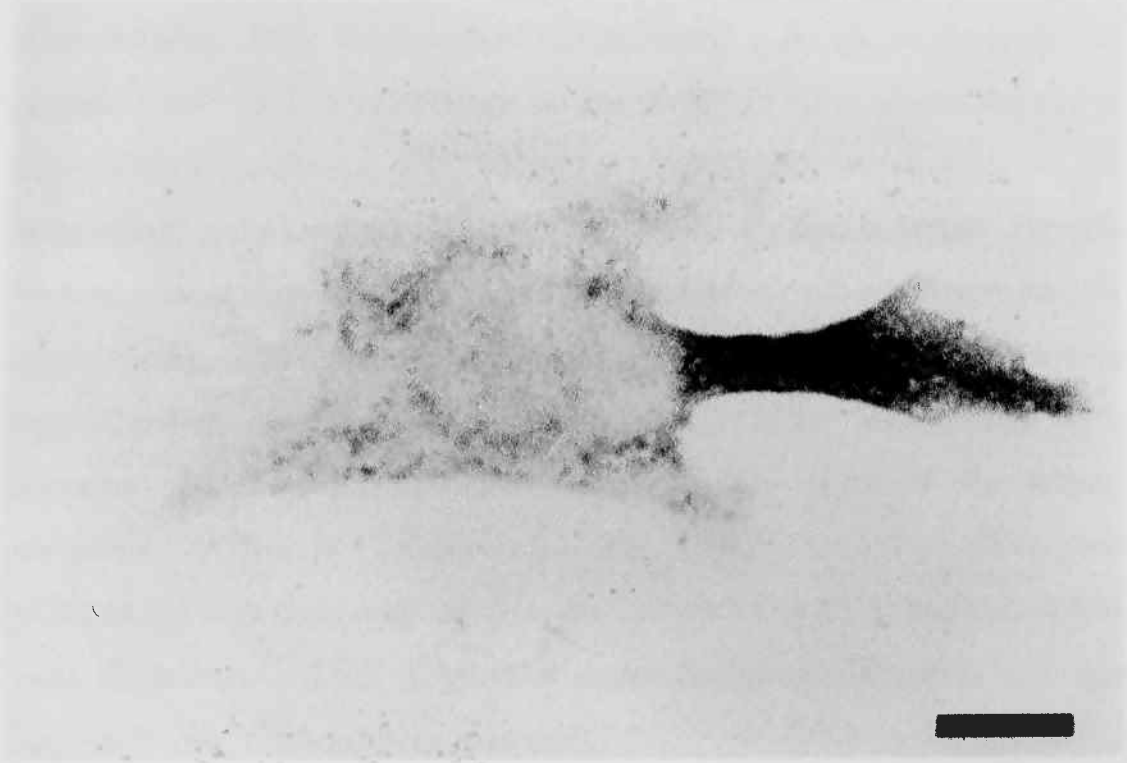

The work of Penman demonstrated that mRNA, and specifically translatable mRNA, is associated with the Triton-insoluble cytoskeletal framework (38-42). This framework contains the three major filament systems of eukaryotic cells; microfilaments, microtubules and intermediate filaments. It is reasonable to suggest that the cytoskeleton is involved in the maintenance of non-uniform mRNA distributions. An understanding of the molecular mechanisms governing mRNA localization would require elucidation of the physical association of mRNA with the cytoskeleton. The development of an electron microscopic in situ hybridization methodology would be directly suited for this purpose. The work presented here describes some of the results obtained utilizing Triton-extracted chick embryo fibroblast cultures for the detection of β-actin, vimentin and tubulin mRNAs (see Results). The important methodological features of our approach are discussed in Methods.

Intracellular visualization of viral nucleic acids has not yet been sufficiently explored by EM in situ hybridization. This technology would be particularly well suited for investigating the cellular location of viral nucleic acids, particularly after viral uncoating. Immunocytochemical techniques alone only provide information concerning viral antigens. There have been two recent reports describing the detection of Herpes Simplex Virus Type II RNA (19) and intranuclear localization of Herpes Simplex Virus Type I DNA (20) in cultured fibroblasts. The purpose of this

review is to discuss some of the more important methodological features in our and others' laboratories which are of particular importance to EM in situ hybridization and will be applicable to future studies of virally infected cells. In Table 1, six protocols are highlighted which encompass EM in situ hybridization applications. The following parameters have been considered:

1. Cell preparation: Procedures which occur before the hybridization step have considerable bearing on the retention and accessibility of target nucleic acids. For instance the choice of fixative, or use of cell proteolytic digestion have important ramifications on hybridization efficiency. The procedures also vary depending on the electron microscopic approach; eg. whole mount or thin sectioning.

2. Probe preparation: A variety of methods exist for the synthesis of nonisotopic DNA and RNA probes which include nick translation, random priming, in vitro transcription and chemical synthesis.

3. Hybridization: The optimization of probe concentration and the duration and stringency of the hybridization reaction has a major impact on the hybridization signal.

4. Detection: A variety of detection methods exist from direct one-step methods to more lengthy amplification schemes. Several types of commercially available colloidal gold reagents exist.

5. Data Analysis: The presentation of the data is critical to a successful publication. Important data includes correlative light

TABLE 1: A COMPARISON OF SIX IN SITU ELECTRON MICROSCOPY PROCEDURES

REFERENCE	TARGET NUCLEIC ACID	PROBE	FIXATION	EMBEDMENT
N.J. Hutchison et al JCB 1982 95: 609-618.	Mouse satellite DNA	Nick Translation biotin-dUTP	Mouse L929 cells 0.5% glutaraldehyde	Whole Mount metaphase chromosomes
M. Binder et al JCB 1986 102: 1646-1653	Mitochondrial rRNA UI small nuclear RNA	Nick Translation biotin-11-dUTP probe size 35-120bp	Drosophila ovaries 4% paraformaldehyde 0.1% glutaraldehyde	Postembedment- Lowicryl
H.F. Webster et al Histochemistry 1987 86:441-445	P_0 mRNA	Nick Translation biotin-11-dUTP probe size 100-300 bp	Rat trigeminal ganglia 4% paraformaldehyde 0.1% glutaraldehyde	Postembedment- Lowicryl Preembedment- Epon
G.I. McFadden et al Histochemical J 1988 20: 575-586	cytoplasmic rRNA	Random priming biotin-11-dUTP	Ornamental tobacco styles (plant cells) 4% paraformaldehyde 0.25% glutaraldehyde	Postembedment- LR Gold
R.A. Wobler et al J Histochemistry & Cytochemistry 1989 37: 97-104	HSV II thymidine kinase mRNA	Biotinated probe from ENZO Biochemical Co. probe size 200-1000bp	Cultured human infected fibroblasts, HSV II 5% formalin	Preembedment- Epon
R.H. Singer et al JCB 1989 108: 2343-2353	Actin, vimentin, and tubulin mRNAs	Nick translation full length cDNAs biotin-11-dUTP probe size 75-200bp	Cultured chicken embryo fibroblasts 4% glutaraldehyde after triton extraction	Triton-extracted whole mounts

TABLE 1 CONT.

HYDBRIDIZATION	DETECTION	CONTROLS	LIGHT MICROSCOPY
Probe concentration 0.8 ng/ul 50% formamide 0.6M NaCl 24 hrs. 37 C	Rabbit anti-biotin goat anti-rabbit-20nm (Lab antibodies) 1-24 hr. incubations RT	No probe micrographs, Internal control-quantitation	^{3}H-autoradiography
Probe concentration not given 50% formamide 0.6M NaCl 24 hrs. 37 C	Enzo rabbit anti-biotin Protein A-14nm (lab prep.) 1-2 hr. incs. RT	No probe micrograph, Internal control and control probe quantitation	silver enhancement
Probe concentration 0.2ng/ul 50% formamide 2XSSC 48 hrs. 40 C	Enzo rabbit anti-biotin Janssen goat anti-rabbit-5nm or biotinated goat anti-rabbit, Streptavidin-20nm 1hr. incs. 37 C	No probe data not shown, Internal control-qualitative	Alkaline phosphatase
Probe concentration 2ng/ul 50% formamide 0.75M NaCl 16 hrs. 40 C	Enzo rabbit anti-biotin Janssen goat anti-rabbit-15nm 1 hr. incs. RT	RNAase micrographs with signal to noise quantitation, internal controls	^{32}P autoradiography
Probe concentration 12ng/ul 40% formamide 0.6XSSC 18 hrs. 37 C	Janssen Streptavidin-5nm overnight RT	DNAase, RNAase and control probe quantitation	None
Probe concentration 2ng/ul 50% formamide 2XSSC 3 hrs. 37 C	Enzo rabbit anti-biotin Janssen goat anti-rabbit -10nm 1-2.5 hr. incs. RT	Control probe quantitation	^{32}P in situ dot blots and immunogold montage reconstruction

microscopy, use of sufficient controls and quantitation of signal to noise ratios.

METHODS

Cell Preparation

Embedment and Whole Mount Electron Microscopy

As described in Table 1, there are basically three types of procedures for preparing a cell for electron microscopic visualization of in situ hybridization. Preembedment techniques employ hybridization and immunogold detection to either cultured cells or tissue sections prior to embedment into plastic. Wobler (19) hybridized and subsequently stained fibroblast cell suspensions which were then pelleted and embedded in Epon. Similarly, Webster (24) processed vibratome sections of rat brain trigeminal ganglia prior to Epon embedment.

Postembedment techniques involve hybridization and detection directly on the thin section. This approach can provide superior ultrastructural morphology. Different embedment procedures have been assessed for RNA retention and accessibility. Binder (15) used Lowicryl K4M embedded Drosophila tissue wherein semi-thin sections were stained with acridine orange to assess RNA retention before subsequent hybridizations on ultrathin sections were performed. McFadden (12-14) successfully hybridized rRNA in tissue embedded with LR

Gold, an acrylic hydrophilic resin with limited cross-linking properties.

The permeability of probes and detection reagents are of general concern with both preembedment and postembedment procedures, however the limiting factors are different. With preembedment techniques, reagent permeability within cells or tissues is directly affected by various cellular pretreatments: e.g. fixation, protease digestion, detergent lysis, etc. (discussed later). However, with the postembedment approach the cell is sectioned and the resin becomes the rate-limiting permeability barrier. Only the nucleic acids exposed at the surface of the section are directly accessible to probe and detector reagents. It is not currently clear as to whether some probe and detection system reagents can penetrate and hybridize to nucleic acids directly within the thin section. The more permeable acrylic resins might be desirable in order to overcome the limited diffusibility of probe and antibodies (12).

Whole mount electron microscopy involves no embedment or sectioning and three dimensional structure is maintained by critical-point drying. The large depth of field of the microscope allows the entire cell preparation to be directly analyzed. Hamkalo (2), has analyzed satellite DNA, by depositing metaphase spreads onto EM grids, fixing in glutaraldehyde and processing for in situ hybridization. The biotinated probe was detected with colloidal gold conjugated antibodies and the preparation examined

after air drying. A whole mount technique in our laboratory involved growing chick embryo fibroblasts on carbon/formvar coated EM grids. Cells were extracted with 0.5% Triton, allowing ultrastructural analysis of the association of mRNAs with the remaining cytoskeleton. Since this detergent extraction removes at least 75% of total cell protein, sufficient contrast was provided and allowed the structural elements of the cell to be easily visualized. The spatial organization of specific mRNAs could then be studied with high resolution. The nucleoplasm is less extracted by Triton and remains relatively opaque to the electron beam; hence analysis of nuclear nucleic acid sequences would benefit by a thin sectioning approach, or additional pretreatments to remove dense material.

There are several reasons to use Triton extraction before fixation. First, we are interested in the distribution of mRNA molecules within the cytoskeletal framework of individual cells. Second, this procedure is directly suitable to whole mount electron microscopy in which the entire complement of the mRNA in the cell is visible and hence increases the signal per field of view. Third, the limited cytoplasmic penetrability associated with colloidal gold reagents are less of a concern. It should be emphasized however that membrane systems are either partially or completely solubilized by Triton-extraction.

Cell Fixation and Pretreatments

As we have shown previously, the choice of a cell fixation procedure can directly influence the success of an in situ hybridization procedure (43-44). For example, an analysis of hybridization to actin mRNA in cultured chick fibroblasts showed that precipitative fixatives e.g. ethanol:acetic acid caused a loss of 75% of the RNA, whereas glutaraldehyde (4%) resulted in the highest retention of RNA (43). However, glutaraldehyde crosslinked too extensively and rendered the mRNA inaccessible to hybridization. Paraformaldehyde (4%) produced the best compromise in RNA retention and accessibility and gave highest signal to noise ratios. In contrast, when cells are extracted in detergent (as discussed above), paraformaldehyde-fixed cytoskeletons resulted in a substantial loss of mRNA during hybridization (16). Glutaraldehyde-fixed Triton-extracted cells resulted in the highest signal to noise ratio (16). Most of the fixatives used in the reports highlighted in Table 1 are glutaraldehyde or paraformaldehyde/glutaraldehyde mixtures, and several labs have reported the need for optimizing this most important parameter for use with each particular model system.

Two prehybridization procedures which warrant some discussion are DNA denaturation and proteolytic digestion. The need for the first is obvious since DNA must be strand-separated before hybridization. Wobler digested (19) formalin fixed cells

with protease and HSV viral DNA was denatured in 50% formamide 3XSSC at 60°C for thirty minutes. However, despite cytopathic evidence of nuclear swelling, chromatin peripheralization and the presence of many icosohedral HSV capsids in each nucleus, only viral RNA hybridization occurred. DNAse digestion before hybridization did not effect labelling. RNAse treatment reduced the nuclear signal by 97%. Interestingly, viral RNA was often observed adjacent to nuclear capsids.

The additional use for proteolytic digestion of cells prior to hybridization has often been included in procedures aimed at detecting viral nucleic acids (45,46). The rationale for this procedure is that viral DNA complexed with protein might be crosslinked in a configuration which warrants a more rigorous denaturation treatment prior to hybridization. Proteolytic digestion followed by DNA denaturation at 100°C in 45% formamide 5XSSC was successfully used for hybridization to formalin-fixed CMV DNA (46). Optimal signal to noise ratios required both proteolytic digestion and denaturation at unusually high temperatures.

In our own experience, we have been able to hybridize to Epstein Barr Virus DNA in cells either fixed with methanol:acetic acid or with paraformaldehyde and denaturated in 70% formamide 2XSSC at 70°C for 2 minutes (47) without need for proteolytic digestion. However, we found that protease digestion increased

efficiency of hybridization to mRNA in cells fixed with glutaraldehyde but decreased this efficiency when fixed in paraformaldehyde (43). Hence, the requirement for proteolytic digestion before hybridization to viral DNA appears to be dependent on the method of fixation. These parameters need to be optimized for each particular system. RNAse treatments and/or omission of DNA denaturation before hybridization are particularly useful for specifically determining which nucleic acid is responsible for the visualized signal and how it might be affected by modification of specific parameters (48).

Probe Preparation

There are a variety of methods for preparing biotinated probes for in situ hybridization. Much of our experience has been with probes wherein the desired DNA has been labelled with an analog using nick-translation. This is the favored method (Table 1). Although the protocol is simple and straightforward to perform, it is important to evaluate the size of the resulting probe fragments using gel electrophoresis (43,44). In our own experience, the same ratio of DNA polymerase I to DNAse in the labelling reaction can yield probe fragments of different sizes from one experiment to another. It has been appreciated that smaller probe molecules show better penetrability but even more important is the fact that large probe molecules exhibit non-specific binding. We have observed optimal signal to noise ratios

with probe fragments between 200-400 bp for hybridization to actin mRNA in paraformaldehyde-fixed cultured fibroblasts. Three of the four reports in Table 1 which utilized nick translation appear to be aware of the importance of probe size.

Another important aspect of probe preparation is the choice of the particular biotinated nucleotide. We have noticed varying degrees of biotin substitution in probes prepared with different commercial sources of labelled nucleotide. Our previous work was based on biotin-11-dUTP (Bethesda Research Laboratories, Gaithersburg, MD) which was discontinued and we now prefer biotin-16-dUTP (Boehringer-Mannheim).

Hybridization

Most of the procedures listed in Table 1 use probe concentrations between 0.2-2 mg/ml in 50% formamide 2XSSC for 16-48 hours. We have found that hybridization for such extended periods was both unnecessary and deleterious to cells fixed for short times in paraformaldehyde (43,44). Hybridization to actin mRNA, present at approximately 1000 copies per cell, was completed in three hours (43,44). Longer hybridizations frequently resulted in loss of signal from paraformaldehyde-treated cells presumably because of solubilization of cellular components. Tissue sections or glutaraldehyde fixed cells can withstand longer hybridizations.

The concentration of probe is an essential feature of successful hybridization as the reaction only goes to saturation at greater than 2mg/ml (probe plus vector, approx. 6 Kb). Less than complete hybridization results in inability to distinguish signal from noise at the EM level (see below).

Detection

Our EM work has used immunogold exclusively to detect the biotinated probe. A few recent references focus on the synthesis and application of colloidal gold reagents for electron microscopy and discuss their advantages and limitations in greater detail (49-50). Colloidal gold-labelled antibodies are the marker of choice for in situ hybridization at the electron microscopy level for a number of reasons. First, the electron opacity of colloidal gold gives higher contrast than enzymatic reaction products. Furthermore, because the colloidal gold is closer to the site of hybridization, the resolution is also higher. Individual hybridization events can be correlated with each gold particle allowing a quantitative approach to the hybridization (16). Second, reagents are stable and easy to use, and the quality of most commercial sources is excellent. Particle diameter and the presence of minimal particle clusters is rigidly controlled. This is particularly advantageous for multiple labelling approaches. We have not observed background problems with these reagents even when used undiluted. Background is usually attributed to the

primary antibody. Commercial suppliers have been helpful with technical information and assistance with research applications e.g. Janssen, Biocell Laboratories.

The variety of immunogold detection schemes should be considered. Most EM in situ hybridization detection procedures (Table I) utilize antibiotin-primary antibodies from Enzo Biochemicals (New York, NY). In our laboratory, this reagent provided the best signal when compared to several other commercially available polyclonal and monoclonal antibodies. Detection of the primary antibody can be accomplished by several methods. Excellent results were obtained with colloidal gold labelled secondary antibodies from Janssen Laboratories (12,16). Binder (15) used Protein-A gold, an F_c receptor for detection of antibiotin primary antibodies. Webster (24) used a biotinated antibody bridged between antibiotin and streptavidin-gold. Wobler (19) utilized streptavidin-gold directly to detect hybridized probes. We (16) and others (51) have tried a number of streptavidin-gold conjugates from several sources without success. This may be attributable to unfavorable steric or charge interactions of the gold-streptavidin complex with the hybridized DNA probe. It might be worthwhile to investigate the use of longer linker arms between the pyrimidine ring and biotin moeity. Interestingly, allyl arms shorter than eleven carbon atoms reduced the sensitivity of detection using alkaline phosphatase labelled antibodies (52).

Theoretically, when streptavidin is adsorbed to colloidal gold and then used for detection of biotinated probes, one gold particle should correspond to the direct visualization of one biotinylated nucleotide (a single-step procedure). For a two step procedure, protein-A should bind a primary antibiotin antibody at a 1:1 ratio, thereby also giving one gold particle per biotinated nucleotide. In contrast, gold labelled secondary antibodies are polyclonal and therefore can potentially recognize multiple epitopes on a single primary antibody. Steric factors, however, will limit this amplification, depending upon the size of gold particle and number of immunoglobulin molecules coating the gold colloid. We have observed approximately a three-fold increase in signal when using polyclonal secondary antibodies instead of Protein-A labelled with gold. A "biotin bridge" method (Table 1, Webster et al.) potentially allows for the greatest number of gold particles per biotinated nucleotide. This three step method involves antibiotin antibodies followed by biotinated antiprimary antibodies and finally streptavidin-gold. Two important considerations in any amplification procedure are that with each additional step, both signal and noise increase, and the gold particle is further removed from the site of hybridization. Amplification is thereby accompanied by a loss in resolution, and increased sensitivity only if minimal background is contributed by the additional antibody incubation.

The size of the colloidal gold labelled antibodies is also important. In reality, they actually are "antibody labelled colloidal gold particles". For example, a 5nm particle is coated with 2-3 whole antibody molecules or 4-5 Protein-A molecules (53-54). Increasing the size of the gold particle to 10nm increases the number of adsorbed antibodies and the resulting surface area of the sphere with the protein coat increases approximately eight-fold (53-54). It is therefore reasonable to expect problems with penetration and diffusibility of these reagents. By extracting cells with Triton before fixation we have eliminated these problems. However on fixed cells, limited permeabilization is necessary to presumably solubilize lipid-rich membrane regions. Treatment of the cells with Triton or Triton-saponin as well as longer incubations with more concentrated antibody solutions were required to obtain adequate signal to noise ratios (18,25).

Data Analysis

Due to the microscopic nature of the subject, the presentation of micrographs must be selected to be representative of the data. In order to represent these microscopic observations objectively some quantitation of the data is required. The following questions must be answered by any new procedure which provides visual information.

- Could it be artifactual?
- How representative are the figures to the entire cell?

- How representative is the cell to the population of cells?

The first step in addressing these considerations is to provide data showing that the signal observed (gold particles) represent bona fide sequence specific hybridization. There are several types of controls which can be used for this purpose. The primary control is to demonstrate that non-homologous biotinated probes (usually the vector alone) which are of the same fragment size and at the same concentration result in the deposition of significantly reduced amounts of gold particles. Another suitable control would be to demonstrate that the signal was significantly reduced by competitive hybridization with excess amounts of unlabelled probe fragments of homologous sequence or by ribonuclease treatment of the sample in the case of an RNA target. Statements that "control probes were negative (data not shown)", or even to show a negative micrograph at high magnification is insufficiently convincing without quantitative information concerning specific hybridization signal versus background noise. The most important information is to determine reproducibility by investigating multiple independent experiments (different probe preparations and samples). This reduces errors attributed to variations in probe preparations, the most common cause of background.

In our study (see Table 1) on hybridization to β-actin mRNA in Triton-extracted fibroblast cultures, gold particles were counted

from fifty micrographs (taken at 20,000 X magnification). Half were taken from hybridizations with biotinated β-actin DNA probes (including the vector), and half from only biotinated vector DNA probes. In total, the data represented analysis of twelve cells from three independent experiments. Quantitation of overall gold densities demonstrated an average signal/noise ratio of >6:1. Furthermore, the electron microscopic appearance of specific hybridization was often in the form of tightly linked clusters of gold particles, thereby giving both a qualitative and quantitative difference of signal from noise. As the number of gold particles in a cluster increased, progressively fewer clusters were observed with the control probe compared to the actin probe. This resulted in a proportional increase in signal to noise ratios (i.e., number of clusters in each size category for actin probe divided by the number for the control probe) which began at 3:1 for individual gold particles and increased logarithmically to 30:1 for clusters of eight or more gold particles. When as many as eight particles are seen in a cluster, the probability is 97% that this signal represents authentic hybridization to actin mRNA. These results are presented in Figure 10. This approach will be discussed in a later section. Wobler (19) also quantitated signal to noise ratios with specific probes compared to nonhomologous control probes. Similarily, quantitation of nuclear and cytoplasmic hybridization to HSV RNA resulted in a 36% background level when only individual gold particles were considered, whereas hardly any

FIGURE 10: Quantitative analysis of biotinated actin probe hybridization using immunogold. Twenty-five micrographs (photographed at 20,000X) were analyzed for each probe (β-actin cDNA plus vector, pBR322 vector only) and the gold label was divided into categories depending on their presence as singles, doubles, etc. The histogram is a plot of the relationship between the number of gold particles per cluster and their observed frequency per unit area (16). Signal to noise ratios were obtained by dividing the frequency of β-actin mRNA over pBR322 for each gold particle cluster size category. When as many as eight gold particles are observed in a cluster, the noise level diminishes essentially to zero and the mRNA is detected with high confidence (97%).

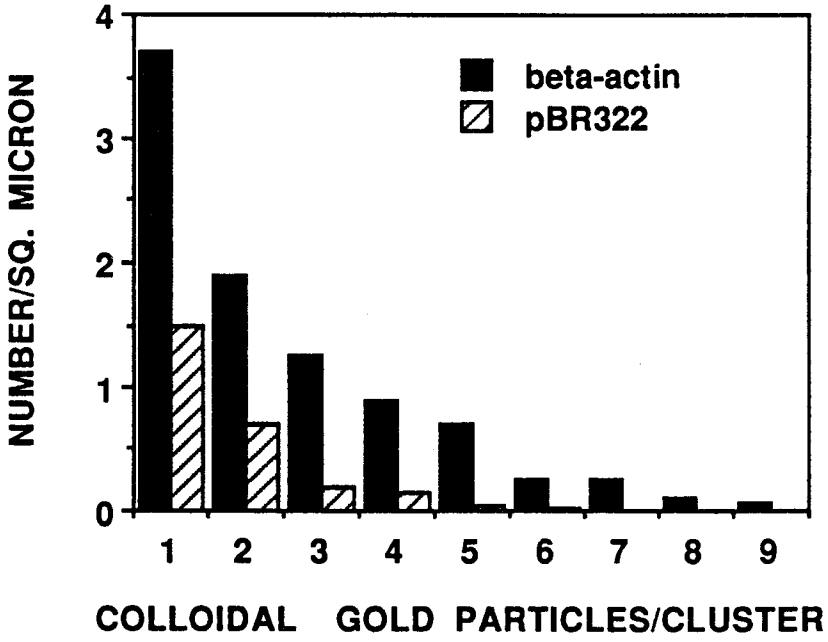

gold particle clusters were observed with control hybridizations using a nonhomologous CMV probe.

Other types of experimental controls can provide additional information. Nuclease digestions can help determine that probe specific hybridization is dependent on the presence of RNA. Nuclease controls have often been used to substitute for nonhomologous probes. The rationale is that if signal is eliminated by nuclease digestion, it can be attributed to probe hybridization rather than non specific sticking. These experiments are particularly helpful if done in addition to the use of control probes (16,19). This helps to eliminate nonspecific binding to nucleic acids or their associated proteins possibly attributed to errors in probe preparation methods. Using only a nuclease digestion control could lead to erroneous conclusions.

Internal controls were used by several of the reports listed in Table 1. McFadden hybridized a probe specific for nuclear encoded rRNA labelled nucleoli and cytoplasm. Hybridization of a probe specific for chloroplast rRNA labelled chloroplasts and not heterologous rRNA in nuclei or mitochondria (12-14). The successful use of this control was further supported by showing that hybridization to rRNA was reduced by digestion with RNAse allowing the determination of a signal/noise ratio of 10:1. Binder (15) provided convincing quantitative data of mitochondrial rRNA hybridization by comparing the subcellular density of gold label in mitochondria with other cellular regions using both mitochondrial

rDNA and a nonhomologous control probe. Again, the use of an internal control to illustrate intracellular specificity can be presented effectively along with controls for sequence specific hybridization. Hamkalo (Table 1) evaluated hybridization to mouse satellite DNA by comparing gold particle densities of centromeric regions with noncentromeric regions on 36 chromosomes. The ratios obtained ranged from 3.7 to 37, with an average value of 9.4. A control chromosome gave only a 0.9 specificity ratio. Webster (24), hybridized to Po mRNA in myelin forming Schwann cells and compared this to lack of staining in cell types which do not express Po mRNA (e.g. fibroblasts). Quantitative data was not provided. The above reports by Webster and Hamkalo did not use probe on the control samples. This is important for evaluating non-specific binding of detection system reagents, but does not control for probe sticking or non-specific hybridization.

The development of a sucessful electron microscopic in situ hybridization protocol begins at the light microscope. Most of the reports listed in Table 1 have some correlative light microscopic information. There are several advantages for this approach. First, light microscopic experiments are faster to perform. This can allow convenient evaluation of parameter manipulation and promote effective technological optimization. For example, determining whether a probe is effective, or whether an RNAse protocol reduced signal can be readily assessed by looking at a

population of cells at 250X with the LM rather than counting gold particles in a single cell with the EM. This also gives an assessment of the whole population of cells and provides an overview. Also, LM information can be obtained rapidly using acridine orange or propidium iodide for evaluation of RNA retention during fixation (15). We have used a rapid ^{32}P-labelled probe in situ procedure to quantitatively evaluate parameter manipulation on thousands of coverslips (43) by scintillation counting. In this report (Section III) we present a method which provides for both LM and EM investigations on the same sample.

RESULTS

Detection of mRNA in Triton-Extracted Fibroblast Cultures

Identification of Individual Molecules

Figure 11a-d illustrates the clustered appearance of colloidal gold particles when actin mRNA hybrids are visualized by the above immunogold detection procedure. This data demonstrated that visualization of the mRNA sequences associated with the cytoskeleton was possible. As discussed in the text to Figure 10, sequence specific hybridization was qualitatively distinguished from background and individual sites of hybridization could be identified with very high confidence (97%). As evident from Fig. 11, the clusters of gold particles were not simply in an aggregate, but rather in a characteristic array with relatively constant spacing, and a linear dimension proportional to

FIGURE 11: Ultrastructural visualization of actin mRNA hybrids visualized in the electron microscope (16). Triton-extracted chick embryo fibroblasts were hybridized with a biotinated β-actin cDNA probe (2 kb, full length) and detected by the immunogold procedure described in Table 1. (a-d) Various conformations of hybridized mRNA seen in association with the cytoskeleton. (e-h) Double label detection of actin mRNA (10nm gold particles) and actin protein (5nm gold particles). Bar, 100nm.

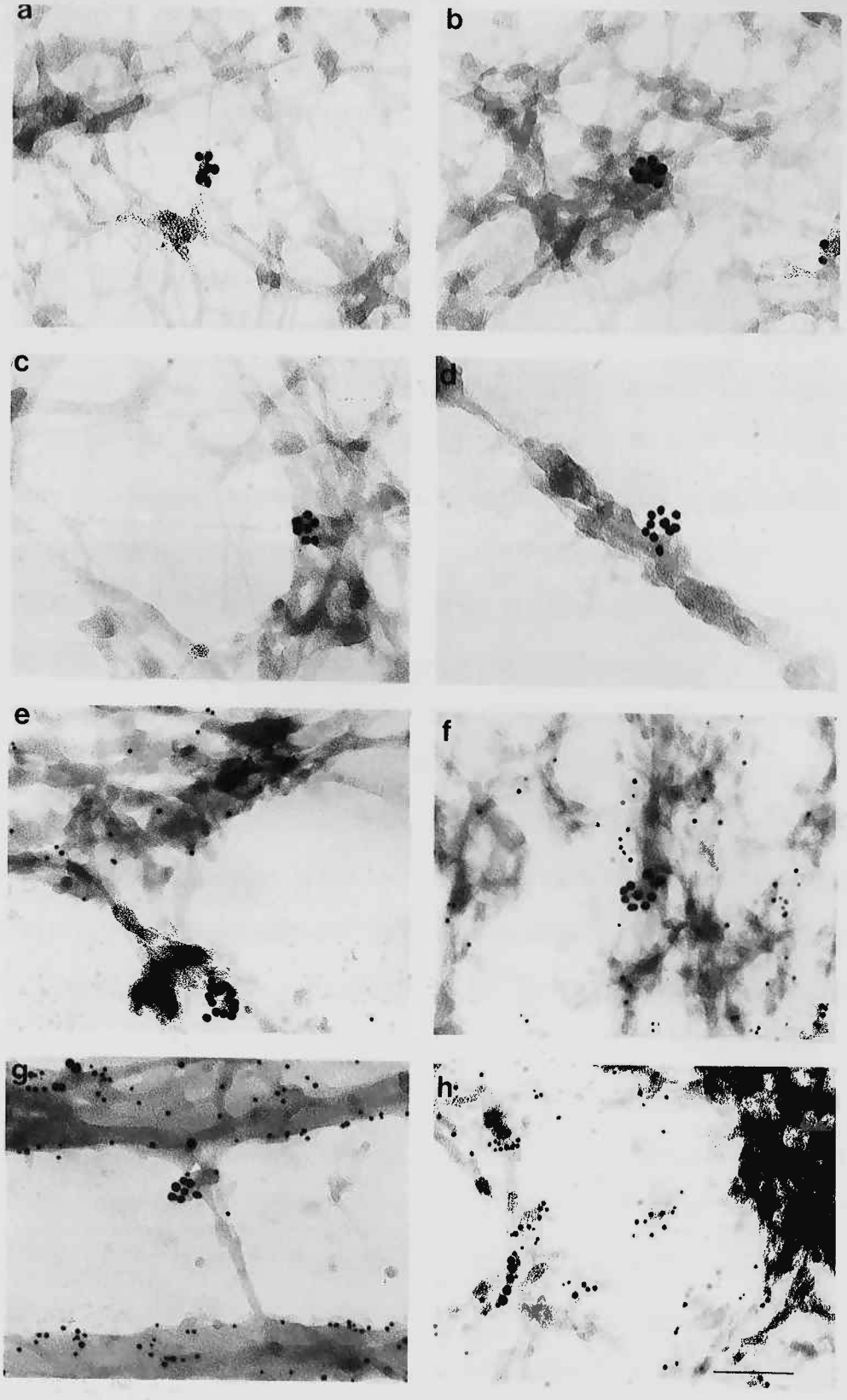
a
b
c
d
e
f
g
h

the number of gold particles involved. This appearance is consistent with biotinated actin probe molecules hybridizing to a template. The structure of the cluster appears to indicate that the template hybridized has a circular or spiral geometry. These conformations of gold particles are consistent with the hypothesis that several small probe molecules hybridized along an individual 2 kb β-actin mRNA molecule, and subsequent detection of biotin by indirect immunocytochemistry resulted in the visualization of an iterated array of gold particles. Non-specific sticking of probe or antibody molecules would occur as independent events and would fail to produce clustering of gold particles.

A schematic describing the observed quantitative and qualitative findings is shown in Figure 12. This illustration is not intended to be an accurate description of the number of secondary antibodies per colloidal gold particle or the number of secondary antibody-gold complexes per primary antibody. Furthermore, the small probe molecules are depicted as having only one biotinated nucleotide when in fact probes were nick translated with only labeled dUTP thereby giving approximately 25% substitution. The schematic however is meant to indicate that immunogold detection, not biotin substitition, is the rate limiting step. More than 7% probe substitution with biotin-dUTP does not result in additional signal (55) because steric factors preclude the binding of more than one 1^{o}Ab per 50 nts (16). It is important to appreciate that in order to template probe molecules along target

FIGURE 12: Schematic showing the basis for detection of bona fide signal from mRNA-biotinated DNA hybrids (16). The schematic presented here explains the iterative detection of a mRNA molecule using a biotinated DNA probe cut into small fragments so that each segment hybridizes independently. When the antibody detection of the biotin groups results in a string of colloidal gold particles, this distinguishes the signal from the noise generated by nonspecific sticking, either of probe or of antibody. The schematic is not intended to represent the number of secondary antibody molecules adsorbed per gold particle, or the number of secondary antibody complexes per primary antibody.

THE BASIS OF SIGNAL TO NOISE ENHANCEMENT FOR THE DETECTION FOR HYBRIDS BY ELECTRON MICROSCOPY

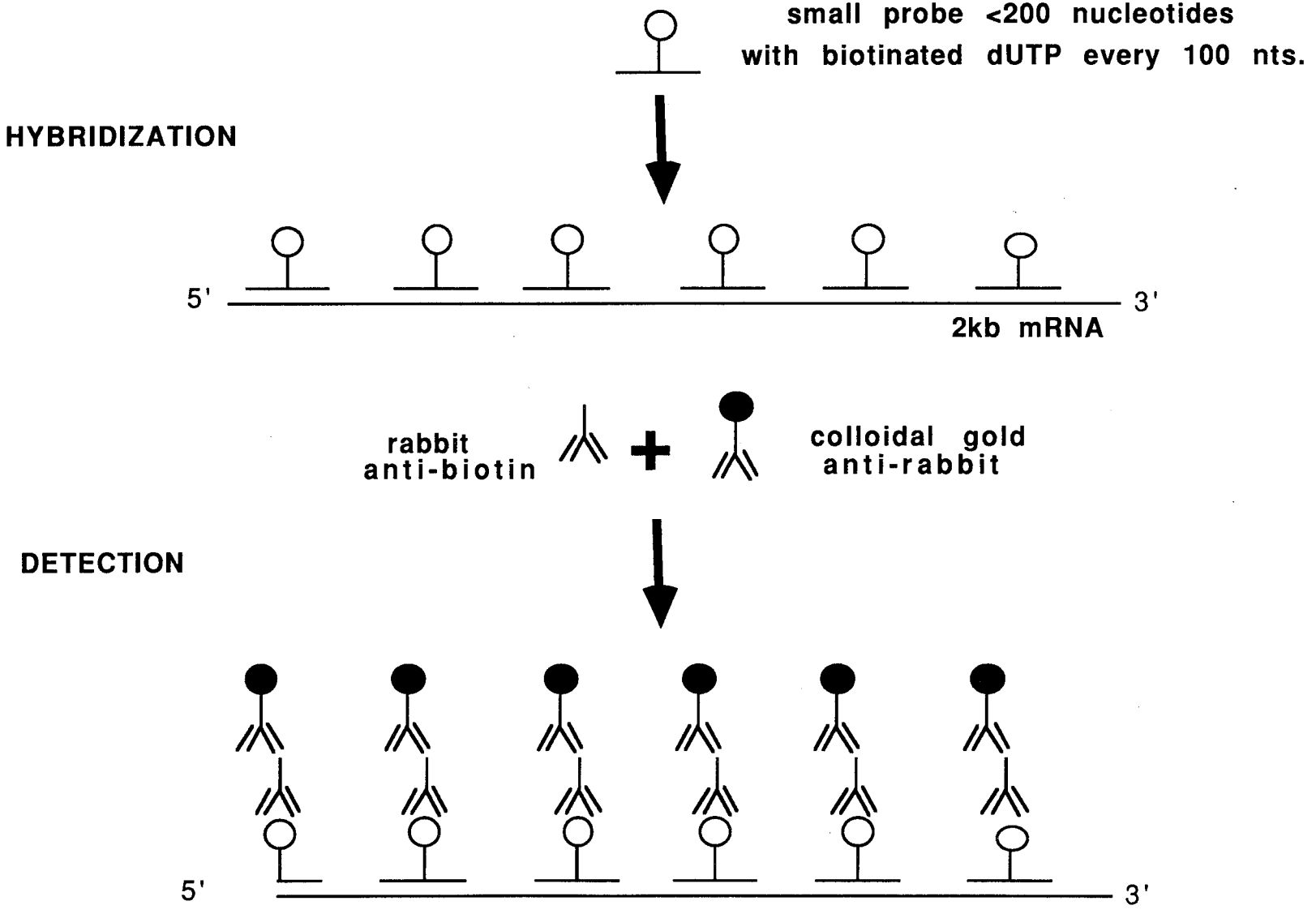

mRNAs such that signal is both qualitatively and quantitatively distinguishable from noise, probe fragment length must be tightly controlled and the probe concentration must be high enough so that multiple hybridization events occur along a single template.

Colocalization of mRNA and its Corresponding Protein

We developed a double-label technology which can evaluate the spatial relationship of specific nucleic acids and their corresponding proteins using electron microscopy. This methodology enabled us to address the role of the specific cytoskeletal filaments in mRNA attachment. Several commercially available monoclonals were screened by immunofluorescence to evaluate whether the characteristic filamentous staining patterns could be obtained following Triton-extraction, glutaraldehye fixation and hybridization in 50% formamide 2XSSC. Many antibodies showed only poor reactivity under these conditions. Those which reacted strongly were employed for the immunogold detection procedure (Table 1) and coincubated with the rabbit polyclonal antibiotin primary antibody so that both protein and probe would be detected. After washing the primary antibodies, 5nm-gold labelled goat anti-mouse and 10nm-gold labelled goat anti-rabbit secondary antibodies (Janssen) were incubated simultaneously to complete the detection of mRNA and its corresponding protein.

Figure 11e-h illustrates the results obtained using a monoclonal antibody to actin (Amersham). From these micrographs it is evident that actin protein (5nm gold) is distributed throughout the area occupied by actin mRNA (10nm gold). In Figure 11g, actin mRNA is localized to a strand connecting two actin cables. An identical approach using probes for vimentin and tubulin mRNA, in combination with antibodies for their cognate proteins revealed that these messages were not colocalized with their own corresponding proteins, and also exhibited a tendency to be localized near actin filaments. This research provided direct high resolution information which would suggest a more general role of microfilaments in the attachment of these mRNAs to the cytoskeleton.

Localization of Myosin Heavy Chain mRNA in Developing Muscle

Triton-Extracted Myotube Cultures

A useful system by which to investigate the spatial organization of cytoplasmic mRNA is developing muscle. We are particularly interested in elucidating any role mRNA localization may have in sarcomere assembly. Currently little information is available about how a cell can assemble such an intricate structure of enormous biological complexity.

We chose to evaluate the subcellular distribution of myosin heavy chain mRNA. We have already investigated its expression

at the light microscope level in developing chick myotube cultures (56). Due to the thickness of myofibers it was necessary to utilize a thin sectioning approach rather than the whole mount procedure successfully used for single cells. We chose a preembedment method since it was a step removed from the light microscopic protocols, and less likely to require more development. Since myosin heavy chain mRNA is quite large (5.9 kb) and abundant; these features would likely maximize our ability to evaluate signal to noise ratios directly on ultra-thin sections which contain significantly reduced amounts of cellular material.

The tissue culture system consists of a mixed population of fibroblasts and myoblasts. The myoblasts after approximately two days in culture differentiate and fuse together into multinucleated syncytia (myotubes). It is during this time that the genes for muscle specific proteins such as myosin become activated. By four days, the presence of numerous myofibers containing the myofibrillar proteins are evident. In order to allow reagents to penetrate the dense cytoplasm, myotubes were Triton-extracted, fixed in 4% glutaraldehyde, hybridized with a full length cDNA probe (5.9 kb, nick translated with bio-11-dUTP), detected with colloidal gold labelled antibodies, embedded into Epon and sectioned. The details of this methodology have been described (17).

The data was analyzed as described for whole mount cells in which a probe for actin mRNA was used. The number of gold

particles in the section was measured as a function of the number of gold particles per cluster. The results are presented in Figure 13. As with the data on whole-mount cells, increase in cluster size with the myosin heavy chain probe was significantly greater than the control probe. Gold particle clusters of size eight or greater were only rarely observed with control probes. Of interest in this analysis is the observation that the cluster sizes are greater than that observed when hybridizing to actin mRNA, consistent with the larger template size of myosin heavy chain mRNA (2 kb vs. 5.9 kb). This data supports the probe template model discussed earlier and serves as an effective method for both qualitatively and quantitatively distinguishing signal from noise. Using this approach, one can identify hybridization to myosin heavy chain mRNA sequences with high confidence. Fig. 14 illustrates a cluster of 9 gold particles associated with a cytoskeletal filament which is within 260nm from a developing myofibril. The high degree of resolution and the precision of the quantitative results come at some cost: extensive and time consuming analysis of thin sections is required in order to obtain a statistically significant sample size.

Embryonic Tissue

We have investigated the extension of the above preembedment approach to muscle tissue from developing embryos in collaboration with Susan Billings-Gagliardi (25). Since some membrane structure was necessary to identify cellular

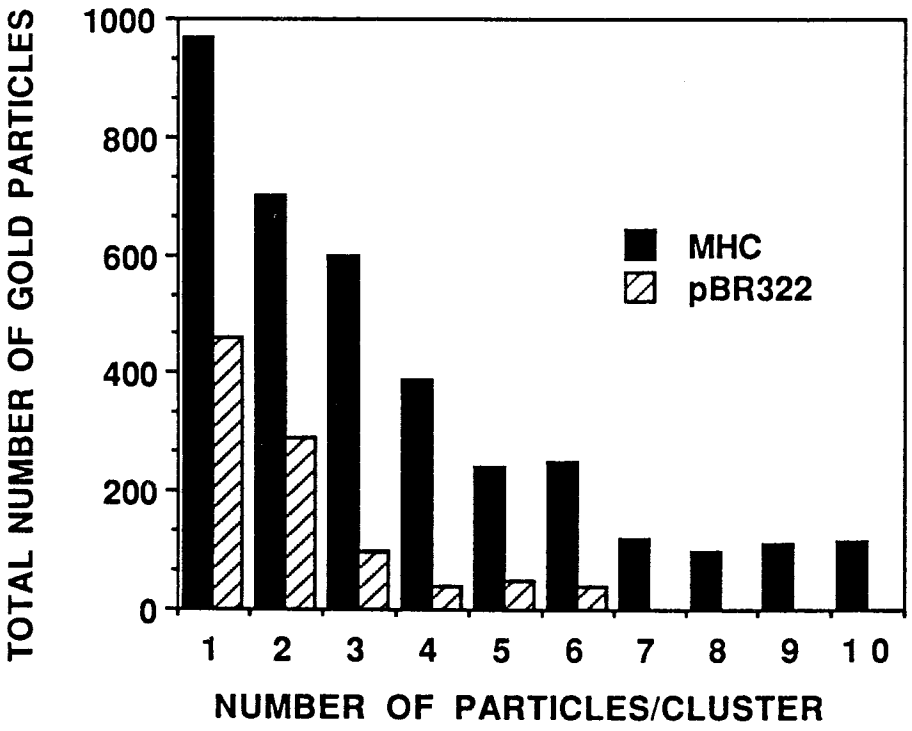

FIGURE 13: Quantitation of myosin heavy chain mRNA hybridization and detection. Histogram showing the relationship between colloidal gold particle clusters per unit area and the number of particles per cluster (17). The signal to noise ratio increased proportionately with the size of the gold particle clusters.

FIGURE 14: Myosin heavy chain mRNA-biotinated DNA hybrid (17). A full length myosin heavy chain cDNA (5.9 kb) was nick translated with biotin-11-duTP (Boehringer-Mannheim). The probe was hybridized to Triton-extracted glutaraldehyde fixed muscle cultures and detected by the immunogold procedure described in Table I. A cluster of nine colloidal gold particles can be seen associated with a nonmyofibrillar cytoskeletal filament, but within 260nm from a developing myofibril. Bar, 100nm.

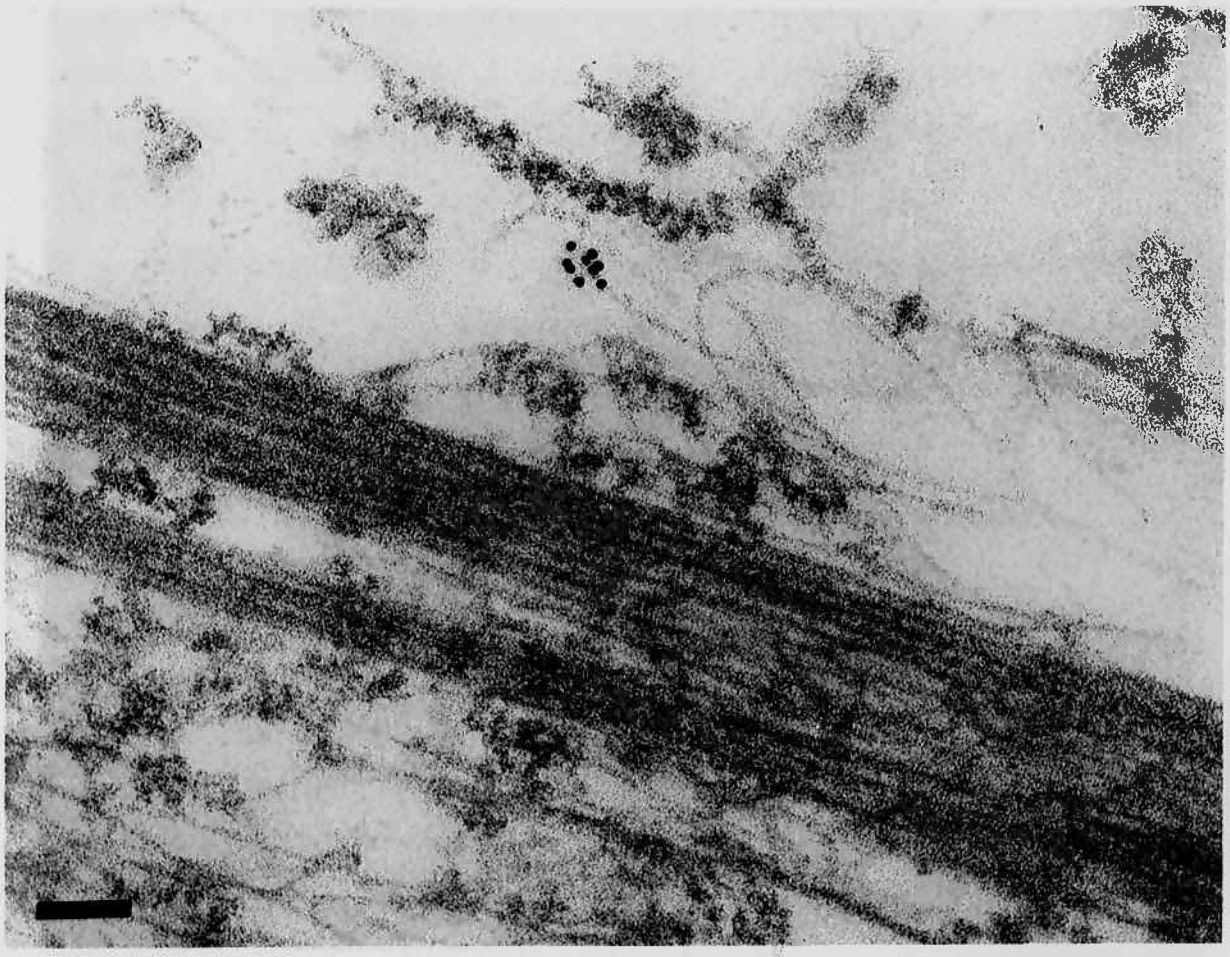

features, it was important to obtain optimal morphological information as well as significant signal to noise ratios from in vivo material. To visualize internal membranes, it was not feasible to continue using triton extraction with these samples before fixation, but some permeabilization was necessary. Therefore it was important to be able to develop an modified approach in order to obtain information by thin section.

The key features of the developed methodology include:

a) Fixation of small strips of embryonic pectoral muscle in 1% paraformaldehyde, 0.2% glutaraldehyde.

b) Permeabilization with 0.5% Triton, 0.5% Saponin before hybridization

c) Immunogold detection with longer and more concentrated antibody incubations.

Again, quantitation of gold particle clusters on thin sections represents an arduous task. Several hundred ultra-thin sections were cut from four blocks (two from MHC probe, 2 from control probe). The data from each block assessed at 20,000 X, represented $2300m^2$ of sectioned muscle tissue.

The results allowed unambiguous visualization of authentic hybridization and provided credibility for subsequent biological observations. A signal to noise ratio of 6:1 was obtained in the 1-2 particles per cluster category and increased to unmeasurably high ratios in cluster sizes of >14 particles. Figure 15 illustrates

FIGURE 15: Localization of myosin heavy chain mRNA in thin sections from 14-day chick pectoralis muscle (25). The overall morphologic appearance of tissue which was not Triton-extracted before fixation was evaluated. Bar, 2μm. The boxed area enlarged in the inset shows two clusters of 9 and 18 gold particles which are near but not apposed to myofilaments in developing sacromeres. Bar, 0-2μm.

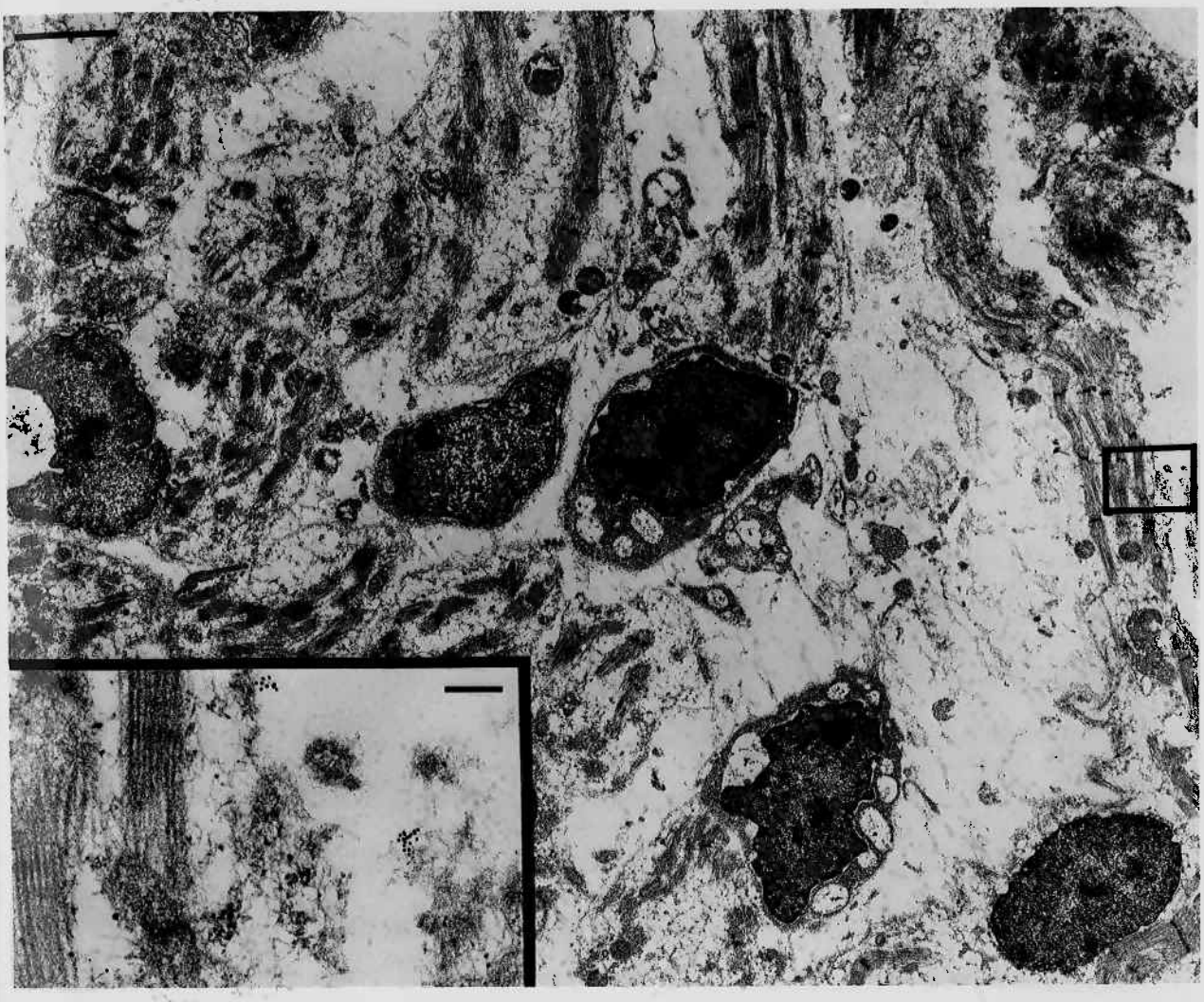

these results. It was interesting to observe that myosin heavy chain mRNA could not be detected in the cytoplasm between individual myofibrils and was frequently localized to non-myofibrillar cytoskeletal filaments of varying diameter (between 4-10 nm). This observation provided physical evidence that myosin heavy chain nascent polypeptides do not assemble directly into polymerizing myosin thick filaments but is consistent with a contranslational assembly model (57) wherein nascent chains assemble onto the cytoskeleton.

One drawback to in situ hybridization procedures at the EM level is the apparent incompatability of the protocol with the quality of morphology as seen in routine preparations. For example, in the muscle tissue experiments described above, the morphology of polysomes appeared to be adversely affected by the hybridization procedure. It remains unclear as to whether ribosomal components were perturbed (preventing optimal heavy metal staining) or solubilized and removed from the mRNA. This observation may be related to the low levels of glutaraldehyde. Nonetheless, the mRNA is expected to remain whether or not polysomes are evident (see below).

A common criticism of this kind of electron microscopic investigation, is that the results might be artifactual. Initially, electron microscopic work which utilized detergent lysis before fixation to illustrate mRNA association with the cytoskeleton was met with some controversy. After fifteen years of research it is

now generally accepted that the cytoskeleton is the cellular compartment where a significant fraction of the mRNAs reside. It is known that polysomes are associated with the cytoskeleton via mRNA (38). Release of polysomes from mRNA does not release mRNA from the cytoskeleton (38). From our own observations presented here, detergent lysis by Triton did not remove a significant fraction of either actin mRNA or myosin heavy chain mRNA. For instance, myosin heavy chain mRNA is found in the same relationship to growing myofibrils irrespective whether cells were extracted before fixation (Compare Fig. 14 with Fig. 15). Therefore the argument that polysomes or mRNA relocate as a result of detergent lysis is not supported by this data.

In summary, the possibility of generating artifactual results was given careful consideration. The data obtained was determined to reflect the actual subcellular distribution of myosin heavy chain mRNA. The objective has been to obtain optimal ultrastructural morphology while permitting superimposition of molecular information. The optimization of in situ hybridization has led to the elimination of commonly used methods (e.g. proteolytic digestion, lengthy hybridization reactions) which were detrimental to cellular morphology. The compatability of postembedment procedures for use with our model system is currently being investigated in attempt to further increase the preservation of morphologic information.

Correlation of Light and Electron Microscopy by Silver Enhancement

Introduction

As discussed previously, the high resolution of an ultrastructural approach for detection of hybridization in situ makes it impossible to view the signal at low enough magnification to survey the cell or the population of cells. The time-consuming analysis of counting hundreds of gold particles in order to obtain statistically significant signal to noise ratios can only generate observations from a few cells. Furthermore, the data from each cell represents only a small fraction of the total cellular area, and its relevance with respect to the "whole" cell is often ambiguous. Our objective was to develop an approach which could directly compare light and electron microscopic observations on the sample or even the same cell. This would have direct bearing on research or diagnostic applications of electron microscopy where quantitation of samples are of critical importance.

A number of works have utilized light microscopy to evaluate an experiment prior to electron miscroscopy (Table 1). The practicality of the light microscopic investigation in the optimization of the protocols has already been discussed. The major improvement presented here is that a single detection system is used which is compatible with both light and electron

microscopy. There are important advantages to this approach. First, the signal to noise ratio after hybridization and detection can be obtained from a large sample size where the probe staining patterns of hundreds of cells can be visualized at light microscopic magnification. Individual cells from the appropriate samples can then be viewed through a continuum of magnification after preparation by thin section or whole mount electron microscopy. In this fashion, the entire cellular complement of probe specific hybridization can be first examined, followed by investigation of specific areas of interest with higher magnification.

An in situ hybridization approach was developed using silver enhancement of colloidal gold labelled antibodies for both the light and electron microscopic detection of biotinylated DNA probes. Colloidal gold amplification by silver enhancement provides higher resolution than amplification by enzymatic methods because the silver precipitation reaction is directly bound to the hybridized probe. Silver enhancement of larger colloidal gold has been a commonly used immunocytochemical procedure at the light and electron microscopic levels (58-59), since its original description by Holgate (60) based on the photochemical method of Danscher (61). Applications for light microscopic in situ hybridization have been described (8,15,62-64). In a comparison of alternate methods for the detection of labelled DNA blotted on nitrocellulose filters, silver enhancement of colloidal gold was observed to be comparable to alkaline

phosphatase and more sensitive than peroxidase detection (8). In the same study however, silver enhanced colloidal gold exhibited lower sensitivity compared to the enzymatic methods when used with in situ hybridization. It is likely that this observation was attributable to the limited penetrability properties of large colloidal gold labelled antibody complexes (discussed earlier). To obviate this problem, we used the recently developed 1 nm gold colloid conjugated to antibodies. As discussed earlier, the larger colloidal gold reagents are complexes of several antibody molecules coating an individual gold particle. With 1nm gold an individual antibody molecule is labelled with more than one gold particle (Auroprobe-one, Janssen). This increases the number of sites for silver enhancement, improves penetrability, reduces steric hindrance, lowers the net negative charge, and hence there is a concomitant improvement in sensitivity. In commercial tests, silver enhanced 1nm labelled gold antibodies were found to compare effectively to enzymatic methods and offer improved penetrability (65-66). An interesting application by Earnshaw (67) used 1nm-colloidal gold probes to localize centromeric proteins beneath the kinetochore of heterochromatin.

Light Microscopy Results

The methodological development for the silver enhancement of colloidal gold used synthetic oligo-dT probes which were 3'-end labelled with biotin-16-dUTP using terminal transferase and

hybridized to total cellular poly-A mRNA (68). The abundant target nucleic acid sequence facilitated this development due to the strong signal. Once optimized, the procedure can be evaluated further by hybridization to less abundant sequences.

Hybridization to poly-A mRNA of cultured fibroblasts, myoblasts and myotubes was done in 15% formamide, 2XSSC for three hours with a probe concentration of 0.25 mg/ml. Due to the lower melting temperature of A:T hybrids, less stringent hybridization conditions were used than with nick-translated cDNA probes. Oligonucleotide hybridization was detected as described in Table 1, with the exception that 1nm gold labelled secondary antibody was used in place of the 10nm gold complex. Coverslips were washed thoroughly with distilled water, blotted and placed in plastic multiwell plates. Silver enhancement solution (300 ml, Janssen) was applied to oligo-dT and oligo-dA (control probe) samples. Two experimental and two control samples were used. The enhancement was observed in progress by using a 40X water immersion objective to view the samples in the plates. Visualization of a brown cellular staining indicated a positive signal and the reactions were stopped by the addition of excess water. Samples were transferred to a a clean multiwell dish and washed thoroughly with distilled water to remove any residual silver enhancement solution. Coverslips were then mounted for light microscopic photography.

FIGURE 16: Light microscopic visualization of poly A mRNA using silver enhancement of one-nanometer gold labelled antibodies. (a) hybridization to cellular poly A mRNA with biotin labelled oligo-dT probes. (b) hybridization performed with a biotinated oligo-dA control probe. Bar, 25μm.

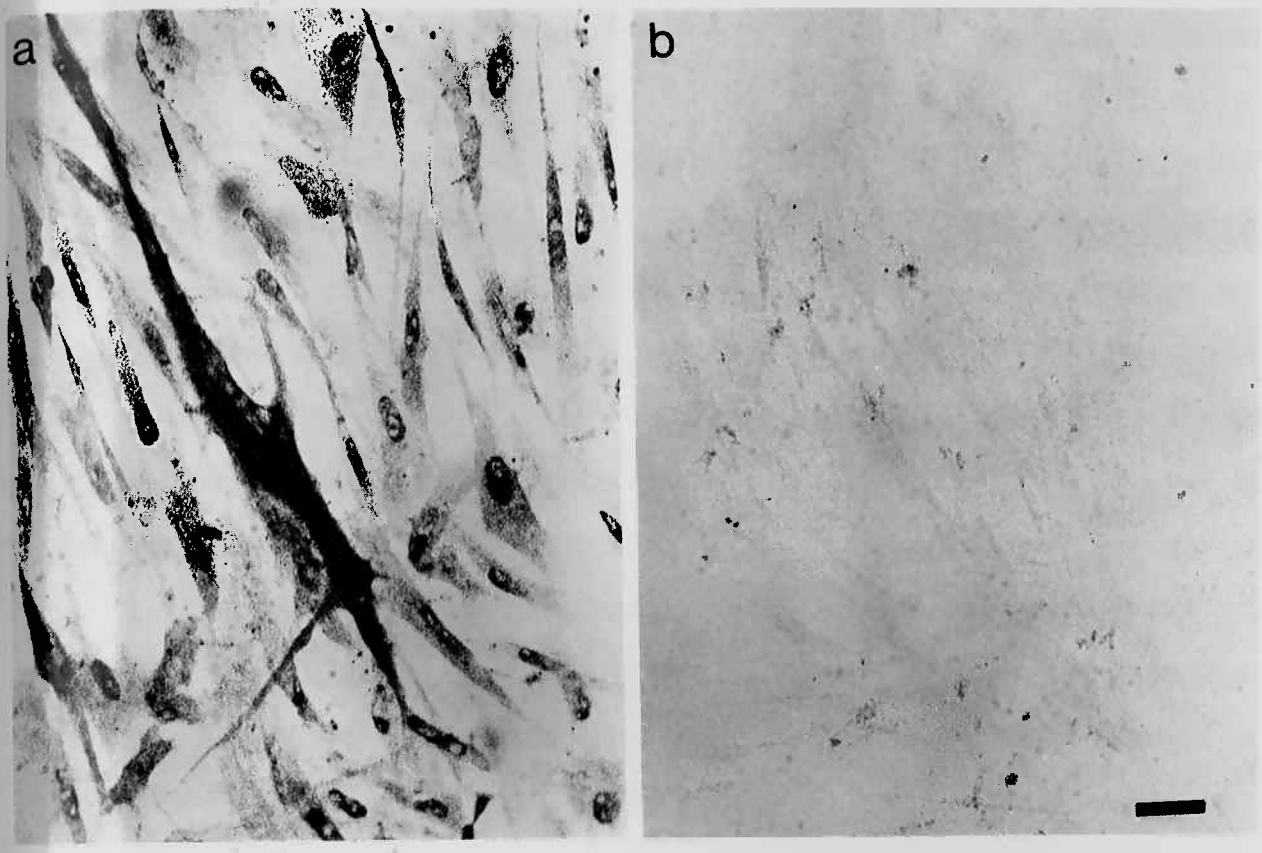
a
b

Figure 16 illustrates the results of silver enhancement after hybridization to total poly-A mRNA of Triton-extracted cultures. Strong positive staining was seen in >95% of the cells. Virtually no staining was observed with the control probe. Little variation was observed between duplicate coverslips for a visual signal to be observed. Table 2 lists the reaction times for three independent experiments utilizing three different primary cultures. Silver enhancement of one-nanometer gold exhibited improved penetrability characteristics for the detection of poly-A mRNA within nuclei of Triton-extracted cells and the cytoplasm of unextracted cells. The effect of gold particle size on the detection of poly-A mRNA in extracted and unextracted cells is shown in Figure 17. The 1nm gold labelled antibody exhibited the strongest signal for both extracted and unextracted cells. The 5nm gold-antibody complex produced an acceptable signal to noise ratio on extracted cells, but the reaction took longer and no intranuclear staining was observed. Since the nucleus is a rich source of poly A, this indicates poor penetrability of the colloidal antibody. The 5nm antibody complex failed to produce any signal on unextracted cells under the conditions employed

There are several factors which contribute to superior signal obtained by silver enhancment of 1nm colloidal gold. It is likely that the 1nm gold labelled antibody was more efficient than the 5nm gold complex in penetrating the cell, generating multiple binding sites on the primary antibody, and was less influenced by

TABLE 2. Biotin labelled (bio-16-dUTP, Boehringer Mannheim) oligo dT probes (55 nucleotides) were hybridized to three different batches of primary muscle cultures. The reaction times listed indicated the time at which maximal staining was observed with the experimental probes, prior to appearance of any background staining with control probes. Each cell batch was evaluated with duplicated coverslips which were processed for either light or electron microscopic photography.

TABLE 2: SILVER ENHANCEMENT REACTION TIMES FOR TRITON-EXTRACTED CELLS

EXPERIMENT	TIME (MINUTES)
1	**8.5, 9.0**
2	**6.2, 7.0**
3	**7.5, 8.0**

FIGURE 17: Light microscopic comparison of silver enhanced 1nm and 5nm gold labelled secondary antibodies. (a) Oligo-dT hybridization to Triton-extracted cells detected using the 1nm gold labelled secondary antibody. (b) Oligo-dT hybridization to cells not extracted before fixation detected with the 1nm gold labelled antibody. (c) Triton-extracted cells; 5nm-gold labelled secondary antibody. (d) Unextracted cells, 5nm-gold labelled antibody. Bar, 10μm.

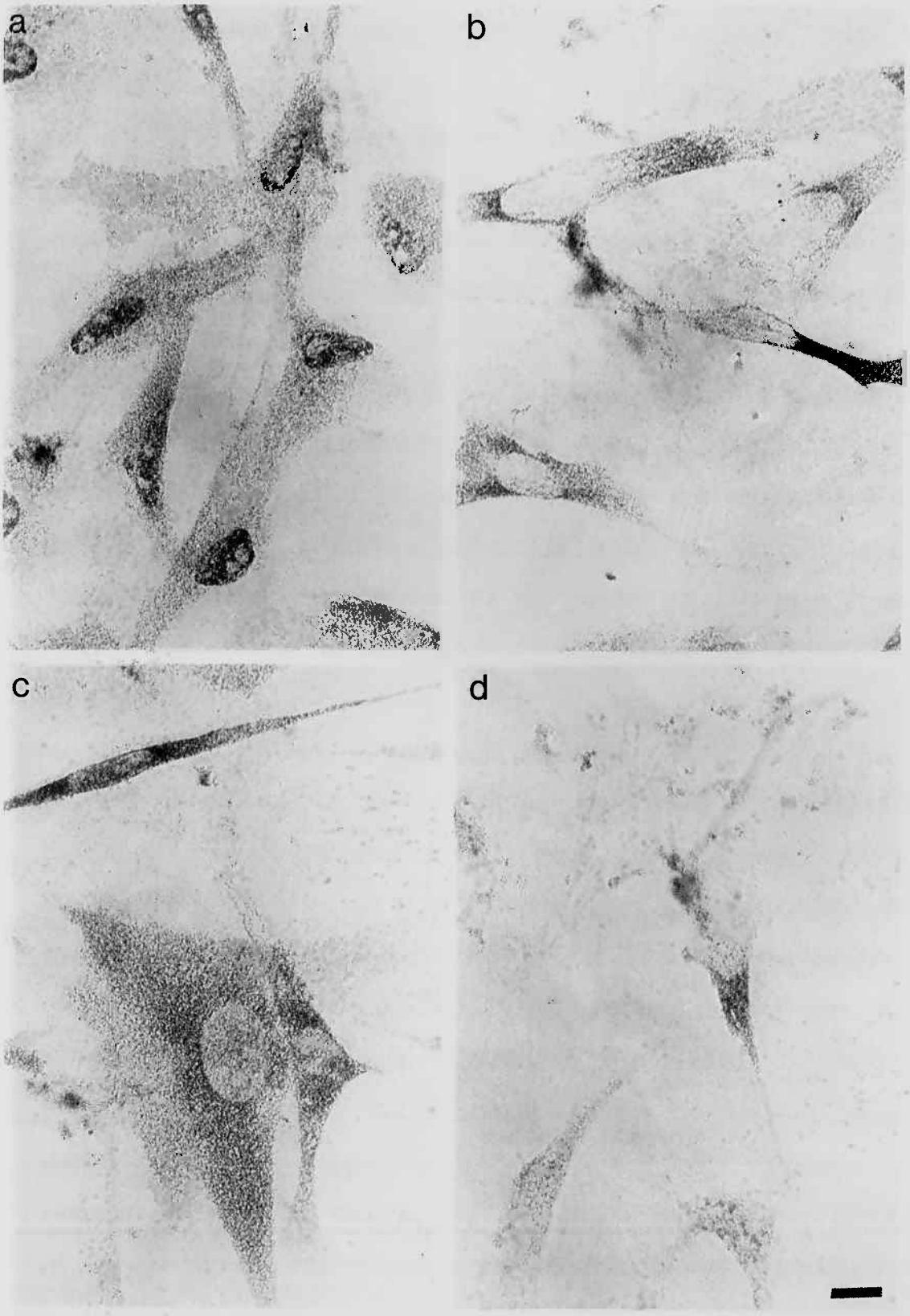
a
b
c
d

charge repulsion and steric hindrance. Furthermore, since the ratio of gold particles to secondary antibody is >1 for the one-nanometer system and <1 for the other sizes of colloidal gold, more nucleation sites exist, possibly producing further signal amplification. It may be possible to improve signal from 5nm gold antibodies by utillizing harsher experimental conditions (e.g. proteolytic digestion) but these would have deleterious effects on ultrastructural morphology. It was expected that the penetrability of larger gold complexes would not be adversely affected in Triton-extracted cells. Therefore the improved signal with 1 nm gold antibodies cannot be attributed to penetrability alone but rather must be due to the secondary factors discussed above (e.g. amplified stoichiometry, increased nucleation sites, etc.).

Electron Microscopy

Coverslips from the above samples were then embedded into Epon, sectioned and stained with heavy metals. Figures 18a&b are illustrative of thin sections from Triton-extracted cells hybridized with either oligo-dA or oligo-dT probes. The outline of the "whole" cell and its corresponding label are readily identified at the electron microscope (2000X). The ability to visualize hybridization with low magnification electron microscopy permits evaluation of the overall spatial distribution with resolution not afforded by the light microscope. At higher magnification (5000X) of the preceding thin sections, the localization of poly-A mRNA

FIGURE 18: Electron microscopic visualization of poly A mRNA at low magnification. Coverslips first evaluated at the light microscope level and determined to exhibit strong probe specific staining were embedded into Epon and sectioned. With the electron microscope, silver enhanced gold particles were visualized at 2000X. (a) A typical thin section from a control probe sample. (b) A typical thin section from the oligo-dT hybridized sample. Bar, 5µm.

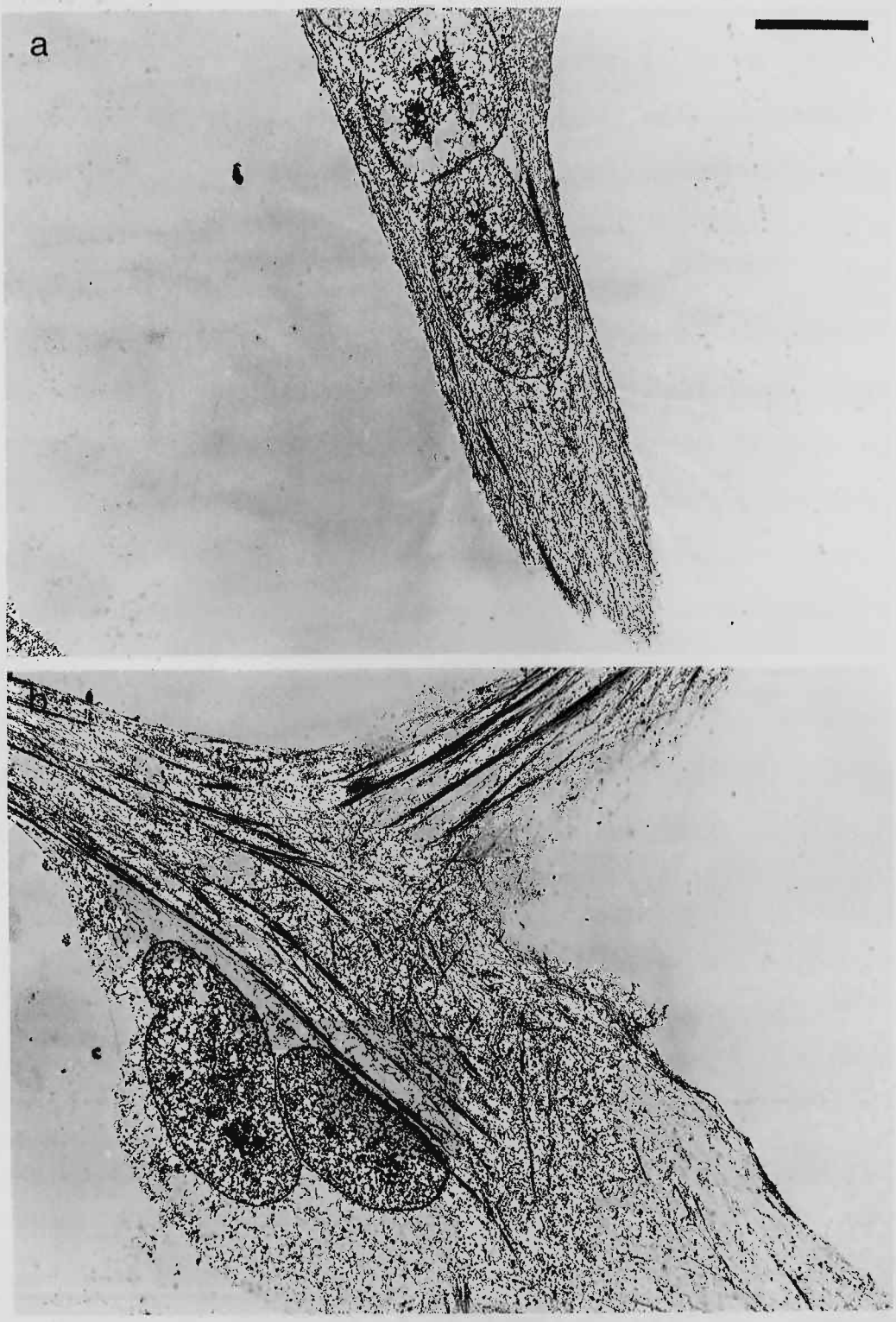
a

near developing myofibrils, on cytoskeletal filaments, and within nuclei is evident (Figure 19a-b). At even higher magnification (20,000X), hybridization can be localized with polysomes on cytoskeletal filaments (Figure 19c) and associated with a proteinaceous fibrillogranular network within the nucleus (Figure 19d).

The approach described the utilization of one-nanometer gold labelled antibodies for correlative light and electron microscopic in situ hybridization. The observations of high signal to noise ratios in hundreds of cells at the LM provides valuable support for subsequent analysis of spatial distributions of polyadenylated RNA at the single cell level using low magnification EM. Through a continuum of magnification with the electron microscope, the total cellular distribution can be assessed coordinate with its interaction with specific cellular structures. Data obtained by this approach has the advantage of proceding from general to more specific observations, (e.g. from cell populations to specific high resolution areas of a single cell.)

CONCLUDING REMARKS

In situ hybridization techniques for electron microscopy provide a powerful approach for investigating the spatial organization of nucleic acids in single cells at high resolution. Our emphasis on the detection of specific sequences has implications

FIGURE 19: Electron microscopic visualization of poly A mRNA at higher magnifications. The thin sections represented in Figure 10 were photographed at 5000X (Bar, 1μm). (a) Control hybridization with the oligo-dA probe. (b) Hybridization to poly A mRNA with the oligo-dT probe. Label is localized to the nonmyofibrillar cytoskeleton. (c) Higher magnification showing the colocalization of poly A mRNA with polysomes. Bar, 0.5mm. (d) Intranuclear localization. Bar, 0.5mm.

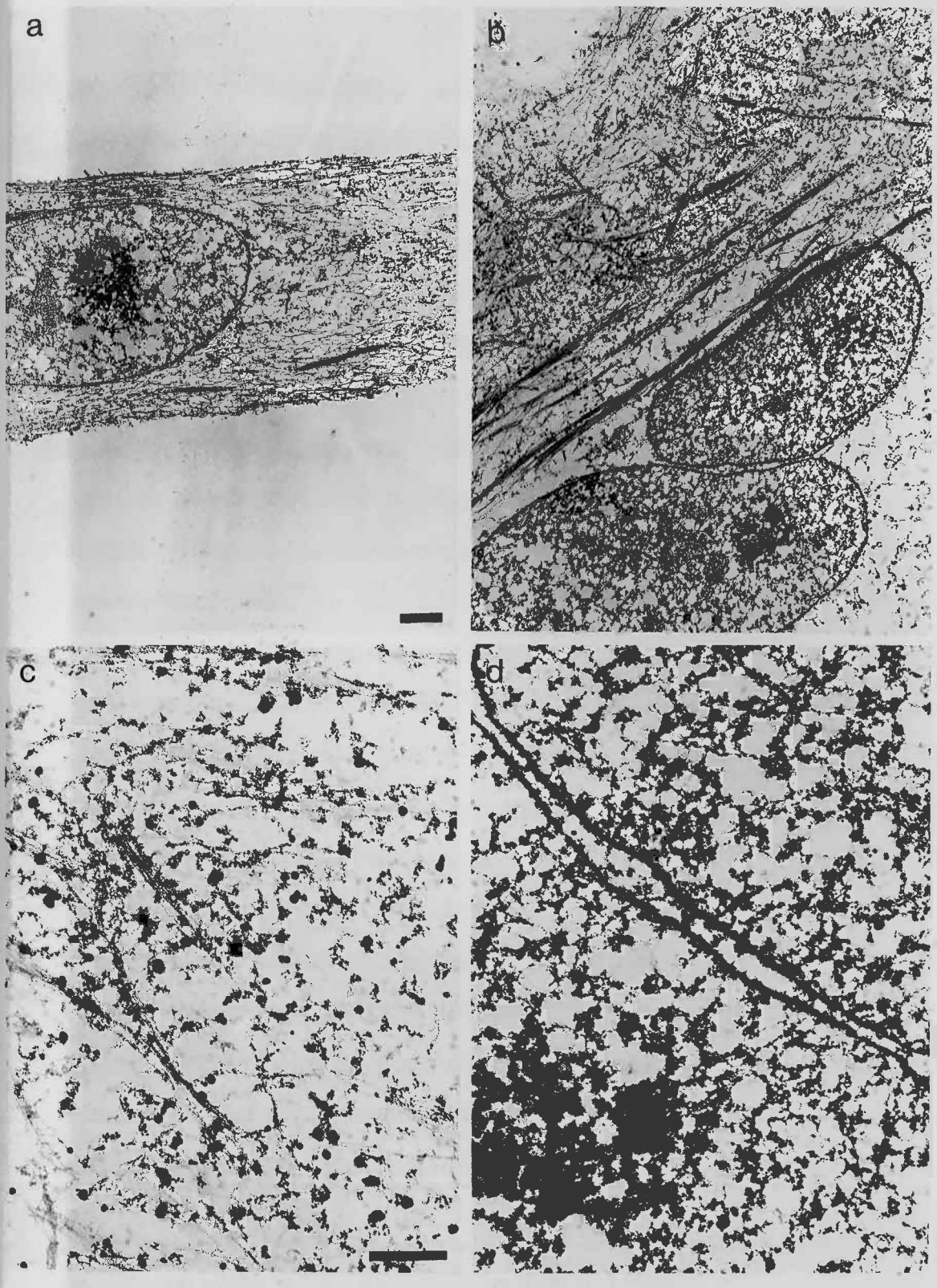
a
b
c
d

for a wide range of research interests. Any nucleic acid sequence whether endogenous or viral, RNA or DNA, is available to this approach. Historically, viral model systems such as poliovirus (40) and adenovirus (69), showed that the preferential expression of viral genes could be attributed to the replacement of host mRNAs by viral mRNAs on the cytoskeleton. These studies suggested that the cytoskeleton may play an important role in the translational regulation of endogenous mRNAs.

It is anticipated that the use of silver enhancement to interface both light and electron microscopic observations will have a broad range of applications toward virology. An example of the technical sophistication provide by this approah is evident from recent work in our laboratory on the subcellular localization of HIV RNA. At the light microscopic level using fluorescence in situ hybridization, the HIV RNA was localized intranuclearly in a punctate pattern (Lawrence et al, 1990). Cytoplasmic label did not exhibit any evidence of a nonuniform mRNA distribution. This observation was consistently observed with several light microscopic detection methods, including silver enhancement. Figure 20 illustrates cytoplasmic detection of HIV mRNA using silver enhancement at the ultrastructural level. Interestingly, HIV RNA appeared associated with mitochondria. This is the first evidence for a relationship between HIV infection and mitochondria. The biological significance of this observation is

FIGURE 20: Mitochondrial localization of HIV using in situ hybridization and silver enhancement detection for electron microscopy. Cultured T-lymphocytes were HIV infected and fixed at 48hrs. Biotinated HIV DNA probe (8.9 Kb genomic clone) was hybridized to nondenatured cells and detected using antibiotin and gold labeled secondary antibodies. Silver enhancement reaction was followed with a water immersion objective and stopped at 6 minutes. Strong cellular staining was observed with the HIV probe. Parallel control botin labeled pBR322 probes showed no staining. Samples were processed for thin sectioning. Silver particles are observed associated with mitochondria (arrow).

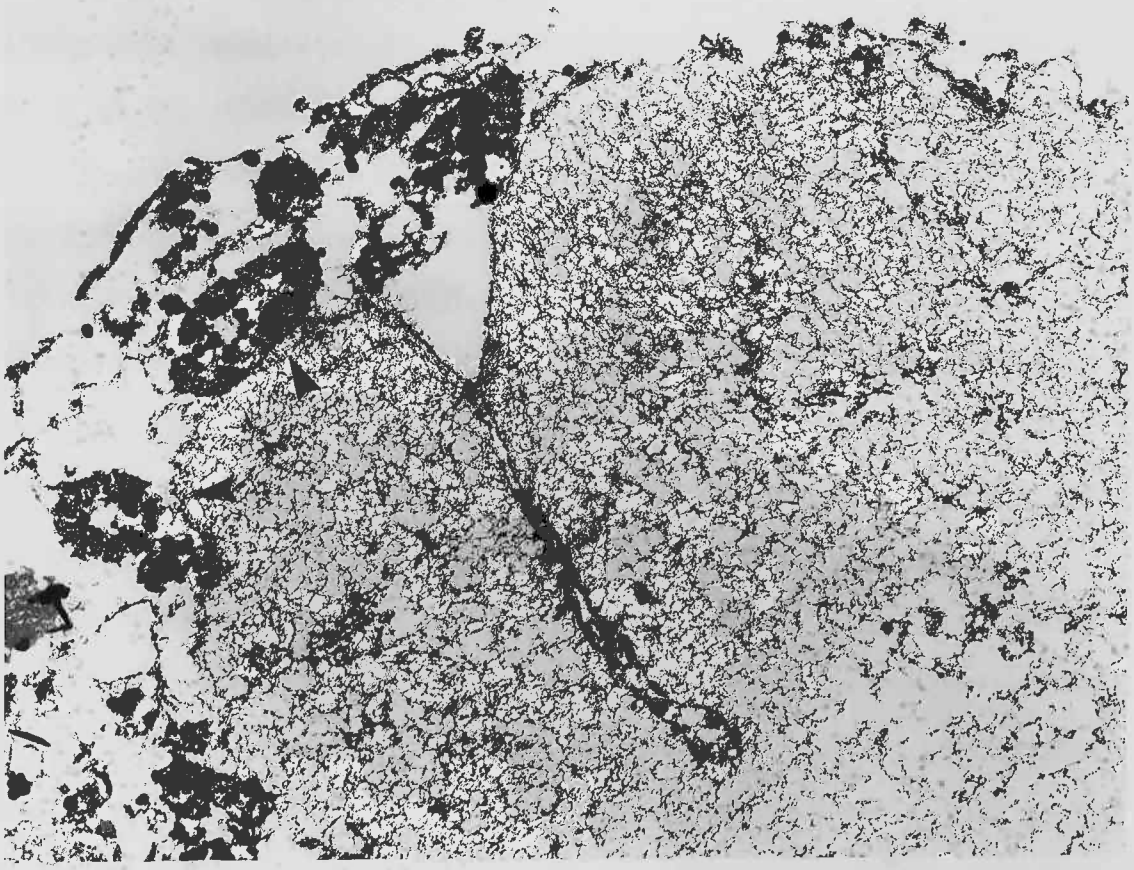

unknown, and this relationship needs to be further clarified. The observation is presented here as an example of biological information obtained by ultrastructural in situ hybridization which is not revealed by light microscopy.

Future directions for electron microscopic visualization of in situ hybrids will continue to intertwine methodology development with biological observations. One step will likely be toward detection of less abundant sequences. Much of the work done in the field to date has been with abundant target nucleic acid sequences as evident from the reports cited in Table 1. We are currently developing a high sensitivity in situ transcription technique (70) for use with electron microscopy. Another area of focus will be toward double labelling techniques which permit the simultaneous visualization of two nucleic acid sequences. Hamkalo (71-72) has recently described a gene mapping technique with biotin and acetylaminofluorene (AAF) labelled DNA probes. McFadden as well as ourselves have developed a method for the detection of digoxigenin (Boehringer Mannheim) labelled DNA probes with colloidal gold (73). The approach described here will make available the power of the electron microscope to dissect out molecular events under high resolution. It is hoped that further technological contributions from a number of laboratories will reveal heretofore unanticipated cellular and molecular relationships.

REFERENCES

1. Wu, M. and Davidson, N. Transmission electron microscopic method for gene mapping on polytene chromosomes by in situ hybridization. PNAS 78, 7059-7063, 1981.
2. Hutchinson, N.J., Langer, P.R., Ward, D.C. and Hamkalo, B.A. In situ hybridization at the electron microscope level: Hybrid detection by autoradiography and colloidal gold. J. Cell Biol. 95, 609-618, 1982.
3. Manuelidis, L., Langer-Safer, P.R. and Ward, D.C. High resolution mapping of satellite DNA using biotin labelled DNA probes. J. Cell Biol. 95, 619-625, 1982.
4. Fostel, J., Narayanswami, S., Hamkalo, B., Clarkson, S.G. and Pardue, M.L. Chromosomal location of a major tRNA gene cluster. Chromosoma 90, 254-260, 1984.
5. Manuelidis, L. Different CNS cell types display distinct and nonrandom arrangements of satellite DNA. PNAS 81, 3123-3127, 1984.
6. Manuelidis, L. and Ward, D.C. Chromosomal and nuclear distribution of the hind III 1.9 kb human DNA repeat segment. Chromosoma 91, 28-38, 1984.

7. Cremers, A.F., Luderus, E.M. Gene localization on human metaphase chromosomes with TEM. Ultramicroscopy 15, 397-405, 1984.

8. Cremers, A.F. de Wal, N.J., Wiegant, J., Dirks, R.W., Weisbeek, P., VanderPloeg, M. and Landegent, J.E. Non-radioactive in situ hybridization: A comparison of several immunocytochemical detection systems using reflection contrast and electron microscopy. Histochemistry 86, 609-615, 1987.

9. Kress, H., Meyerowitz, E.M. and Davidson, N. High resolution mapping of in situ hybridized biotinylated DNA to surface-spread Drosophila polytene chromosomes. Chromosoma 93, 113-122, 1985.

10. Ferguson, D.J., Burns, J., Harrison, D., Jonasson, J.A. and McGee, J.O. Chromosomal localization of genes by scanning EM using in situ hybridization with biotinylated probes: Y chromosome repetitive sequences. Histochem. J. 18, 266, 1986.

11. Radic, M.Z., Lundgren, K. and Hamkalo, B.A. Curvature of mouse satellite DNA and condensation of heterochromatin. Cell 50, 1101-1108, 1987.

12. McFadden, G.I., Bonig, I., Cornish, E.C. and Clarke, A.E. A simple fixation and embeding method for use in hybridization histochemistry of plant tissues. Histochemical J. 20, 575-586, 1988.

13. McFadden, G.I. In situ hybridization in plants: From macroscopic to ultrastructural resolution. Cell Biology International Reports 13, 3-21, 1989.

14. McFadden, G.I. Evidence that cryptomonad chloroplasts evolved from photosynthetic eukaryotic endosymbionts. J. Cell Biol. 95, 303-308, 1990.

15. Binder, M., Tourmente, S., Roth, J., Ren, M. and Gehring, W.J. In situ hybridization at the electron microscope level: Localization of transcripts on ultrathin sections of Lowicryl K4M-embedded tissue using biotinylated probes and protein-A gold complexes. J. Cell Biol. 102, 1646-1653, 1986.

16. Singer, R.H., Langevin, G.L. and Lawrence, J.B. Ultrastructural visualization of cytoskeletal mRNAs and their associated proteins using double-label in situ hybridization. J. Cell Biol. 108, 2343-2353, 1989.

17. Silva, F.G., Lawrence, J.B. and Singer, R.H. Progress toward ultrastructural identification of individual mRNAs in thin section: myosin heavy chain mRNA in developing myotubes. In: Techniques in Immunocytochemistry, Vol. 4, G. Bullock and P. Petrusz (eds.), 147-165, 1989.

18. Singer, R.H., Lawrence, J.B., Silva, F., Langevin, G.L., Pomeroy, M. and Billings-Gagliardi, S. Strategies for ultrastructural visualization of biotinated probes hybridized to messenger RNA in situ. In: Current Topics in Microbiology and

Immunology-In Situ Hybridization. A.T. Haase and M.B. Oldstones (eds), 55-69, 1989.

19. Wobler, R.A., Beals, T.F. and Maassab, H.F. Ultrastructural localization of herpes simplex virus RNA by in situ hybridization. J. Histo. Cyto. 37, 97-104, 1989.

20. Puvion, D.F. and Puvion, E. Ultrastructural localization of viral DNA in thin sections of herpes simplex virus type 1 infected cells by in situ hybridization. Eur. J. Cell Biol. 49, 99-109, 1989.

21. Langer, P.R., Waldrop, A. and Ward, D.C. Enzymatic synthesis of biotin-labeled polynucleotides: novel nucleic acid affinity probes. PNAS 78, 6633-6637, 1981.

22. Langer, P.R., Levine, M. and Ward, D.C. An immunological method for mapping genes on Drosophila polytene chromosomes. PNAS 79, 4381-4385, 1982.

23. Singer, R.H. and Ward, D.C. Actin gene expression visualized in chicken muscle tissue cultures by using in situ hybridization with a biotinated nucleotide analog. PNAS 79, 7331-7335, 1982.

24. Webster, H.F., Lamperth, L., Favilla, J.T., Lamke, G., Tesi, D. and Manuelidis, L. Use of a biotinylated probe and in situ hybridization for light and EM localization of Po mRNA in myelin forming Schwann cells. Histochemistry 86, 441-444, 1987.

25. Pomeroy, M.E., Lawrence, J.B., Singer, R.H. and Billings-Gagliardi, S. Electron microscopic localization of myosin heavy chain mRNA in embryonic muscle tissue. Dev. Biol., in press.

26. Thiry, M. and Thiry-Blaise, L. In situ hybridization at the EM level: an improved method for precise localization of ribosomal DNA and RNA. Eur. J. of Cell Biol. 50, 325-243, 1989.

27. Lawrence, J.B. and Singer, R.H. Intracellular localization of mRNA for cytoskeletal proteins. Cell 45, 407-415, 1986.

28. Taneja, K.L. and Singer, R.H. Detection and localization of actin mRNA isoforms in chicken muscle cells by in situ hybridization using biotinated oligonucleotide probes. J. Cellular Biochem. 44, 1-12, 1990.

29. Sundell, C.L. and Singer, R.H. Actin mRNA localizes in the absence of protein synthesis. J. Cell Biol., in press.

30. Colman, D.R., Kreibich, G., Frey, A.B., Sabatini, D.D. Synthesis and incorporation of myelin polypeptides into CNS myelin. J. Cell Biol. 95, 598-608, 1982.

31. Trapp, B.D., Moench, T., Pulley, M., Barbosa, E., Tennekoon, G., and Griffin, J. Spatial segregation of mRNA encoding myelin specific proteins. PNAS 84, 7773-7777, 1987.

32. Garner, C.C., Tucker, R.P. and Matus, A. Selective localization of mRNA for cytoskeletal protein MAP2 in dendrites. Nature 336, 674-677, 1988.

33. Fontaine, B., Sassoon, D., Buckingham, M. and Changeux, J.P. Detection of the nicotinic acetylcholine receptor subunit mRNA by in situ hybridization at neuromuscular junctions of 15-day-old chick striated muscles. EMBO J. 7, 603-609, 1988.

34. Jeffrey, W.R., Tomlinson, C.R. and Brodeur, R.D. Localization of actin mRNA during early ascidian development. Dev. Biol. 99, 408-417, 1983.

35. Jeffrey, W.R. Spatial distribution of mRNA in the cytoskeletal framework of Ascidian eggs. Dev. Biol. 103:482-492, 1984.

36. Rebagliati, M.R., Weeks, D.L., Harvey, R.P. and Melton, D.A. Identification and cloning of localized maternal mRNAs from Xenopus eggs. Cell 42, 769-777, 1985.

37. Frigerio, G., Burri, M., Bopp, D., Baumgartner, S. and Noll, M. Structure of the segmentation gene paired and the Drosophila PRD gene set as part of a gene network. Cell 47, 735-746, 1986.

38. Lenk, R., Ransom, L., Kaufmann, Y. and Penman, S. A cytoskeletal structure with associated polyribosomes obtained from HeLa cells. Cell 10, 67-78, 1977.

39. Farmer, S.R., Ben-Zeev, A., Benecke, B.J. and Penman, S. Altered translatability of mRNA from suspended anchorage-dependent fibroblasts: reversal on cell attachment to a surface. Cell 15, 627-637, 1978.

40. Lenk, R. and Penman, S. The cytoskeletal framework and poliovirus metabolism. Cell 16, 289-301, 1979.

41. Fulton, A.B., Wan, K.W. and Penman, S. The spatial distribution of polyribosomes in 3T3 cells and the associated assembly of proteins into the skeletal framework. Cell 20, 849-857, 1980.

42. Cervera, M., Dreyfuss, G. and Penman, S. mRNA is translated when associated with the cytoskeletal framework in normal and VSV-infected HeLa cells. Cell 23, 113-120, 1981.

43. Lawrence, J.B. and Singer, R.H. Quantitative analysis of in situ hybridization methods for the detection of actin gene expression. Nuc. Acids Res. 13, 1777-1799, 1985.

44. Singer, R.H., Lawrence, J.B. and Villnave, C. Optimization of in situ hybridization using isotopic and non-isotopic detection methods. Biotechniques 4, 230-250, 1986.

45. Brigati, D.J., Myerson, D., Leary, J.J., Spolholz, B., Travis, S.Z., Fong, C.K.Y., Hsiung, G.D. and Ward, D.C. Detection of viral genomes in cultured cells and paraffin embedded tissue sections using biotin labelled hybridization probes. Virology 126, 32-50, 1983.

46. Unger, E.R., Budgeon, H.T., Myerson, D. and Brigati, D.J. Viral diagnosis by in situ hybridization. Am. J. Surg. Path. 10, 1-8, 1986.

47. Lawrence, J.B., Villnave, C.A. and Singer, R.H. Sensitive high resolution chromatin and chromosome mapping in situ:

presence and orientation of two closely integrated copies of EBV in a lymphoma cell line. Cell 52, 51-61, 1988.

48. Lawrence, J.B., Singer, R.H. and Marselle, L.M. Highly localized tracks of specific transcripts within interphase nuclei visualized by in situ hybridization. Cell 57, 493-502, 1989.

49. Verkleij, A.J. and Leunissen, J.L.M. (eds.) Immuno-gold labeling in cell biology. CRC Press, 1989.

50. Hayat, M.. (ed.) Colloidal gold: principles, methods and applications. Volumes I & II. Academic Press, 1989.

51. McFadden, G.I. In situ hybridization techniques for electron microscopy: molecular cytology goes ultrstructural. In: Electron Microscopy of Plant Cells. J.L. Hall and C.J. Hawes (eds.). Academic Press, pp.1-38, 1990.

52. Leary, J.J., Brigati, D.J. and Ward, D.C. Rapid and sensitive colorimetric method for visualizing biotin-labelled DNA probes hybridized to DNA or RNA immobilized on nitrocellulose: Bio-blots. PNAS 80, 4045-4049, 1983.

53. Romano, E.L. and Romano, M. Protein-A bound to colloidal gold: A useful reagent to label antigen-antibody sites in EM. Immunochem. 14, 711-718, 1977.

54. Kehle, T. and Herzog, V. Interactions between protein-gold complexes and cell surfaces: A method for precise quantitation. Euro. J. Cell Biol. 45, 80-85, 1987.

55. Gebeyehu, G., Rao, P.Y. Soo Chan, P., Simms, D.A. and Klevan, L. Novel biotinylated nucleotide-analogs for labeling and

colorimetric detection of DNA. Nuc. Acids Res. 15, 4513-4534, 1987.

56. Lawrence, J.B., Taneja, K.L. and Singer, R.H. Temporal resolution and sequential expression of muscle-specific genes revealed by in situ hybridization. Dev. Biol. 133, 235-246, 1989.

57. Isaacs, W.B. and Fulton, A.B. Cotranslational assembly of myosin heavy chain in developing cultured skeletal muscle. PNAS 84, 6174-6178, 1987.

58. Scopsi, L. Silver-enhanced colloidal gold method. In: Colloidal Gold: Principles, Methods and Applications. Volume I. M.A. Hayat (eds.). Academic Press, Inc., pp.252-290, 1989.

59. Hacker, G.W. Silver-enhanced colloidal gold for light microscopy. In: Colloidal Gold-Principles, Methods and Applications. Volume I. M.A. Hayat (eds.). Academic Press, Inc., pp.300-318, 1989.

60. Holgate, C.S., Jackson, P., Cowen, P.N. and Bird, C.C. Immunogold-Silver staining: New method of immunostaining with enhanced sensitivity. J. Histochem. Cytochem. 31, 938-944, 1983.

61. Danscher, G. Localization of gold in biological tissue: A photochemical method for light and electron microscopy. Histochem. 71, 81-88, 1981.

62. Liesi, P., Julien, J.P., Vilja, P., Grosveld, F. and Rechardt, L. Specific detection of neuronal cell bodies: in situ hybridization with a biotinated neurofilament cDNA probe. J. Histochem. 34, 923-926, 1986.

63. Jackson, P., Lewis, F.A. and Wells, M. In situ hybridization technique using an immunogold silver staining system. Histochem. J. 21, 425-428, 1989.

64. VandenBrink, W., VanderLoos, C., Volkers, H., Lauwen, R., VandenBerg, F., Houthoff, H. and Das, P. Combined α-galactosidase and immunogold/silver staining for immunohistochemistry and DNA in situ hybridization. J. Histochem. 38, 325-329, 1990.

65. Leunissen, J.L.M., van de Plas, P.F. and Borghgraef, P.E. Auroprobe-one: A new and universal ultra small gold particle based immunodetection system for high-sensitivity and improved penetration. Janssen Life Science Products, Aurofile No. 2.

66. Volkers, H.H., van de Brink, W.J., Leunissen, J.L.M., DeBrabander, M., Zijlmans, H.J., Houthoff, H.J. and van den Berg, F.M. DNA in situ hybridization: towards a routine technique-new developments in detection methods using Auroprobe-one. Janssen Life Science Products. Aurofile No. 3.

67. Cooke, C.A., Bernat, R.L. and Earnshaw, W.C. CENP-B: A major human centromere protein located beneath the kinetochore. J. Cell Biol. 110, 1475-1488, 1990.

68. Bassell, G.J., Powers, C.M., Lawrence, J.B., Taneja, K.L. and Singer, R.H. Spatial organization of poly A mRNA on the fibroblast cytoskeleton. Submitted for publication.

69. van Venrooij, W., Sillekens, P., van Eekelene, A. and Reinders, R. On the association of mRNA with the cytoskeleton in uninfected and adenovirus-infected human KB cells. Exp. Cell Res. 135, 79-91, 1981.

70. Tecott, L.H., Barchas, J. and Eberwine, J.H. In situ transcription: specific synthesis of cDNA in fixed tissue sections. Science 240, 1661-1664, 1988.

71. Hamkalo, B.A., Narayanswami, S. and Lundgren, K. Localization of nucleic acid sequences by EM in situ hybridization using colloidal gold labels. Am. J. Anat. 185, 197-204, 1989.

72. Narayanswami, S. and Hankalo, B.A. High resolution mapping of Xenopus laevis 5S and ribosomal RNA genes by EM in situ hybridization. Cytometry 11, 144-152, 1990.

73. McFadden, G., Bonig, I. and Clarke, A. Double label in situ hybridization for electron microscopy. Transactions of the Royal Microscopy Society, in press.

CHAPTER IV

SPATIAL COMPARTMENTALIZATION OF POLY(A) mRNA WITHIN THE CYTOSKELETON VISUALIZED BY ULTRASTRUCTURAL IN SITU HYBRIDIZATION

INTRODUCTION

A cell contains thousands of proteins organized into highly complex structures reflecting specific cellular functions. A major challenge of cell biology is to understand the organizational principles by which newly synthesized proteins are targetted intracellularly and assembled into these macromolecular complexes. Several reports have observed that the synthesis of specific proteins can be localized to discrete cellular regions by localization of their corresponding mRNAs (Lawrence and Singer, 1986; Taneja and Singer, 1990; Sundell and Singer, 1991; Colman et al., 1982; Trapp et al., 1987; Garner et al., 1988; Fontaine et al., 1988; Jeffrey et al., 1983; Jeffrey, 1984; Rebagliati et al., 1985; Frigerio et al., 1986). Analogous to protein sorting which occurs by recognition of peptide sequences (Sabatini et al., 1982; Schatz and Butow, 1983; Walter et al., 1984), mRNA sorting occurs by recognition of nucleic acid sequences (Macdonald et al., 1988). The ability of a cell to sort and target mRNAs may add a new

dimension to the regulation of gene expression, since the positioning of specific mRNAs within a cell could promote the localized synthesis of proteins near their sites of function and hence directly influence cellular organization (Lawrence and Singer, 1986; Trapp et al., 1987; Garner et al., 1988; Fontaine et al., 1988).

The ability of a cell to localize mRNA may depend on internal cellular structures which would anchor mRNAs at specific locations. mRNA has been shown to be associated with the cytoskeleton (Lenk et al., 1977; Fulton et al., 1980; Jeffrey, 1982; Adams et al., 1983; Zambetti et al., 1985) and this may play a role in its translation (Farmer et al., 1978; Lenk and Penman, 1979; Cervera et al., 1981; Venrooij et al., 1981; Ben-Ze'Ev et al., 1981; Bonneau et al., 1985; Ornelles et al., 1986). It is likely that the cytoskeleton is involved in the mechanism which localizes mRNAs to discrete cellular regions (Singer et al., 1989; Yisraeli et al., 1990; Sundell and Singer, 1991; Pokrywka and Stephenson, 1991). It has been proposed that mRNA localization involves a two-step process (Yisraeli et al., 1990) (1) the movement of a newly synthesized mRNA from its entrance into the cytoplasm to its region of localization, and (2) the subsequent anchoring of that mRNA to prevent its diffusion. In Xenopus oocytes, the targeting of veg-1 mRNA to the vegetal pole required intact microtubules; whereas the attachment of veg-1 mRNA within the vegetal pole could be disrupted by microfilament depolymerization (Yisraeli et

al., 1990). By contrast, in our laboratory actin mRNA localization to the fibroblast lamella required only intact microfilaments (Sundell and Singer, 1991). These data from different systems suggest that mRNA can be associated within different cytoskeletal compartments. Is the localization of mRNAs to different cellular regions within an individual cell mediated by different filament systems, or can mRNAs be localized to different regions of an individual filament system?

The identification of the filament systems involved in the attachment of mRNAs to the cytoskeleton has been through biochemical approaches, utilizing drugs to perturb filament system(s), and comparing the relative amounts of mRNA in soluble and cytoskeletal cell fractions. A number of studies have provided conflicting results. Using the actin depolymerizing drug cytochalasin, some studies have demonstrated release of polysomal RNA from the cytoskeleton (Lenk et al., 1977; Ornelles et al., 1986). In other cytochalasin studies, the majority of mRNA was found not associated with actin (Raemakers et al., 1983; Bagchi et al., 1987). The association of actin mRNAs with the cytoskeleton was shown to be dependent (Bird and Sells, 1986) and independent (Jeffrey et al., 1986) of actin. Similarly contradictory findings have been shown for histone mRNAs (Bird and Sells, 1986; Zambetti et al., 1985). Fluorescence detection to analyze the intracellular distribution of cap binding protein indicated an overlap with an intermediate filament network

(Zumbe et al., 1982). It is impossible however with the level of resolution provided by LM (0.2 μ) to determine that cap binding protein was directly associated with intermediate filaments.

The most direct approach to study the association of mRNA with the cytoskeletal framework is to visualize it at the ultrastructural level. The high resolution provided by the EM (0.3nm) would allow mRNA molecules to be unequivocally proximated to individual filaments. Toward this goal, we have developed improved in situ hybridization approaches for electron microscopy (Singer et al., 1989a; Silva et al., 1989; Singer et al., 1989b; Pomeroy et al., 1991; Bassell and Singer, in press). We have evaluated the association of actin, vimentin and tubulin mRNA with the cytoskeleton using EM (Singer et al., 1989a). However, there were important motivations to expand these observations to include the total complement of cellular mRNA. First, in the previous study, microfilaments appeared to be solely involved in the attachment of mRNA to the cytoskeleton. However, since only three mRNA species were evaluated, this did not adequately test the hypothesis that multiple filament systems are involved in anchoring mRNA on to the cytoskeleton. Since most eukaryotic mRNAs are polyadenylated (Sheiness and Darnell, 1973; Brawerman, 1981), this served as a convenient sequence to probe, permitting observations of a more general significance to cellular mRNA, and allowing the relative involvement of each filament system to be evaluated. Another advantage to

visualizing poly(A) mRNA is to understand how mRNA molecules are positioned with respect to each other within the cytoskeleton. These observations are important toward ellucidating mechanisms whereby functionally related protein synthesis could be spatially controlled. Lastly, recent work in the laboratory has indicated that the poly(A) sequence itself is involved in the mechanism of mRNA attachment to the cytoskeleton (Taneja, in preparation), therefore, it was of interest to investigate this direct relationship ultrastructurally.

The above goals required further advances in the in situ hybridization/EM technology which permitted ultrastructural detection of poly(A) mRNA attachment sites with resolution concomitant with the visualization of polysomes and labelled cytoskeletal filaments. Furthermore, by using 1nm gold conjugated antibodies, we have been able to evaluate the distribution of total poly(A) mRNA within unextracted cells, in addition to whole mount preparations. The application of this high resolution in situ hybridization technology illustrated that the distribution of poly(A) mRNA was not homogeneously distributed on the cytoskeleton, or on one filament system. In contrast, the distribution was observed to be compartmentalized at several levels, exhibiting specific interactions with different cytoskeletal proteins and structures. Poly(A) was principally localized to the actin cytoskeleton, but was not uniformly distributed; and localized primarily to microfilament intersections

colocalizing with the actin binding proteins, filamin and α-actinin. Specific associations of poly(A) were also observed with intermediate filaments. This data taken together with our previous work permit the formulation of a model to describe localized mRNA distributions within the cytoskeletal framework.

RESULTS

Methodological Considerations

This work required the development of several novel detection methods for in situ hybrids, the salient features of which are summarized below. Procedures were developed to obtain first light and then electron microscopic observations on the same sample, using a single detection methodology. One-nanometer colloidal gold labelled antibodies were used for the detection of biotinated probes hybridized in situ followed by silver enhancement of the signal. Use of the 1nm gold antibodies allowed effective penetration of the intact cell and permitted comparison to Triton-extracted cells. The distribution of morphologically identifiable polysomes with respect to poly(A) mRNA and labelled cytoskeletal filament systems was evaluated at the ultrastructural level in thin sections. The ability to visualize polysomes concomitant with hybridization indicates that the hybridization conditions have not adversely affected the translational apparatus, provides information on the translational

status of hybridized mRNA molecules, and allows the study of spatial relationships between poly(A) mRNA, the cytoskeleton and the polysome.

Double labelling methods allowed characterization of specific proteins involved in the attaching of mRNPs to the cytoskeleton. The identification of the cytoskeletal filament system(s) associated with poly(A) required several improvements in the existing methodology. Previous protocols followed a 3 hr. hybridization in 50% formamide, and monoclonal antibody labelling was sparse and did not uniformly decorate microfilaments or intermediate filaments. A statistical analysis was performed where the proximity of poly(A) (10nm gold particles) was assessed with respect to anticytoskeletal antibodies (5nm gold particles). With this approach it was possible to conclude that mRNAs were likely to be close (within 5nm) to actin protein. Our objective was to improve the CSK labelling such that mRNA- filament associations could be directly visualized.

The use of silver enhancement of 1nm gold labelled antibodies allowed correlation of light and electron microscopic observations and proved essential for the optimization of the double label colloidal gold method. Fixation and hybridization conditions were optimized to ensure that the characteristic filament staining patterns seen with cytoskeletal antibodies at the light microscope level were not compromised. An immediate advantage of hybridization to poly(A) with oligo-dT probes was

that due to the lower melting temperature of A-T hybrids, significantly less stringent hybridization conditions were required than with actin mRNA hybrids. In addition, the reduction of the oligo-dT hybridization time from 3 hrs. to 30 minutes resulted in an increase in the density of antibody labelling along filaments. Alternative fixation methods were also evaluated. The best compromise in morphology, labelling and reproducibility was obtained with fixations in 2% paraformaldehyde/0.2% glutaraldehyde. These combined optimizations were sufficient to obtain characteristic light microscopy staining patterns for microtubules, intermediate filaments and microfilaments (Fig. 21) and permitted their ultrastructural identification (see below). The specificity of all antibodies used was confirmed by Western Blot (see Appendix-1).

Intracellular Poly(A) mRNA Distribution - Light Microscopy

By light microscopy, general distribution patterns of poly(A) mRNA were compared to cells labelled with antibodies to actin, vimentin or tubulin. Figure 21 illustrates the intracellular distribution of poly(A) mRNA in both Triton-extracted (21A) and unextracted cultured fibroblasts (1CD). Strong positive cytoplasmic signal was seen in > 95% of the triton-extracted and

FIGURE 21: Light Microscopic Visualization of Poly(A) mRNA and Cytoskeletal Proteins.

Detection using silver enhancement of one-nm colloidal gold labelled secondary antibodies. (A) Oligo-dT-biotin hybridization to Triton-extracted, glutaraldehyde fixed fibroblasts. Bar, 25μm. (B) Control hybridization with oligo-dA-biotin probe. (C,D) Oligo-dT-biotin hybridization to unextracted paraformaldehyde fixed fibroblasts. Bar, 25μm. (E) Antiactin staining in Triton-extracted fibroblasts. Bar, 15μm. (F) Antivimentin distribution, Triton-extracted fibroblast. (G) Antitubulin distribution, Triton-extracted fibroblasts. (H) Oligo-dT-biotin hybridization to Triton-extracted fibroblasts, phase microscopy.

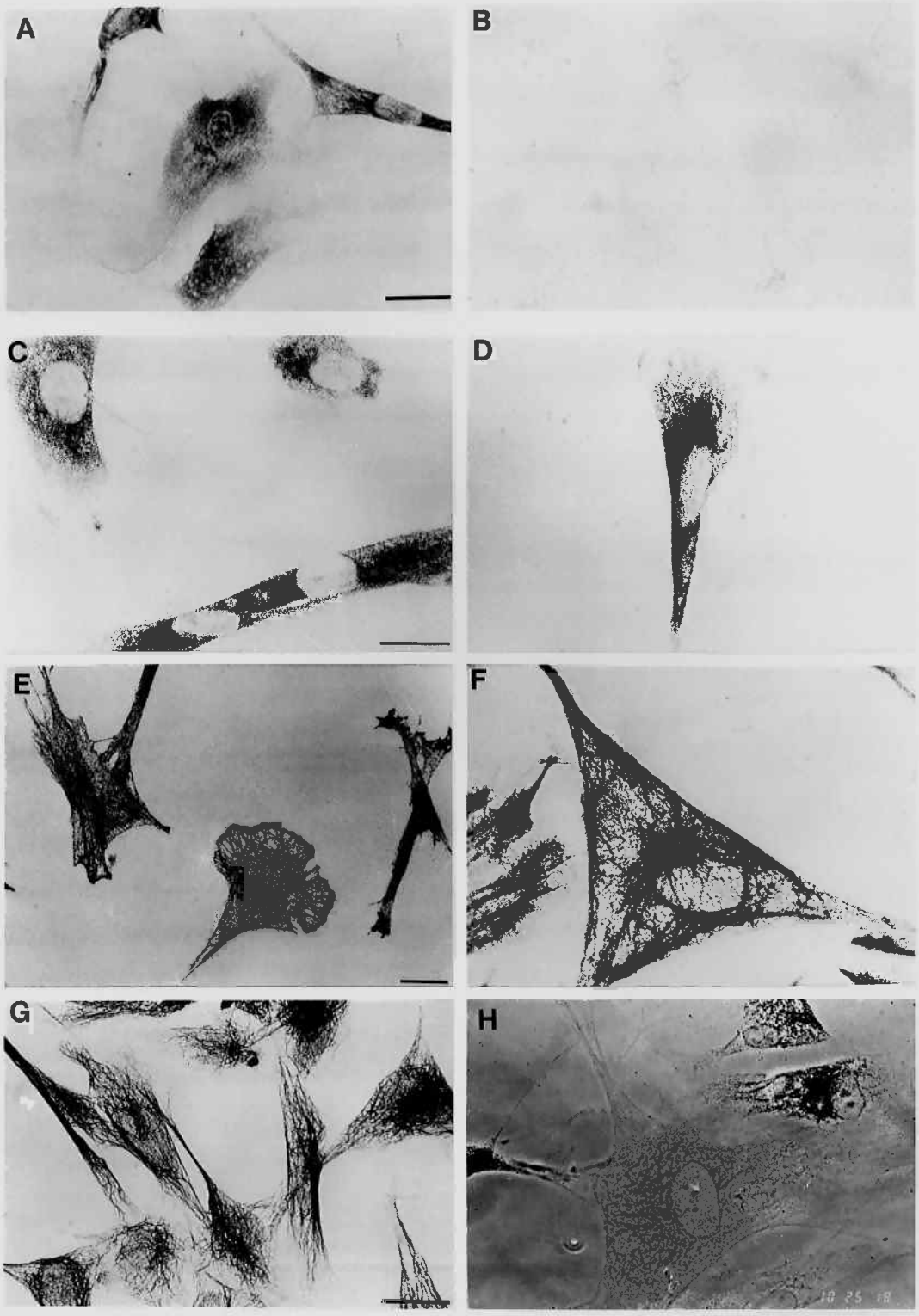
A
B
C
D
E
F
G
H

Appendix-1. Western Blot of Cytoskeletal Monoclonal Anitbodies.

(Lane 1) Anti-actin (East Acres Inc.), 42kD.

(Lane 2) Anti-vimentin (Amersham Inc.), 55kD.

(Lane 3) Anti-α-actinin (Sigma Chemicals), 190kD.

(Lane 4) Anti-filamin (Amersham Inc.), 280kD Doublet.

Polyacrylamide (10%) gel electrophoresis. Chemiluminescent detection (Tropic Corp.)

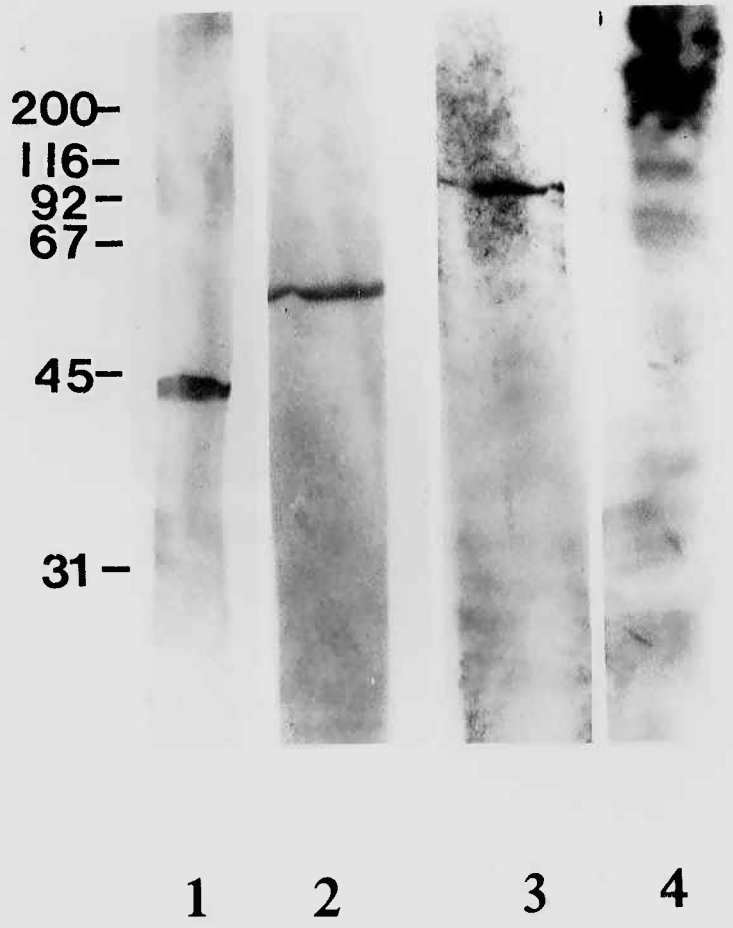
200–
116–
92–
67–
45–
31–
1
2
3
4

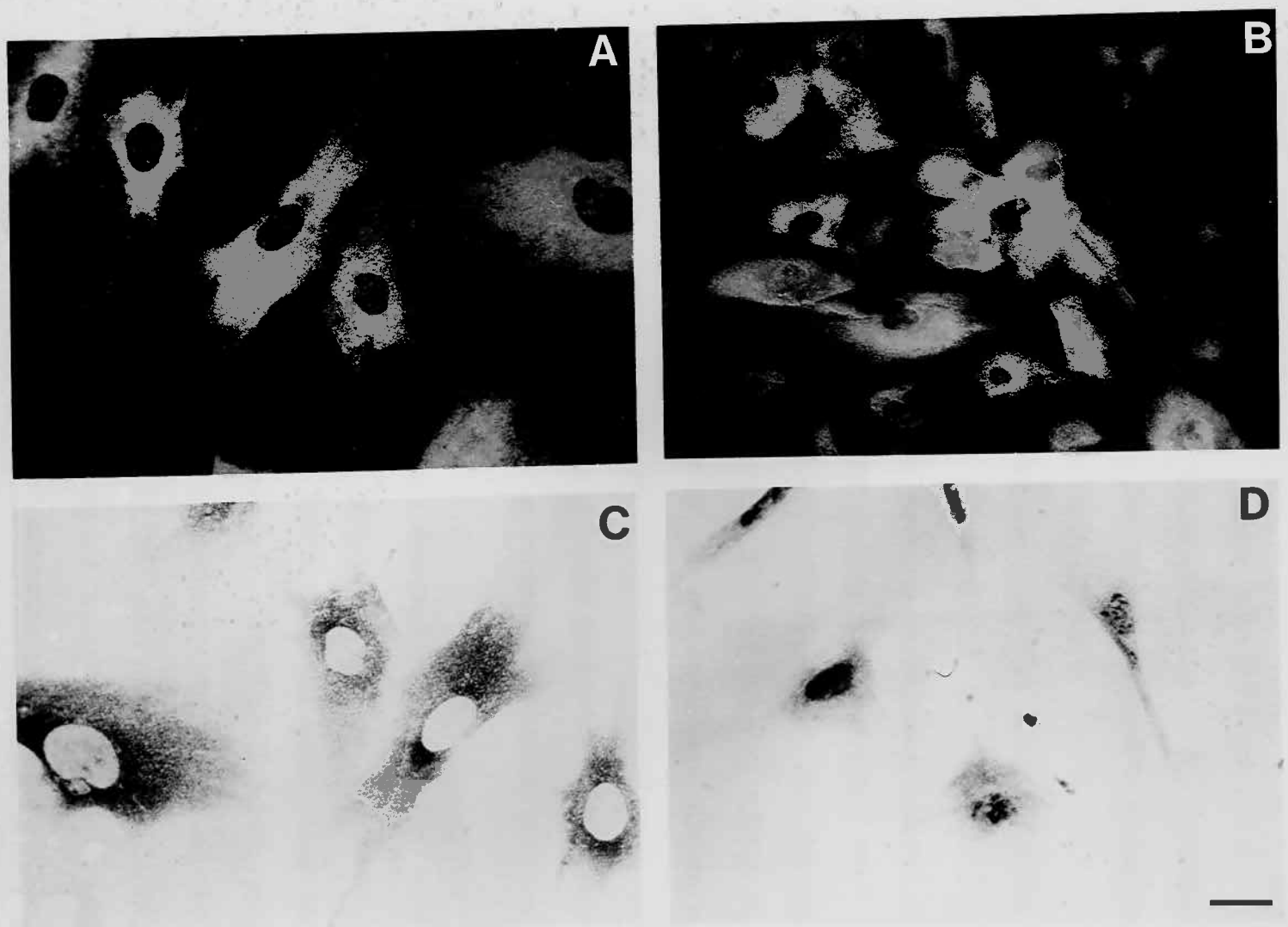
A
B
C
D

unextracted cell populations. From correlative RNA slot blot analysis (Taneja et al., submitted), greater than 90% of mRNA is retained following a one-minute triton-extraction. No specific cellular signal was observed with the control oligo-dA probe at the same time of silver enhancement (Fig. 21B).

The light microscopic distribution poly-(A) mRNA in the nucleus was nonhomogeneous, and localized in the form of discrete foci (Figure 21A). These domains have been shown to involved in RNA processing (Carter, Taneja and Lawrence, 1991). Quantitation by RNA slot blot of cell fractions and image processing of fixed cells has shown that 18% of poly(A) mRNA is localized to the nucleus (Taneja et al, in preparation). Although the focus of this report is on the cytoplasmic distribution of poly(A), the visualization of nuclear poly(A) foci using the silver enhancement detection methodology provided an internal positive control for the system.

The relative amounts of poly(A) detected in the nucleus and cytoplasm was shown to vary with different fixation conditions. This is illustrated in Appendix-2. Triton-extracted cells fixed in 4% glutaraldehyde exhibited the stongest cytoplasmic label, but nuclear label was only observed in approximately 25% of the cells. Triton-extracted cells fixed in 2% paraformaldehyde 0.2% glutaraldehyde exhibited slightly reduced cytoplasmic label, but nuclear poly (A) was frequently detected i.e. >60% cells. Unlabeled nuclei were thicker and appeared less extracted.

Appendix-2. Effect of Fixation on Cytoplasmic and Nuclear Poly(A) mRNA Detection.

A. Triton-extracted cells fixed in 2% paraformaldehyde 0.2% glutaraldehyde. B. Triton-extracted cells fixed in 4% glutaraldehyde. Note stronger nuclear detection in (A) compared to (B). Dark field optics. C. Triton-extracted fibroblasts fixed in 4% glutaraldehyde. D. Triton-extracted fibroblasts fixed in 4% paraformaldehyde. Note stronger cytoplasmic detection in (A) compared to (B). Bright field optics. Bar, 25μm.

Triton-extracted cells fixed in paraformaldehyde had intense nuclear label, but only poor cytoplasmic detection. Therefore, the intensity of nuclear detection was increased with lower crosslinking concentrations. It is likely that the variations in nuclear label are attributed to reduced penetrability of antibodies at higher crosslinking concentrations. By contrast, the cytoplasmic label increased at higher crosslinking concentrations. Since the cytoplasm is considerably more extracted than the nucleus, it is likely that cytosolic penetrabilty is not adversely compromised with higher crosslinking. Support for this explanation is shown in Chapter 3, where only 1nm gold labeled antibodies are able to detect nuclear poly(A) in Triton-extracted cells, whereas considerably larger conjugates (10nm) produced only strong cytoplasmic detection. An explanation for stronger cytoplasmic detection with higher crosslinking has been that the mRNP-cyoskeletal linkage is more stable during hybridization conditions (Singer et al., 1989). Supportive of this explanation is observation of decreased tritiated uridine retention in Triton-extracted paraformaldehyde fixed cells versus Triton-extracted glutaraldehyde fixed cells following hybridization (Sundell and Singer, 1990).

Poly(A) mRNA was not uniformly distributed throughout the cell, but was most evident in the perinuclear cytoplasm. Peripheral regions exhibited comparatively less staining, and extreme edges or lamellipodia did not appear to be labelled.

These patterns were observed in both extracted and unextracted fibroblasts. Figure 21E-G illustrates characteristic light microscopic silver enhancement staining patterns obtained for various cytoskeletal proteins possibly involved in mRNA attachment to the CSK. Actin protein staining was characterized by the labelling of stress fibers, peripheral lamellipodia and microspikes. Intermediate filament labelling was concentrated in the perinuclear cytoplasm. Microtubule labelling was characterized by a swirly fibrillar distribution throughout the cytoplasm. The distribution of poly(A) mRNA did not exhibit an obvious fibrillar appearance, and did not visually resemble any of the individual filament staining patterns seen for microfilaments, microtubules or intermediate filaments (Fig. 21). In some extracted cells photographed in phase (Fig. 21H), poly(A) mRNA retained on the cytoskeleton was observed to have a diffuse filamentous appearance, but still contrasted with the highly fibrillar staining seen with antibodies to each of the major filament systems.

It is unlikely that the diffuse fibrillar distribution of poly(A) is a result of hybridization conditions which might impart this pattern, since the intense fibrillar staining of actin, vimentin and tubulin are also observed after hybridization. The relatively mild hybridization conditions (i.e. 15% formamide 2X SSC, 0.5 hrs) has been optimized to preserve cellular morphology as well as antigenicity of the cytoskeletal filaments (see below). Therefore,

the distribution of poly(A) perhaps could be explained by its association with more than one filament system, or localization to a subset or domains within one system.

Ultrastructural Distribution of Poly(A) mRNA and Polysomes

Thin Sections

Samples from the experiment shown in Figure 21 were processed for thin section electron microscopy. At the ultrastructural level, the silver particles are visible at low magnification, permitting a continuous integration of optical and ultrastructural observations. The outline of the "whole" cell and its corresponding label were easily visualized at low magnification (2800X). As was seen with light microscopy, the distribution of poly(A) was not uniform when viewed by the electron microscope (Fig. 22A). Even at this higher magnification and resolution, there appears to be no apparent identifiable fibrillar pattern to this distribution. The cytoskeletal filaments, however, are not visible in unextracted cells. Although poly(A) is distributed throughout the cytoplasm, localized areas of concentration were indicated by aggregates of silver particles, surrounded by unlabelled regions. At higher magnification, silver particles were often close together or fused, suggestive of the presence of clusters of mRNA molecules

FIGURE 22: Thin Section Analysis of Poly(A) mRNA Distribution.

Detection using silver enhanced one-nm colloidal gold labelled secondary antibodies. (A) Oligo-dT-biotin hybridization to a paraformaldehyde fixed fibroblast. A clustery distribution of silver particles is observed throughout the cytoplasm (small arrows). Label can be seen over mitochondria (large arrow). Bar, 1μm. (B) Oligo-dA-biotin hybridization to a paraformaldehyde fixed fibroblast demonstrated little nonspecific binding. (C) Oligo-dT-biotin hybridization to a Triton-extracted fibroblast. Bar, 0.5μm. (D) Oligo-dA-biotin hybridization to a Triton-extracted fibroblast. (E) Colocalization of poly(A) mRNA with morphologically preserved polysomes (arrow) in Triton-extracted fibroblasts (84% of silver particles are within 5nm of a polysome, n=175). Bar, 200nm. (F) Aggregates of poly(A) mRNA in perinuclear cytoplasm and nuclear membrane (arrow) in a paraformaldehyde fixed fibroblast (N, nucleus).

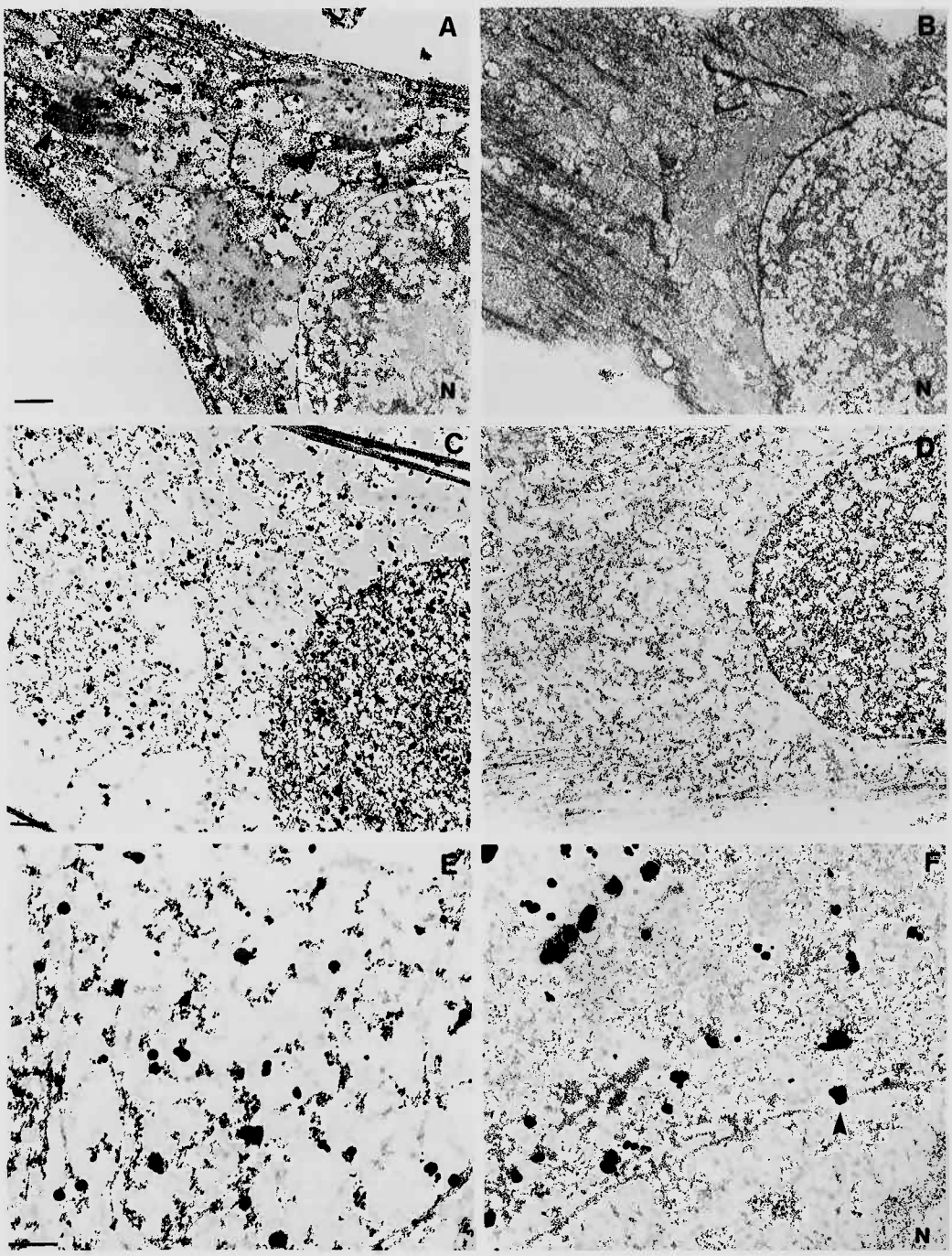
A
N
B
N
C
D
E
F
N

(Fig. 22F). Unfortunately, the preservation of ultrastructural morphology in paraformaldehyde fixed cells was insufficient to preserve polysomes and RER membranes when exposed to in situ hybridization conditions. Clusters of poly(A) mRNA could not be unequivocally correlated with respect to specific cellular structures nor could membrane associated poly(A) mRNA be compared to non-membrane bound mRNA. Some clusters were detected over mitochondria (Fig. 22A). Cells fixed in glutaraldehyde exhibited improved ultrastructural morphology following hybridization, but did not permit detection of poly(A) mRNA (data not shown). This was attributed to poor penetrability of antibodies into the heavily crosslinked cytosol.

The best preservation of molecular and morphologic detail occurred in triton-extracted cells fixed in glutaraldehyde (Fig. 22C). The cytoskeleton is visible in Triton-extracted cells and permitted analysis of its coordinate relationship to mRNA. It was apparent that the non-uniform distribution of poly(A) mRNA was conferred by the cytoskeleton, as the clustered distribution of silver particles was observed throughout the cytoskeletal framework. At higher magnification, (Fig. 22E) poly(A) was seen associated with cytoskeletal filaments and morphologically identifiable polyribosomes (84% colocalization, n=175). Polysomes were identified by their characteristic morphologic appearance, often present in circular or coiled conformations. Stress fibers,

FIGURE 23: Distribution of Poly(A), Polysome and Cytoskeletal Proteins.

Visualization by silver enhancement and thin sectioning. (A) Oligo-dT-biotin hybridization to Triton-extracted fibroblast. Poly(A) is not localized within stress fibers (arrows). Bar, 1μm. (B) Localization of actin protein to stress fibers. Bar, 0.5μm. (C) Association of polysomes with filaments labelled with actin antibodies (arrow). Bar, 250nm. (D) Visualization of a microtubule organizing center with anti-tubulin-antibody. Polysomes although visible in other sections, are not localized to microtubules. (E) Polysome distribution in a thin section labelled with antivimentin antibodies (arrow). Bar, 250nm. (F) Association of polysomes with vimentin (arrow). Bar, 200nm.

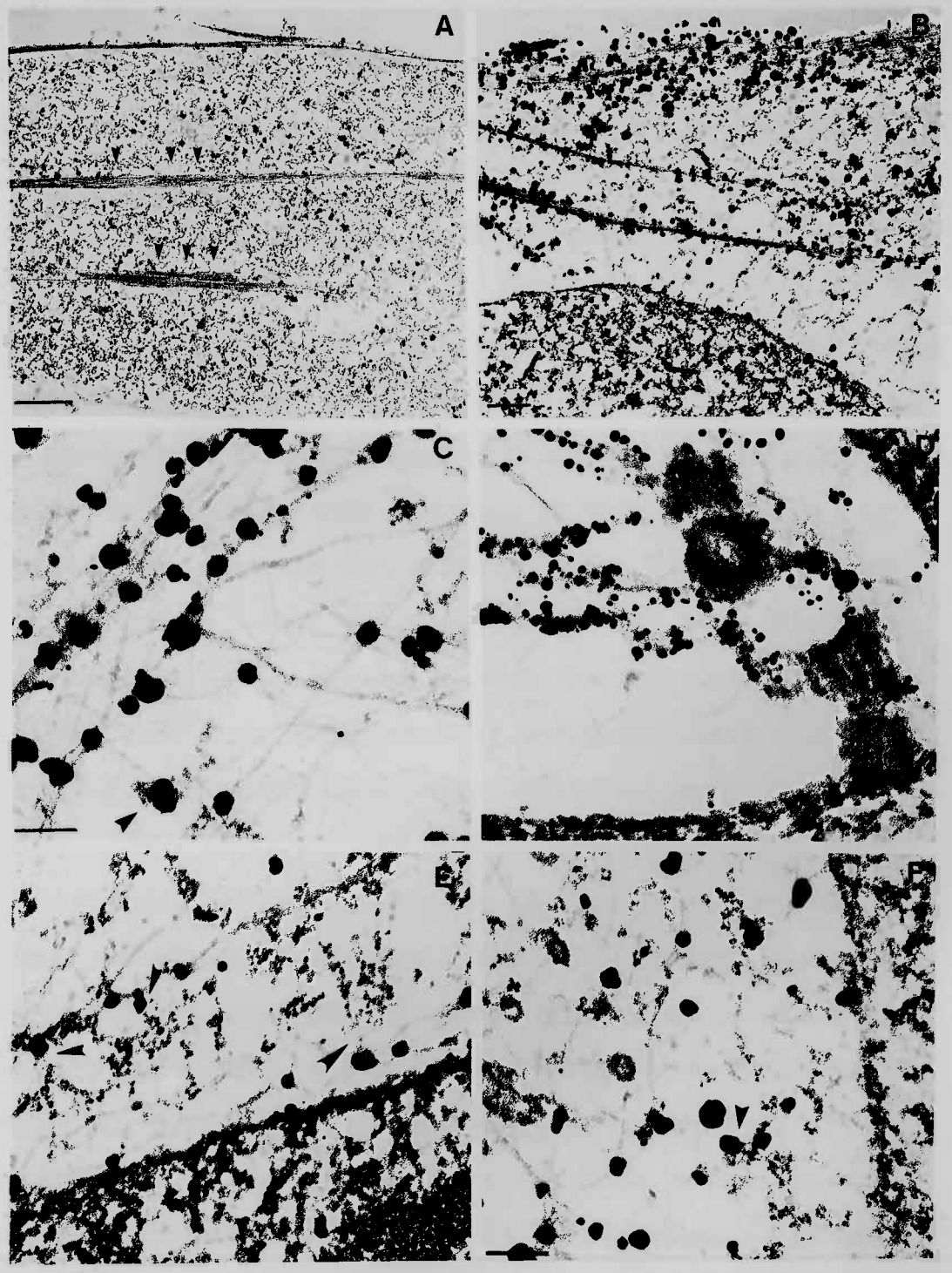
A
B
C
D
E
F

however, were not observed to contain either poly(A) mRNA or polysomes (Fig. 23A). This result could not be attributed to poor penetrability of probe detection system antibodies within these densely packed microfilaments, since they could be labelled by anti-actin antibodies (Fig. 23B). Poly(A) mRNA was, however, frequently associated with the 6nm filaments which associate with the stress fiber surface (data not shown).

The association of polysomes with respect to ultrastructurally identified cytoskeletal filaments has not been studied previously. Triton-extracted cells exposed to antibodies to actin, vimentin or tubulin were identified by light microscopy (Fig. 21) and then processed for thin sectioning (Fig. 23B-F). Regions rich in polysomes could be seen associating with filaments detected using the actin antibodies, with the exception of stress fibers (Fig. 23B). In many sections polysomes were observed associated with filaments that were unlabelled with anti-actin antibodies. This data indicated that a component of the actin cytoskeleton appeared to be principally but not solely involved in anchoring mRNPs to the cytoskeleton. Polysomes were not distributed linearly along microfilaments, but tended to cluster at specific points (Fig. 23C, arrow). Cells labelled with anti-vimentin antibodies revealed distinct associations of polysomes with intermediate filaments (Fig. 23E-F). Polysomes were seen near microtubules labelled with the anti-tubulin antibodies, but were clearly not associated. The analysis of the spatial distribution of

polysomes on the cytoskeleton using this thin sectioning approach was compiled from three experiments and 10-20 cells were photographed per sample. This data implicated the actin cytoskeleton as the major structural component for mRNA attachment. Intermediate filaments demonstrated a secondary role, but clear associations with polysomes could be identified.

Whole Mounts-Silver Enhancement

An evaluation of the spatial distribution of poly(A) mRNA within the cytoskeletal framework is limited by the lack of available three dimensional information provided by using only a thin sectioning approach (Nickerson and Penman, 1991). Epon sections are between 60-80nm thin, and cytoskeletal filaments appear fragmented, producing strictly a two-dimensional viewpoint of associated poly(A) mRNA. Individual cytoskeletons can be viewed in a resinless approach by whole-mount electron microscopy (Lenk et al., 1977; Fulton et al., 1980). Since triton-extraction removes approximately 70% of total cellular protein, sufficient contrast is provided to examine the structural elements of the cells interior using TEM (Lenk et al., 1977).

We utilized the silver enhanced one-nanometer gold technology concomitant with the whole mount procedure. At low magnification with the electron microscope, a synoptic view of poly(A) mRNA could be visualized with respect to the cytoskeleton. The spatial organization of poly(A) mRNA was

nonhomogeneous, but did not resemble specific fibrillar networks (Fig. 24). The amount of poly(A) mRNA varied markedly from one cytoskeletal region to another. The perinuclear region was the most heavily labelled (Fig. 24A). This observation is consistent with previously reported data on the density of polysomes in whole mounts (Fulton et al., 1980). Although poly(A) mRNA was more concentrated in the cell body, the highly branched cytoskeletal network within the leading edge contained appreciable amounts of poly(A) mRNA. However, poly(A) was not found in the extreme periphery, i.e. lamellipodia (Fig. 24B). Many cells exhibited very steep gradients in the amount of poly(A) mRNA: higher in perinuclear regions and dropped precipitously toward the cell periphery i.e. lamellipodia. These thin actin rich regions have been previously shown to be devoid of polysomes (Abercrombie et al., 1971); suggesting that the close apposition of ventral and dorsal membranes precludes entry of polysomes.

Examination at higher magnification revealed a clustery appearance (Fig. 24C) which suggested that poly(A) mRNA was not uniformly distributed along cytoskeletal filaments, but was preferentially concentrated to areas of filament intersection (Fig. 24D). This could explain the aggregated appearance of silver particles which was apparent in thin sections (Fig. 22).

FIGURE 24: Spatial Organization of Poly(A) mRNA- Whole Mounts

(A) Perinuclear cytoplasm. Bar, 1μm.

(B) Fibroblast leading edge. Bar, 1μm.

(C) Microheterogeneous patterns of poly(A) mRNA distribution (arrows). Bar, 0.5μm.

(D) Association of poly(A) mRNA near regions of filament intersection. Bar, 200nm.

A
N
B
L
C
D

Based on the description of the ultrastructural distribution of mRNA can be formulated specific hypotheses. The observation that poly(A) mRNA is clustered at intersections within the cytoskeleton raises the question that the filament themselves might not be solely involved in mRNP attachment, but rather that the above specialized structures contain an intermediate component i.e. bufunctional protein, which bridges mRNP to the filament. The observation that the intracellular poly(A) distribution does not visually resemble any single filament system suggests that poly(A) may be associated with more than one type of filament. The localization of polysomes to both microfilaments and intermediate filaments (Fig. 23) provided the first experimental support for this hypothesis. To further test these hypotheses, the localization of poly(A) to cytoskeletal intersections and the identification of the filament systems involved were quantitatively evaluated using colloidal gold labelled antibodies (5 and 10nm particles) which are not silver enhanced.

Quantitation Using Immunogold

Antibodies labelled with either 10nm or 5nm colloidal gold were used to quantitate the association of poly(A) mRNA in pairwise combination with actin, vimentin and tubulin in whole mounts. Five cells were evaluated for each pair wise combination and between 6-10 micrographs were taken from each cell (magnification 28,000X). Ten nm particles (poly(A)) were scored

as to whether they were or were not associated with labelled filaments (5nm particles). Poly(A) mRNA molecules which were determined to be associated with a filament met two stringent criteria: (1) the 10nm particle(s) was within 5nm of a series of 5nm particles, and (2) both sizes of colloidal gold visually appeared to be associated with the same filament. These strict criteria therefore limit the number of poly(A) mRNA molecules which can be evaluated in a whole mount preparation. For example, in thick cytoskeletal regions, it is frequently not possible to distinguish whether a 10nm particle is associated with a labelled filament or an immediately adjacent unlabelled filament. Only unequivocal associations were included in the analysis. This approach yields substantially more scorable poly(A) mRNA than thin sectioning since more of the cell is visible. The results of this analysis is summarized in Table 3 and Figure 25A-C, and is compiled from three independent experiments.

The majority of poly(A) mRNA was observed to be associated with the actin cytoskeleton. From double label colloidal gold experiments, 72% of detected poly(A) localized within 5nm of labelled microfilaments. This result was consistent with the thin section analysis (see Figure 23), where polysomal dense regions were primarily composed of actin filaments. However, one-third of detected poly(A) was consistently observed to be associated with vimentin filaments. In early double label colloidal gold experiments on Triton-extracted whole mounts (Singer et al.,

TABLE 3: Association of Poly(A) mRNA with Cytoskeletal Proteins

A.	dT-B/μ^2	dA-B/μ^2	S/N	%S
	4.7	0.5	9.4/1	90

B.	ACTIN	VIMENTIN	TUBULIN
	72.0 $\pm$ 10.5	33.6 $\pm$ 7.2	#9.8 $\pm$ 1.5
		# 39.6	
		* 24.3	

C	FILAMIN	α-ACTININ	VINCULIN
	56.7 $\pm$ 4.2	59.4 $\pm$ 6.0	12.6 $\pm$ 2.5

A. Signal-to-noise ratio determination from counting GPCs of size >2 particles in oligo-dT (biotin) and oligo-dA (biotin) hybridizations. The number of GPCs per μ^2, their ratio and percent of significant GPCs in oligo-dT (biotin) samples are indicated.

B. Percentage of poly(A) mRNA (GPCs >2 particles X %S) which localized within 5nm of labelled filaments with standard deviation between three experiments. #, A second monoclonal antibody to vimentin. *, Analysis of vimentin poly(A) colocalization in RK13 cells. #, Signal-to-noise ratio of 8.3:1 was obtained by directly comparing oligo-dT and oligo-dA labelling on labelled microtubules.

C. Percentage of poly(A) mRNA (10nm particles) localized within 5nm of labelled actin binding proteins (5nm particles).

The above quantitative analysis is compiled from over 1200 poly(A) cytoskeletal interactions (approx. 100 micrographs).

FIGURE 25: Associations of Poly(A) mRNA with Specific Cytoskeletal Proteins.

Double label colloidal gold analysis by whole mount electron microscopy. Poly(A) is detected with 10nm gold, and the cytoskeletal protein with 5nm gold.

(A) Poly(A) mRNA molecules are attached to microfilaments labelled with antibody to actin. Bar, 100nm.

(B) Poly(A) mRNA (small arrows) is localized to vimentin filaments, while some poly(A) mRNA is not (large arrow).

(C) Poly(A) mRNA-intermediate filament association using a second monoclonal antivimentin antibody.

(D) Microtubules are strongly labelled with 5nm gold particles, but poly(A) mRNA is associated with unlabelled cytoskeletal filaments.

(E) Association of poly(A) with α-actinin.

(F) Localization of poly(A) mRNA to microfilament intersection. Filamin labelling detected by 5nm gold particles.

(G) Thin section of an antifilamin sample. Filamin is localized to microfilament intersection (large arrow), while polysomes are distributed peripherally (small arrows).

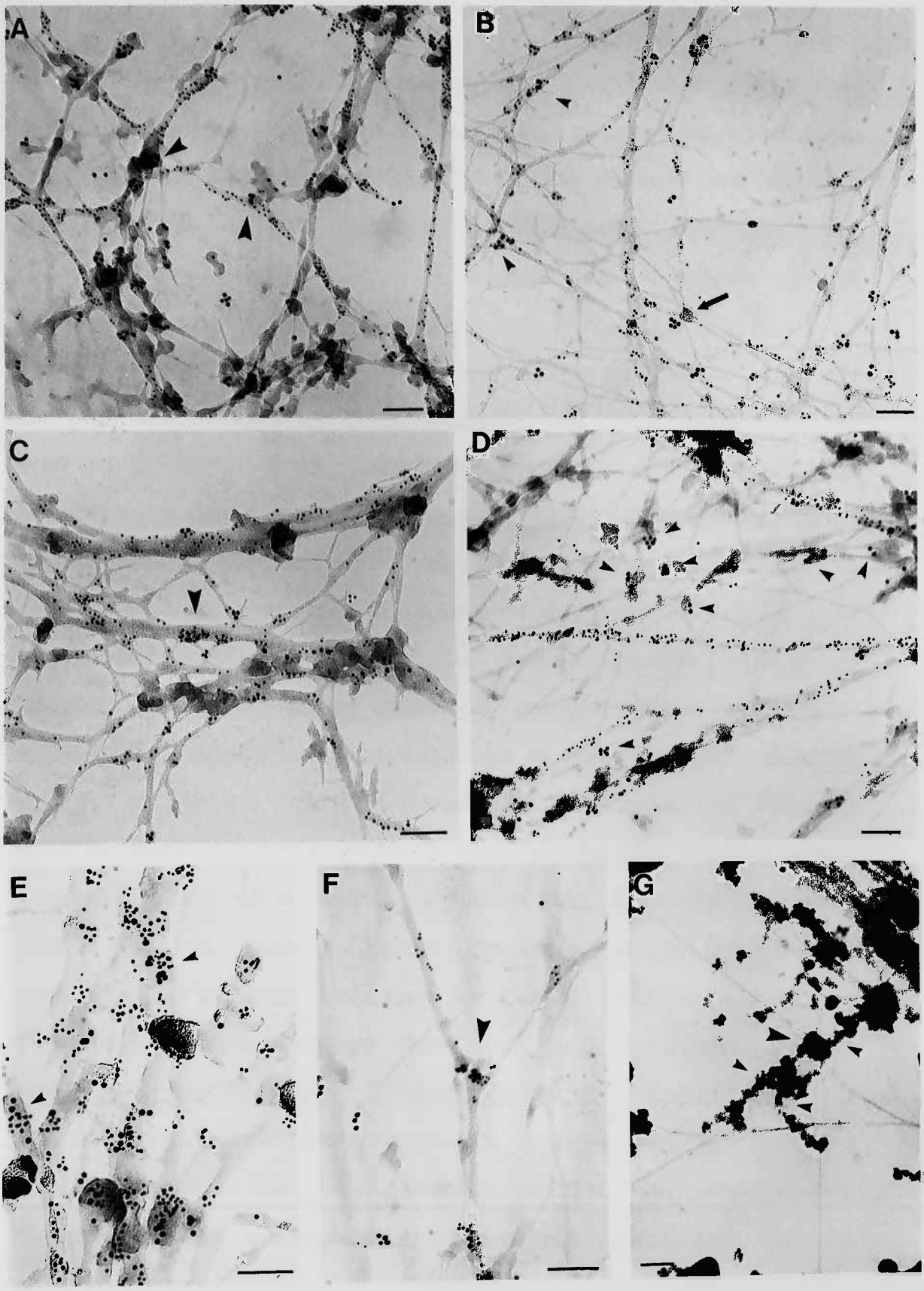
A
B
C
D
E
F
G

1989), we were unable to demonstrate involvement of filament systems other than actin. How then could it be explained that the overall spatial distribution of poly(A) mRNA did not look like the actin cytoskeleton? In fact, at the light microscopic level, the distribution of poly(A) mRNA lacked resemblance to any one of the three major filament systems.

The above observations were corroborated ultrastructurally in both thin sections of Triton-extracted and unextracted cells, as well as in critical point dried whole mounts. These descriptive observations were important because they implied that actin might not be the sole player, and therefore provided the motivation to develop an improved double label gold methodology. Quantitation of the poly(A)-vimentin association suggested that a significant amount of poly(A) mRNA localized to intermediate filaments. It is important to note, however, that the poly(A) mRNA colocalization percentages with actin and vimentin total to 106%. An interesting explanation for this finding would be the presence of actin-vimentin junctions. However, since the above data is generated from the independent analysis of separate poly(A)/actin and poly(A)/vimentin samples, it is not possible to directly compare these data in a three way analysis within an individual cell. Furthermore, the Triton-extraction at 4^{o}C depolymerizes microtubules (Lenk et al., 1977), and therefore does not permit their representation in the data (see below). Nonetheless, the comparison of the poly(A) actin with poly(A)

vimentin strongly indicates that intermediate filaments are involved in anchoring poly(A) mRNA to the cytoskeleton. Comparing their relative colocalization percentages, intermediate filaments were associated with approximately half as much poly(A) mRNA as the actin cytoskeleton.

The vimentin poly(A) colocalization data was confirmed in independent experiments, and evaluated using two different monoclonal antibodies and two different cell types (see Table 3-Part B). Furthermore, the mild hybridization conditions preserved intermediate filament architecture and allowed strong labelling with anti-vimentin antibodies. From the numerous micrographs examined of vimentin poly(A) mRNA interactions, the association appeared direct and unambiguous. For example, in many intermediate filament rich regions unencumbered by mixture with other filaments, i.e., actin, the poly(A) mRNA-vimentin association is most clearly evident (Fig. 25B).

The demonstration of dual involvement for microfilaments and intermediate filaments does not conflict with reports which demonstrate release of mRNA from the cytoskeleton following actin perturbation with pharmacologic agents. Cytochalasins have been widely used to demonstrate actin dependent processes. These heterocyclic compounds bind to barbed ends of F-actin and induce the severing and aggregation of the actin cytoskeleton (Reviewed in Schliwa, 1986). There exists some controversy on the quantity of mRNA released from the cytoskeleton following

cytochalasin treatment (Bagchi et al 1987; Raemakers et al,1983; Ornelles et al 1986); with reported values ranging from 15 to 60%. Part of this discrepancy can be explained by varied cytochalasin concentrations or different cytochalasin species. The important observation relevant to this study, is that complete release of mRNA from the cytoskleton was never observed, even at high cytochalasin doses which dramatically altered the morphology of the cell i.e. 50% at 10ug/ml (Ornelles et al,1986). The inability to release one-third of the cytoskeletal associated mRNA has been recently observed in our laboratory using image processing (Taneja and Singer, submitted).

An unanswered question concerning these observations is whether the mRNA which is still retained on the cytoskeleton is bound to intermediate filaments or to microfilaments which were not perturbed by cytochalasin treatment. This issue is resolved in this study by ultrastructural examination of the mRNA-cytoskeletal association in cytochalasin treated cells. The data are shown in Figure 26-27, and provide additional support for a poly(A) mRNA-intermediate filament interaction. Figure 26A-B illustrates the light microscopic disorganization of the actin cytoskeleton following cytochalasin treatment. Stress fibers are no longer observed, and actin labelling is localized in cytoplasmic aggregates. As a result of cytochalasin treatment, in situ hybridization to poly(A) mRNA is substantially, but not completely eliminated (Fig. 26C-D). The distribution of the

retained poly(A) mRNA did not seem to parallel the disorganized actin cytoskeleton. Intermediate filaments still retain their unique light microscopic appearance following cytochalasin treatment i.e. perinuclear concentration (Fig.26F).

At the ultrastructural level, the majority of poly(A)mRNA in actin labelled cytochalasin treated cells was clearly associated with an unlabelled and unperturbed cytoskeletal network (Figure 27C-D, arrowheads). These are intermediate filaments (Figure 27A-B). In the vimentin labelled cytochalasin treated cells, mRNA-intermediate filament associations are directly observed (arrows). Aggregates of actin are unlabelled by the antibody to vimentin (Fig. 27B).

The whole mount procedure utilized to study the association of mRNA with the cytoskeleton results in microtubule depolymerization. In order to investigate the possibility that a small component of mRNA was bound to microtubules, Triton-extractions were performed at room temperature in the presence of EGTA (Singer et al., 1989a). These conditions, although suboptimal for mRNA retention on the other filament systems did allow preservation of many microtubules. The majority of poly(A) mRNA was clearly associated with filaments other than microtubules (see Fig. 25D). Only 10% of poly(A) mRNA colocalized to microtubules. This actually represents <10% of total cytoskeletal associated mRNA, since less mRNA is retained by this method (data not shown). This label represented bonafide

Figure 26. Cytochalasin Effects on the Retention and Distribution of Poly(A) mRNA: Light Microscopy.

Bar, 50μm.

A. Antiactin binding detected by silver enhancement in Triton-extracted RK13 cells.

B. Antiactin binding following cytochalasin treatment (0.5μg/ml, 30 minutes) and triton-extraction.

C. Hybridization to poly(A) mRNA in triton-extracted cells.

D. Hybridization to poly(A) mRNA following cytochalasin treatment and triton-extraction.

E. Control hybridization with biotinated oligo-dA probe following cytochalasin treatment and triton-extraction.

F. Antivimentin binding following cytochalasin treatment and triton-extraction.

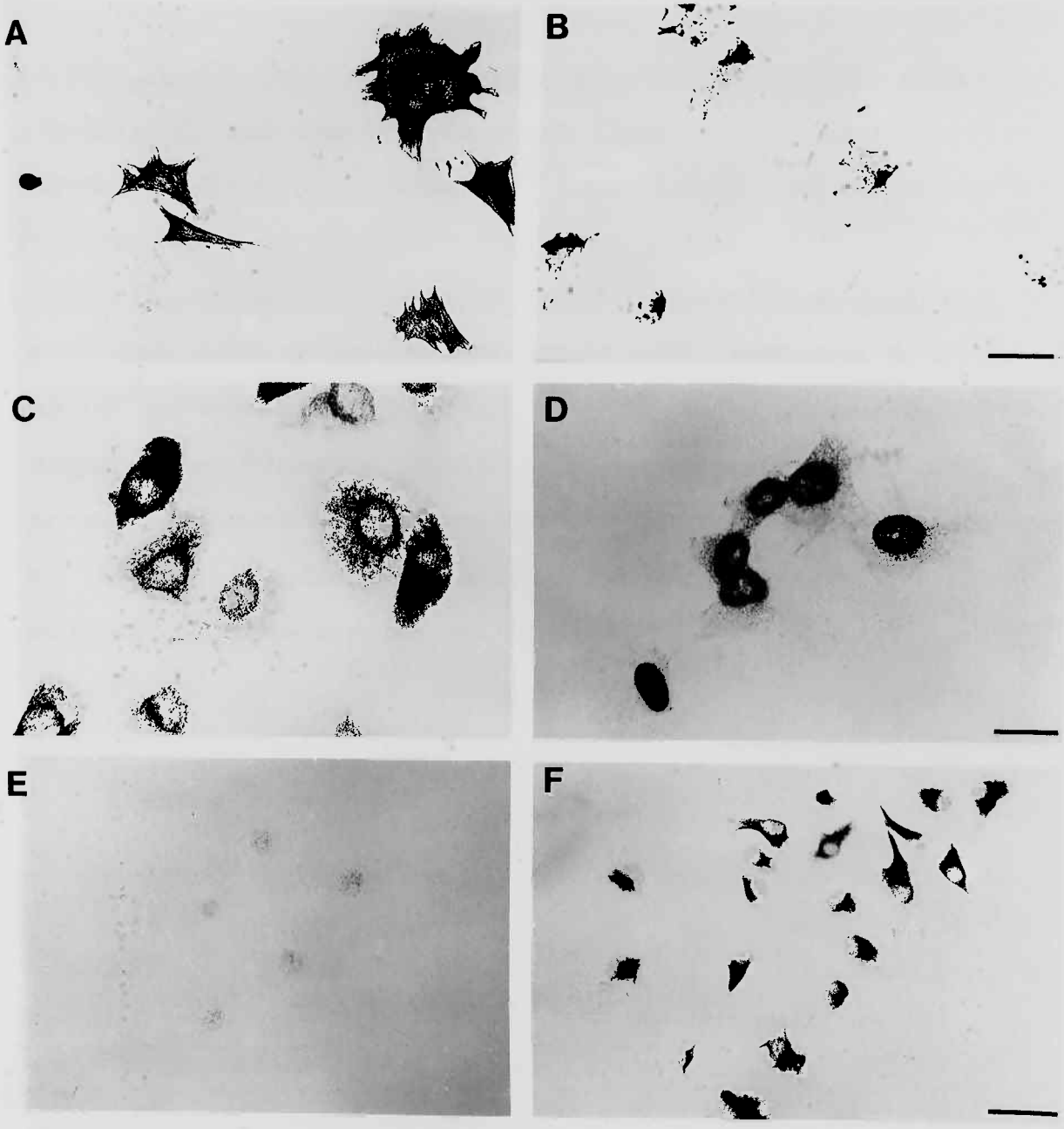
A
B
C
D
E
F

Figure 27. Cytochalasin Effects on the Association of Poly(A) mRNA with Microfilaments and Intermediate Filaments.

(A,B) Double label ultrastructural detection of poly(A) mRNA (10nm gold) and vimentin filaments (5nm gold). Associations between mRNA and vimentin (arrowheads) are observed following actin disorganization using cytochalasin.

(C,D) Double label detection of poly(A) mRNA (10nm gold) and actin (5nm gold) in cytochalasin treated cell. Numerous poly(A) mRNA molecules are observed attached to unlabelled and nonperturbed filaments (arrowheads). Aggregates of actin (arrows) are unlabelled by antivimentin (B) and heavily labelled by antiactin (C) further demonstrating the specificity of the antibodies and separation of the labelling.

Bar, 100nm.

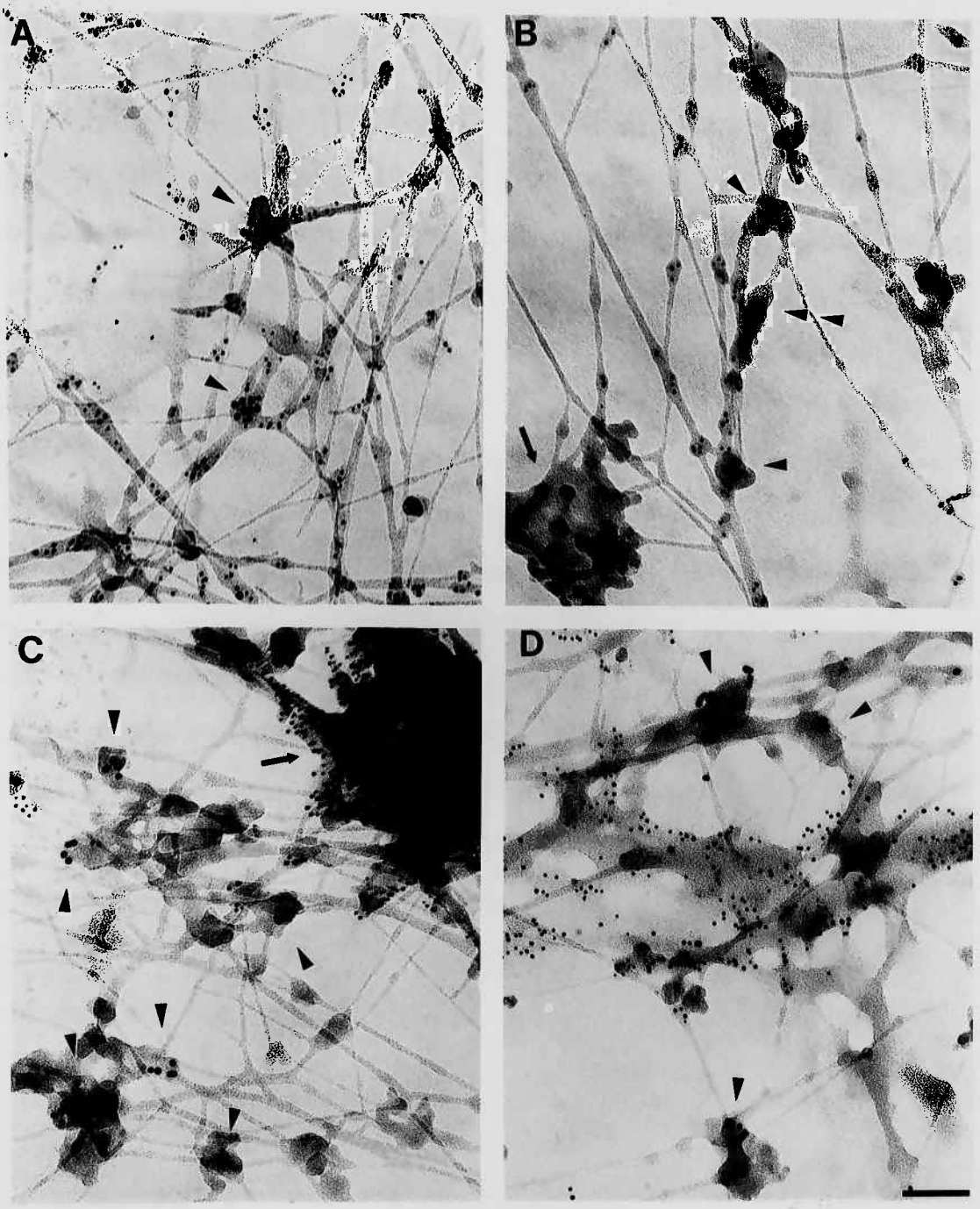
A
B
C
D

hybridization to poly(A) mRNA, since nonspecific binding of control oligo-dA probes on the labelled microtubules was minimal (signal to noise ratio, 8.3:1).

From the analysis of Triton-extracted whole mounts using actin antibodies the distribution of poly(A) mRNA with respect to the actin CSK was nonhomogeneous. Since poly(A) mRNA was associated with intersections (Fig. 24D), we sought to determine whether they would colocalize with the actin binding proteins, filamin, alpha-actinin or vinculin which are involved in crosslinking microfilament(s) (For review, see Vandekerckhove, 1990; Hartwig and Kwiatkowski, 1991). Poly(A) mRNA which localized to points of contact between branched actin filaments showed strong colocalization with filamin (Fig. 25F). Greater than half of poly(A) colocalized within 5nm of filamin and α-actinin (Table 3-Part C). In contrast, poly(A) was significantly less colocalized with vinculin, a separate class of ABP which binds actin to the plasma membrane (12%). Polysome association with filamin and α-actinin was also observed in thin section analysis (For filamin, see Fig. 25G).

mRNA-Cytoskeletal Association- Artifacts Considered

The original report by Penman demonstrated that >97% of cellular polysomes are associated with the cytoskeleton, despite

extraction of >75% of cellular protein (Lenk et al., 1977). Their further use of viral model systems demonstrated that mRNA is translated only when bound to the cytoskeleton; therefore, this association may be obligatory (for review see Nielsen et al., 1983). These data were met with considerable controversy and it was suggested that the Triton-extraction procedure might have generated an artifactual association of mRNA with the cytoskeleton.

Over the past decade, evidence has accumulated which indicates that the association of mRNA with the cytoskeleton is indeed a real cellular relationship. Moreover, this association appears to function in translation and the nonuniform intracellular localization of mRNA. The supporting research can be organized into the following areas: (1) The actin binding protein, ABP-50, is a translation factor (EF-1a) which is active only when bound to the cytoskeleton (Dharmawardhane et al. 1991). (2) The localization of mRNAs to distinct morphologic regions is mediated by specific cytoskeletal filament systems (Sundell and Singer,1990; Pokryka and Stephenson,1991;Yisraeli et al,1990). Specific mRNA localization patterns are observed in both intact and Triton-extracted cells (Singer et al., 1989a; Silva et al., 1989; Singer et al., 1989b; Bruckenstein, 1990). (3) The above mRNA-cytoskeletal interaction requires specific nucleic acid sequences within the 3'UTR (Macdonald and Struhl,1988; Mowry and Melton,1992). (4) RER membrane and nonmembrane bound

mRNAs are associated with the cytoskeleton by different mechanisms (Zambetti et al,1990).

In this study, the distribution of poly(A) mRNA was nonuniform and localized to specific cytoskeletal domains i.e. actin intersections, intermediate filaments; while avoiding others, i.e. stress fibers, lamellipodia, microtubules. This thesis along with the above recent studies provides much evidence that the association of mRNA with the cytoskeleton plays a basic role in controlling translation and the intracellular location of translation. The original suggestion that the Triton-extraction procedure had generated an artifactual association of mRNA with the cytoskeleton has not been supported.

We will continue, however, to experiment with kinder and gentler protocols, in order to further understand the relationship of mRNA with internal cell structure. For example, the Triton-extraction procedure solubilizes much of the RER membrane, and therefore does not permit the distinction between membrane and non-membrane associated polysomes. It has been shown that membrane associated mRNAs can be similarly retained on the cytoskeleton (Cervera et al., 1981; Zambetti et al., 1990a), but it is unclear whether this occurs by a different mechanism. It is anticipated that an improved ultrastructural in situ hybridization approach will prove valuable. We are currently investigating the use of post-embedment approaches (McFadden et al., 1988; Binder

et al., 1986) which involve hybridization and detection directly on the thin section, offering improved membrane morphology.

DISCUSSION

We have investigated the spatial organization of poly(A) mRNA within the cytoskeletal framework of single cells through the direct visualization of hybridization with ultrastructural resolution. This work required the development of an approach which permitted a synoptic view of the cell while at the same time providing for resolution sufficient to identify the specific proteins involved in the attachment of mRNA to the cytoskeleton. Interactions with both microfilaments and intermediate filaments has been demonstrated.

The actin cytoskeleton has been previously implicated in the attachment of mRNA to the cytoskeleton from cell fractionation studies which demonstrated that mRNA could be released from the cytoskeleton using actin depolymerizing drugs (Lenk et al., 1977; Ornelles et al., 1986; Adams et al., 1983). Other reports, however, have not observed release of mRNA utilizing this approach (Bagchi et al., 1987; Jeffrey et al., 1986). The ambiguity inherent in a drug study is obviated by direct visualization. The ultrastructural in situ hybridization study described here has shown, to within a few nanometers of resolution, that the actin

cytoskeleton is principally involved in anchoring poly(A) mRNA. Moreover, visualization has provided information on the way which poly(A) is assembled on to actin filaments.

Cytoplasmic actin is assembled into several structurally and functionally distinct arrangements (Heuser and Kirschner, 1990; Small and Celis, 1978). This complexity is achieved through the actions of a diverse group of actin binding proteins which regulate filament polymerization, length, spatial organization and interactions with other cellular components (Hartwig and Kwiatkowski, 1991; Pollard and Cooper, 1986). Three basic domains within the actin cytoskeleton have been identified in non-muscle cells: peripheral processes, stress fibers and orthogonal networks. Using the approaches described here, the distribution of poly(A) mRNA was seen to be non-homogeneous within the actin cytoskeleton, and was localized to orthogonal microfilament networks.

Within branched actin networks, poly(A) mRNA molecules were not uniformly distributed along microfilaments, but were predominately concentrated at actin filament intersections. Poly(A) mRNA colocalized ultrastructurally with the actin binding proteins, filamin and alpha-actinin which are known to be involved in the assembly of branched microfilament networks (Hartwig and Kwiatkowski, 1991; Vandekerckhove, 1990). Both are high molecular weight homodimers (500,400 kD respectively) which possess amino terminal actin binding sequences, and hence

crosslink adjacent microfilaments (Hartwig and Kwiatkowski, 1991; Vandekerckhove, 1990). In contrast to its association with branched intersections, poly(A) mRNA was not observed to exhibit significant localization to tightly packed microfilaments i.e. stress fibers, nor did poly(A) colocalize with vinculin, a separate class of actin binding protein which binds actin to the ventral plasma membrane surface.

The observation that poly(A) is localized to intersections of actin orthogonal networks has several implications. First, it is likely that components of the actin vertex, rather than the actin filament, are involved in the mechanism of mRNP attachment to the cytoskeleton. It is important to note, however, that the majority (>50%) of sites containing filamin or alpha-actinin do not contain poly(A) mRNA. Therefore, although filamin or alpha actinin may be actin binding proteins involved in the attachment of mRNP to the cytoskeleton this is not their sole function. Other proteins may be specific for poly(A) mRNA binding and further work may reveal them. The localization of poly(A) to actin vertices may also be involved in promoting translation of mRNA on the cytoskeleton. A relationship between the actin cytoskeleton and protein synthesis has been directly demonstrated in Dictyostelium, where ABP-150, which crosslinks microfilaments was shown to be elongation factor 1A (Yang et al., 1990). This data is in agreement with the localization of poly(A) to actin intersections reported here, and suggest that the branched

actin intersection is a translationally competent domain which mRNPs are localized.

The localization of poly(A) to actin vertices also provides insight into mechanisms of mRNA localization. The ability to segregate mRNAs to distinct cellular regions requires a model wherein specificity in the cytoskeleton determines the localization. How might a cell localize one mRNA peripherally and another proximal to the nucleus, if both mRNAs are associated with the actin cytoskeleton? The ultrastructural distribution of poly(A) mRNA may offer insight into this process. Since the poly(A) mRNA has an affinity for actin intersections, rather than actin filaments, the cell could segregate mRNAs by targetting to different intersections. Work done in our laboratory on the localization of actin mRNAs to the fibroblast lamella demonstrated that this process was dependent on microfilaments (Sundell and Singer, 1991). At the ultrastructural level, recent data indicates that actin mRNAs are localized to the intersections of their own filaments (data not shown). The molecular components of peripheral intersections which confer selectivity for actin mRNPs are unknown.

It is also unknown how microfilaments are involved in the mechanism of mRNP movement. One route could be that mRNPs are actively transported on stress fibers i.e. motor protein, and although poly(A) mRNA was not localized to these structures, it is important to emphasize that the microscopic evaluation in this

work provides only information about the steady-state distribution of molecules. If the transport step is rapid (about 1 hr for actin mRNA) (Sundell and Singer, 1991) compared to the half-life of mRNA in the cell (about 12 hrs) (Kessler-Icekson et al., 1978), molecules in transport would not be a significant component of the current analysis (only about 4%). Alternatively, mRNPs could be transported directly through branched microfilament networks. It is interesting to note that the actin binding proteins filamin and α-actinin are involved in inducing gel-sol transitions of the actin cytoskeleton. These transitions are believed to be involved in cell motility. Perhaps similar mechanisms control mRNP movement along microfilaments. Alternatively, mRNP direction could be controlled by specific mRNP motor molecules, although none have yet been characterized. A model is presented in Figure 28 to illustrate putative roles of actin binding proteins in the localization of mRNAs to different compartments within the actin cytoskeleton.

Specific nucleic acid sequences appear to confer attachment and location within the cytoskeletal framework. Recent experiments in this laboratory demonstrated that RNAse A and T1 digestion which cuts mRNA sequences with the exception of poly(A), failed to release poly(A) from the cytoskeleton (Taneja, in preparation). Interestingly, polysomes did not lie uniformly along an intersection, but made contact at only few sites within

FIGURE 28: Proposed Mechanisms for Intracellular Compartmentalization of mRNA.

(1) Localization of poly(A) mRNA to orthogonal microfilament network. The poly(A) sequence is shown directly associating mRNPs with the intersection. Only one mRNA molecule is shown localized to each site.

(2) Possible localization of poly(A) to stress fiber surfaces during transport.

(3) Possible localization to microtubules during transport.

(4) Localization to intermediate filaments. Interactions of mRNPs with vimentin is illustrated by both poly(A) and nascent peptide associations.

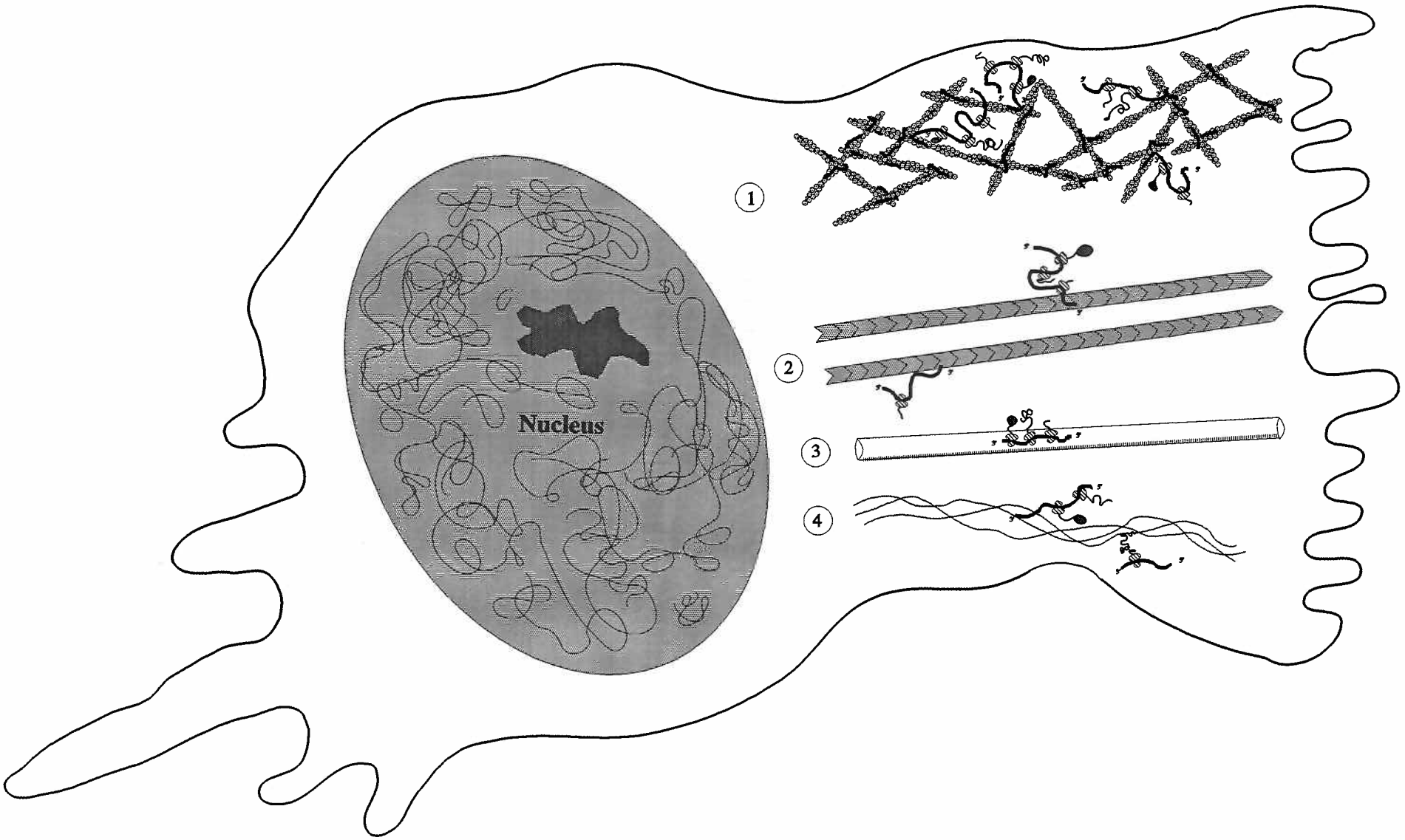
Nucleus
1
2
3
4

the polysome. From Figure 25G, a polysome is seen with only one attachment site for the actin(filamin) intersection, with the bulk of the polysome exhibiting little affinity. These results are suggestive of a more direct role of the poly(A) tail in the attachment of mRNPs to the cytoskeleton (Taneja et al., submitted). Since the poly(A) sequence is generic to most mRNAs, and most mRNAs are cytoskeleton associated, it is speculated that poly(A) serves as the mRNA anchor (see model) for the intersection.

The targeting of actin mRNA to peripheral regions within the actin cytoskeleton was shown not to require protein synthesis (Sundell and Singer, 1990). Recent data has identified a 400bp 3'UTR sequence which confers peripheral mRNA localization (Kislauskis and Singer, in preparation). The non-uniform localization of developmentally regulated mRNAs is also regulated by 3'UTR sequences which contain stem loop structures (Macdonald and Struhl, 1988; Seeger and Kaufman, 1990). Similar motifs have been postulated to be generally involved in RNA-protein interactions (Zamore et al., 1990). The above observations indicate that different sequences within the same mRNA can mediate mRNA attachment or localization. It is certain, however, that other interactions exist between an mRNP and the cytoskeleton. For example, histone mRNAs were released from the cytoskeleton with cytochalasin treatment; whereas RER membrane associated mRNAs required cytochalasin plus

puromycin, suggesting an additional cytoskeletal interaction provided by the signal peptide (Zambetti et al., 1990). How interactions with the cytoskeleton collectively regulate mRNA sorting, mRNA attachment, and mRNA translation will be an important synthesis of all of this information.

The high resolution in situ hybridization methodology we have developed, has revealed that intermediate filaments also provide mRNA binding sites throughout the cytoskeletal framework. Until this work no direct evidence for involvement of IFs in associations of mRNA had been obtained (Singer et al., 1989b). Intermediate filament-like immunofluorescence patterns for scRP antigens (Bachman et al., 1986) and cap binding protein (Zumbe et al., 1982) have been reported. The data presented here directly demonstrates a role for intermediate filaments in the attachment of mRNA to the cytoskeleton, and provide the first comparison of the quantitative contribution of each of the major filament systems as a site of mRNA attachment.

The demonstration that poly(A) mRNA is distributed on microfilaments and intermediate filaments has several implications. First, the cell may utilize multiple mRNA-filament system interactions to localize mRNAs to different cellular regions. Second, different filament systems may have unique functions. For example, one filament system could be involved in mRNP assembly, and another in protein synthesis (see model). The localization of prosome antigens to intermediate filaments was

suggestive of IF involvement in translational repression (Grossi de Sa et al., 1988). The localization of polysomes to vimentin however (Fig 23E,F) indicates that proteins can be synthesized on intermediate filaments. To address these different hypotheses, it will be important to investigate whether specific mRNAs are sequestered to a single filament system. The direct localization of poly(A) mRNA to intermediate filaments reported here reveals the site where IFS may function in gene expression and provides direction toward understanding this historically elusive cytoskeletal component. Currently the mechanism which mRNAs are associated with intermediate filaments is unknown. The localization of poly(A) mRNA to cytoskeletal intersections is, however, a general phenomenon (Table 3), and involves both microfilaments and intermediate filaments. From Figure 25B-C, poly(A) mRNA is observed at intersections between intermediate filaments. To date approximately fifteen IFBPs have been identified, but their functions are unknown (Skalli and Goldman, 1991). It will be interesting to learn whether any are involved in mRNP metabolism.

Microtubules are not believed to play major roles in the attachment of mRNA to the cytoskeleton since during the Triton-extraction procedure done at 4°C, microtubules depolymerize, yet about 90% of mRNA is retained on the cytoskeleton (Lenk et al., 1977). However, it is possible that microtubules play a role in mRNP transport. Microtubule depolymerization with colchicine

disrupted the localization of veg-1 (Yisraeli et al., 1990) and bicoid mRNAs (Pokrywka and Stephenson, 1991). A two step model was proposed whereby mRNA is transported on microtubules and then anchored on microfilaments (Yisraeli et al., 1990). The elucidation of possible mechanisms involved in mRNA movement along microtubules will require techniques which distinguish newly synthesized mRNAs from the steady-state population.

In summary, the development of an ultrastructural in situ hybridization methodology has permitted the direct visualization of the linkage between mRNA and the cytoskelton. This approach has demonstrated that poly(A) mRNA is not homogeneously distributed within the cytoskeleton. Both microfilaments and intermediate filaments were shown to be have major roles in the attachment of poly(A) mRNA to the cytoskeleton. This is the first direct evidence for involvement of intermediate filaments. The mechanism of mRNP attachment to the actin cytoskeleton likely involves components of the actin vertex, and not the actin filament.

The ultrastructural approach described here presents new questions on how mRNA-cytoskeletal interactions might be spatially utilized to synthesize functionally related proteins at common locations. The localization of poly(A) to filament intersections offers an additional microcompartment for mRNAs to be colocalized. The ultrastructural appearance of poly(A) at these sites can be in the form of tightly linked gold particle clusters, i.e.

2-6 particles (Fig. 25). It is possible that these clusters could contain multiple mRNA molecules. It will be essential to identify how many mRNA molecules are contained within these sites of hybridization. If more than one mRNA can exist per vertex, this may be a means for compartmentalizing mRNAs coding for proteins which function as oligomeric-peptide complexes. Alternatively, intersections containing poly(A) may contain only a single molecule. The spacing between intersections may therefore be of interest since hybridization to poly(A) is observed very close together (<50nm) but on separate filaments. Work reported in Chapter V will be directed toward the unequivocal identification of individual mRNA molecules and then determining whether single intersections or groups of intersections serve as vehicles to compartmentalize functionally related protein synthesis. For instance, do the vertices provide a functional mosaic within the cytoskeleton? It is anticipated that the continued development of a visual approach with ultrastructural resolution will be an essential technology toward this goal.

MATERIALS AND METHODS

Cell Culture

Human diploid fibroblasts (provided by Edward Fey) were used for most of this work. Chick embryo fibroblasts isolated from pectoralis muscles of 12-d-old chicken embryos and the NRK epithelium cell line (ATCC) were used for supportive data. Cells were cultured by standard techniques and plated in Falcon six-well tissue culture plates at a density of 2 x 10^5/well for HDFs and NRKs, and 5 x 10^5/well for CFBs. Tissue culture plates contained sterile coverslips (thin section procedure) or carbon and formvar coated gold EM grids on 22-mm circular coverslips (whole mount procedure). The purity of the gold grid was essential for cell viability, and 100% gold grids were obtained from Ladd Inc. (London 200 mesh, 3 mm). Carbon rods and formvar (0.5% in dichloroethane) were purchased from Tousimis Corp. Grid assembles were made by floating a formvar film onto glass coverslips supporting six gold grids. After drying, the film is coated with carbon using a Denton Evaporator. Grid assemblies were sterilized by gamma irradiation from a cesium-137 source.

Cells were Triton-extracted and/or fixed 1-2 days after plating. The Triton-extraction buffer (Lenk et al., 1977) contained: 0.3M sucrose, 0.1m NaCl, 10mM pipes pH6.9, 3mM $MgCl_2$, 10μM leupeptin (Sigma Chemical Co.), 1:40 dilution Vanadal complex (4mM adenosine, 0.2M $VaSO_4$). Cells were

briefly washed with buffer, and then extracted for 60-90s at 4°C in buffer containing 0.5% Triton X-100, followed by a brief wash in the first buffer and then fixed in 2% paraformaldehyde 0.2% glutaraldehyde or 4% glutaraldehyde (PBS, 5mM magnesium). Cells not extracted with Triton X-100 were first washed in Hanks balanced salt solution and then fixed in 4% paraformaldehyde (PBS 5mM $MgCl_2$). All fixations were for 15 minutes at room temperature. Cells were processed for in situ hybridization and immunocytochemistry directly following fixation. For in situ hybridization (probe visualization only) cells could be dehydrated and stored in 70% ethanol at 4°C.

Probe Preparation

Synthetic oligo-dT (55 nts) and oligo-dA (55nts) were 3'-end labelled with biotin-16-dUTP (Boehringer-Mannheim) using terminal transferase (25pM oligo, 25mM biotin dUTP, 140mM potassium cacodylate, 30mM Tris-HCl pH 7.6, 1mM $CoCl_2$, 0.1mM DTT, and 100 units of terminal transferase) at 37°C for 1 hr. Probes were purified using a 20ml G-50 column, and the collected fractions were blotted onto nitrocellulose and detected using a strept- avidin-alkaline phosphatase conjugate (Boehringer-Mannheim). Positive fractions were lyophilized, resuspended and combined and the OD measured. The size of the biotinated terminal transferase tails were approximately ten bases long determined by polyacrylamide gel electrophoresis.

Hybridization

Cells were washed in PBS (5mM $MgCl_2$) and then equilibrated in 15% formamide (Sigma) 2X SSC and 10mM sodium phosphate pH 7.0 at room temperature for not more than 10 minutes. 5-20ng of probe was dried down with E. coli tRNA (10μg) and sonicated salmon sperm DNA (10μg) and then suspended in 10μl of 30% formamide containing 20mM sodium phosphate pH 7.0. Probes were mixed with 10μl of hybridization buffer (20% dextran sulfate, 4X SSC, 0.4% BSA, 20mM sodium phosphate pH 7.0). Coverslips were placed cell side down on parafilm containing 20μl probe mixture and hybridized for 0.5-3 hrs at 37°C. After hybridization coverslips were washed for 20 minutes in 15% formamide 2X SSC at 37°C, and three 10 minute washes in 1X SSC on a rotary shaker at room temperature.

Immunocytochemistry

Detection of biotinated probes was accomplished by a two-step immunogold procedure utilizing rabbit antibiotin primary antibodies (Enzo Biochemicals) and colloidal gold (1, 5 and 10nm) labelled goat anti-rabbit secondary antibodies (Amersham Inc.). Coverslips were pretreated with 8% BSA, RNAse-free (Boehringer-Mannheim) in TBS, pH 7.4 for 10 minutes. Primary antibodies were diluted 1:100 in 1% BSA, 0.1% Triton X-100, TBS, pH 7.4 (BTTBS) and incubated at 37°C for 1 hr. Coverslips were washed three times in BTTBS for 10 minutes each on a rotary shaker at

room temperature. Coverslips were incubated with colloidal gold labelled antibodies (1:100 dilution in BTTBS) for 2 hrs. at 37°C and washed as above.

For silver enhancement of colloidal gold, samples were washed thoroughly in double distilled deionized water and placed into dry multiwell plates (cell side facing up). Approximately 300 µl of silver enhancement reaction solution (Amersham Inc.) was added to each sample, and the enhancement was observed in progress using a 40X water immersion objective. Visualization of brown colored cellular staining indicated a positive signal and the reaction was terminated. The time taken in the silver enhancement reaction for a strong visual signal to be observed reflected the size of the gold particle and extraction/fixation conditions. The methodological development of SAG for correlative light and electron microscopic ISH have been reported in an extended format (Bassell, in press).

Detection of cytoskeletal proteins was accomplished in analogous fashion to biotinated probes. Several monoclonal antibodies were screened by light and electron microscopy using silver enhancement of one nm gold labelled goat anti-mouse secondary antibodies (Amersham Inc.). The objective was to obtain monoclonals which could tolerate glutaraldehyde fixation (2% paraformaldehyde 0.2% glutaraldehyde) in order to preserve the ultrastructural morphology of polysomes and cytoskeletal filaments. Also, the monoclonals had to exhibit strong labelling

following a hybridization in 15% formamide 2X SSC for 30 minutes. The following antibodies were selected for this study: anti-actin (East Acres Inc., Boehringer-Mannheim), antivimentin (Boehringer-Mannheim, Amersham Inc.), anti-tubulin (Amersham), antifilamin (Sigma Chemical Co., Amersham Inc.), anti-alphaactinin (Sigma), anti-vinculin (Sigma). The last two antibodies did not tolerate hybridization conditions and warranted that their detection be performed first, followed by postfixation, hybridization and probe detection. For double labelling of cytoskeletal proteins with poly(A) mRNA, the rabbit antibiotin antibody was co-incubated with the above monoclonals. Similarly, goat anti-rabbit (10nm gold) antibody was co-incubated with goat anti-mouse (5nm gold) antibody in the secondary incubation.

Controls

For in situ hybridization, control biotinated oligo-dA probes were hybridized in parallel to oligo-dT in all experiments. At the light microscope level using silver enhancement, oligo-dT and oligo-dA samples were run simultaneously with the same reaction mixtures. Both oligo-dT and oligo-dA hybridizations were evaluated ultrastructurally. For unenhanced 10nm colloidal gold labelled antibody samples which were evaluated at the electron microscope, quantitation of signal-to-noise ratios was obtained by counting gold particles in oligo-dT and oligo-dA samples. Also,

parallel oligo-dT and oligo-dA samples were silver enhanced for light microscopic signal-to-noise evaluation.

The evaluation of the specificity obtained with the monoclonal antibodies to cytoskeletal proteins was based on light microscopic staining patterns, i.e. actin ruffles, antigen specific ultrastructure i.e. MTOC, stress fiber and filament diameter measurements (thin sections). Antibody specificity was also confirmed on Western blots (see appendix-1). To control for nonspecific binding, control antisera and/or no primary antibody samples were routinely performed in all experiments.

Electron Microscopy

For thin sectioning, coverslips were post fixed in 2% osmium in PBS for 30 minutes. After rinsing in distilled H_2O samples were dehydrated to absolute ethanol through a series of graded EtOH. After treatment with propylene oxide poly/bed 812 (1:1) for 30-60 min at room temperature, samples were placed into 100% Epon for 1 h at room temperature. Beem capsules were filled with fresh 100% poly/bed 812 and quickly inverted onto the surface of the coverslips and polymerized for 48 h at 60°C. To remove the Beem capsules from the coverslip, samples were immersed in liquid nitrogen for a few seconds, and gently tapped to remove the Beem capsule. Thin sections (60-80nm) were stained with uranyl acetate (1.5% in 50% Ethanol), and Reynold's lead citrate for three and five minutes respectively.

For whole mounts, grids were teased from coverslips and dehydrated for critical point drying. All samples were evaluated with a Philips 400 transmission electron microscope.

REFERENCES

Abercrombie, M., J.E.M. Heaysman, and S.M. Pegrrum. 1971. The locomotion of fibroblasts in culture. *Exp. Cell Res.* 67:359-367.

Adams, A., E.G. Fey, S.F. Pike, C.J. Taylorson, H.A. White, and B.R. Rabin. 1983. Preparation and properties of a complex from rat liver of polyribosomes with components of the cytoskeleton. *Biochem. J.* 216:215-226.

Bachman, M., W.J. Mayet, H.C. Schroder, K. Pfeifer, K.-H.M. zum Buschenfelde, and W.E.G. Muller. 1986. Association of La and Ro antigens with intracellular structures HEp-2 carcinoma cells. *Proc. Natl. Acad. Sci. USA* 83:7770-7774.

Bagchi, T., D.E. Larson, and B.H. Sells. 1987. Cytoskeletal association of muscle-specific mRNAs in differentiating L6 rat myoblasts. *Exp. Cell Res.* 168:160-172.

Bassell, G.J., and R. H. Singer. 1991. Ultrastructural in situ hybridization using immunogold. **In** Electron Microscopy in Diagnosis and Research. M.A. Hyatt (ed.), *CRC Crit. Rev. Biochem.*, in press.

Ben-Ze'ev, A., M. Horowitz, H. Skodnik, R. Abulafia, O. Laub, and Y. Aloni. 1981. The metabolism of SV40 RNA is associated with the cytoskeletal framework. *Virology* 111:475-487.

Binder, M., S. Tourmente, J. Roth, M. Renaud, and W.J. Gehring. 1986. In situ hybridization at the electron microscope level: Localization of transcripts on ultrathin sections of lowicryll K4M-embedded tissue using biotinylated probes and protein A-gold complexes. *J. Cell Biol.* 102:1646-1653.

Bird, R.C. and B.H. Sells. 1986. Cytoskeleton involvement in the distribution of mRNP complexes and small cytoplasmic RNAs. *Biochim. Biophys. Acta* 868:215-225.

Bonneau, A.-M., A. Darveau, and N. Sonenberg. 1985. Effect of viral infection on host protein synthesis and mRNA association with the cytoplasmic cytoskeletal structure. *J. Cell Biol.* 100:1209-1218.

Brawerman, G. 1981. The role of the poly(A) sequence in mammalian messenger RNA. *CRC Crit. Rev. Biochem.* 10:1-38.

Bruckenstein, D.A., P.J. Lein, D. Higgins, and R.T. Fremeau,Jr.. 1990. Distinct spatial localization of specific mRNAs in cultured sympathetic neurons. *Neuron* 5:809-819.

Carter, K.C., K.L. Taneja, J.B. Lawrence. 1991. Discrete nuclear domains of poly(A) RNA and their relationship to the functional organization of the nucleus. *J. Cell Biol.* 115: 1191-1202.

Cervera, M., G. Dreyfuss, and S. Penman. 1981. Messenger RNA is translated when associated with the cytoskeletal framework in normal and VSV-infected HeLa cells. *Cell* 23:113-120.

Colman, D.R., G. Kreibach, A.B. Frey, and D.D. Sabatini. 1982. Synthesis and incorporation of myelin polypeptides into CNS myelin. *J. Cell Biol.* 95:598-608.

Dharmawardhane, S., M. Demma, F. Yang, J. Condeelis 1991. Compartmentalization and actin binding properties of ABP-50: The elongation factor-1 alpha of Dictyostelium. *Cell Motility and Cytoskel.* 20.

Farmer, S.R., A. Ben-Ze'ev, B.-J. Benecke, and S. Penman. 1978. Altered translatability of messenger RNA from suspended anchorage-dependent fibroblasts: Reversal upon cell attachment to a surface. *Cell* 15:627-637.

Fontaine, B., D. Sassoon, M. Buckingham, and J.P. Changeux. 1988. Detection of the nicotinic acetylcholine receptor a-subunit mRNA by in situ hybridization at neuromuscular junctions of 15-day-old chick striated muscles. *EMBO J.* 7:603-609.

Frigerio, G., M. Burri, D. Bopp, S. Barumgartner, and M. Noll. 1986. Structure of the segmentation gene paired and the Drosophila PRD gene set as part of a gene network. *Cell* 47:735-746.

Fulton, A.B., K.M. Wan, and S. Penman. 1980. The spatial distribution of polyribosomes in 3T3 cells and the associated assembly of proteins into the skeletal framework. *Cell* 20:849-857.

Garner, C.C., R.P. Tucker, and A. Matus. 1988. Selective localization of messenger RNA for cytoskeletal protein MAP2 in dendrites. *Nature(London)* 336:674-677.

Grossi de Sa, M.T., Martins de Sa, C., Harper, F., Olink-Coux, M., Huesca, M., et al. 1988. The association of prosomes with some of the intermediate filament networks of the animal cell. *J. Cell Biol.* 107:1517-1530.

Hartwig,J.H., and D.J. Kwiatkowski. 1991. Actin-binding proteins. *Curr. Opinion Cell Biol.* 3:87-97.

Heuser, J.E. and M.W. Kirschner. 1980. Filament organization revealed in platinum replicas of freeze-dried cytoskeletons. *J. Cell Biol.* 86:212-234.

Jeffery, W.R. 1982. Messenger RNA in the cytoskeletal framework: Analysis by in situ hybridization. *J. Cell Biol.* 95:1-7.

Jeffrey, W.R. 1984. Spatial distribution of mRNA in the cytoskeletal framework of Ascidian eggs. *Dev. Biol.* 103:482-492.

Jeffery, W.R., J.E. Speksnijder, B.J. Swalla, and J.M. Venuti. 1986. Mechanism of maternal mRNA localization in chaetopterus eggs. In Advances in Invertebrate Reproduction 4. M. Porchet, J.-C. Andries, and A. Dhainaut, editors. Elsevier Science Publishers B.V. (Biochemical Division), pp. 229-240.

Jeffery, W.R., C.R. Tomlinson, and R.D. Brodeur. 1983. Localization of actin messenger RNA during early ascidian development. *Dev. Biol.* 99:408-417.

Lawrence, J.B. and R.H. Singer. 1985. Quantitative analysis of in situ hybridization methods for the detection of actin gene expression. *Nucl.Acids Res.* 13:1777-1799.

Lawrence, J.B. and R.H. Singer. 1986. Intracellular localization of messenger RNAs for cytoskeletal proteins. *Cell* 45:407-415.

Lenk, R. and S. Penman. 1979. The cytoskeletal framework and poliovirus metabolism. *Cell* 16:289-301.

Lenk, R., L. Ransom, Y. Kaufmann, and S. Penman. 1977. A cytoskeletal structure with associated polyribosomes obtained from HeLa cells. *Cell* 10:67-78.

Macdonald, P.M. and G. Struhl. 1988. Cis-acting sequences responsible for anterior localization of bicoid mRNA in drosophila embryos. *Nature* 336:595-598.

McFadden, G.I., I. Bonig, E.C. Cornish, and A.E. Clarke. 1988. A simple fixation and embedding method for use in hybridization histochemistry on plant tissues. *Histochemical J.* 20:575-586.

Nickerson, J.A., and S. Penman. 1991. BioVision: microscopy in three dimensions. *Seminars in Cell Biology* 2:117-129.

Nielson, P., S. Goelz, and H. Trachsel. 1983. The role of the cytoskeleton in eukaryotic protein synthesis. *Cell Biology International Reports* 7:245-254.

Ornelles, D.A., E.G. Fey, and S. Penman. 1986. Cytochalasin releases mRNA from the cytoskeletal framework and inhibits protein synthesis. *Mol. Cell. Biol.* 6:1650-1662.

Pokrywka, N.J., and E.C. Stephenson. 1991. Microtubules mediate the localization of bicoid RNA during Drosophila oogenesis. *Development* 113:55-66.

Pollard, T.D. and J.A. Cooper. 1986. Actin and actin-binding proteins. A critical evaluation of mechanisms and functions. *Ann. Rev. Biochem.* 55:987-1035.

Pomeroy, M.E., J.B. Lawrence, R.H. Singer, and S. Billings-Gagliardi. 1991. Distribution of myosin heavy chain mRNA in embryonic muscle tissue visualized by ultrastructural in situ hybridization. *Dev. Biol.* 143:58-67.

Ramaekers, F.C.S., E.L. Benedetti, I. Dunia, P. Vorstenbosch, H. Bloemendal. 1983. Polyribosomes associated with microfilaments in cultured lens cells. *Biochim. Biophys. Acta.* 740: 441-448.

Rebagliati, M.R., D.L. Weeks, R.P. Harvey, and D.A. Melton. 1985. Identification and cloning of localized maternal mRNAs from Xenopus eggs. *Cell* 42:769-777.

Sabatini, D.D., G. Kreibich, T. Morimoto, and M. Adesnik. 1982. Mechanisms for the incorporation of proteins in membranes and organelles. *J. Cell Biol.* 92:1-22.

Schatz, G., and R.A. Butow. 1983. How are proteins imported into mitochondria? Cell 32:316-318.

Seeger, M.A. and T.C. Kaufman. 1990. Molecular analysis of the bicoid gene from drosophila pseudoobscura: identification of conserved domains within coding and noncoding regions of the bicoid mRNA. *EMBO J.* 9:2977-2987.

Sheiness, D., and J.E. Darnell. 1973. Polyadenylic acid segment in the mRNA becomes shorter with age. Nature 241:265-268.

Silva, F.G., J.B. Lawrence, and R.H. Singer. 1991. Progress toward ultrastructural identification of individual mRNAs in thin section: myosin heavy-chain mRNA in developing myotubes. *Tech. Immunocytochem.* 143:58-67.

Singer, R.H., G.L. Langevin, and J.B. Lawrence. 1989. Ultrastructural visualization of cytoskeletal mRNAs and their associated proteins using double-label in situ hybridization. *J. Cell Biol.* 108:2343-2353.

Singer, R.H., J.B. Lawrence, F. Silva, G.L. Langevin, M. Pomeroy, and S. Billings-Gagliardi. 1989. Strategies for ultrastructural visualization of biotinated probes hybridized to messenger RNA in situ. In Current Topics in Microbiology and Immunology. A.T. Haase (eds.) Springer-Verlag, Berlin-Heidelberg. 55-69.

Skalli, O. and R.D. Goldman. 1991. Recent insights into the assembly, dynamics, and function of intermediate filament networks. Cell Motility and the Cytoskeleton 19:67-79.

Small, J.V., and J.E. Celis. 1978. Filament arrangements in negatively stained cultured cells: the organization of actin. Eur. J. Cell Biol. 16:308-325.

Sundell, C.L. and R.H. Singer. 1990. Actin mRNA localizes in the absence of protein synthesis. *J. Cell Biol.* 111:2397-2403.

Sundell, C.L. and R.H. Singer. 1991. Requirement of microfilaments in sorting of actin messenger RNA. *Science* 253:1275-1277.

Trapp, B.D., T. Moench, M. Pulley, E. Barbosa, G. Tennekoon, and J. Griffin. 1987. Spatial segregation of mRNA encoding myelin-specific proteins. *Proc. Natl. Acad. Sci. USA* 84:7773-7777.

van Venrooij, W.J., P.T.G. Sillekens, C.A.G. van Eekelen, and R.J. Reinders. 1981. On the association of mRNA with the cytoskeleton in uninfected and adenovirus-infected human KB cells. *Exp. Cell Res.* 135:79-91.

Vandekerckhove, J. 1990. Actin-binding proteins. *Curr. Opinion Cell Biol.* 2:41-50.

Walter, P., R. Gilmore, and G. Blobel. 1984. Protein translocation across the endoplasmic reticulum. *Cell* 38:5-8.

Wolosewick, J.J. and K.R. Porter. 1979. Microtrabecular lattice of the cytoplasmic ground substance: Artifact or reality. *J. Cell Biol.* 82:114-139.

Yang, F., M. Demma, V. Warren, S. Dharmawardhane, and J. Condeelis. 1990. Identification of an actin-binding protein from dictyostelium as elongation factor 1a. *Nature* 347:494-496.

Yang, H.-Y., N. Lieska, A.E. Goldman, and R.D. Goldman. 1985. A 300,000-mol-wt intermediate filament-associated protein in baby hamster kidney (BHK-21) cells. *J. Cell Biol.* 100:620-631.

Yisraeli, J.K., S. Sokol, and D.A. Melton. 1990. A two-step model for the localization of maternal mRNA in xenopus oocytes: Involvement of microtubules and microfilaments in the translocation and anchoring of Vg1 mRNA. *Development* 108:289-298.

Zambetti, G., E.G. Fey, S. Penman, J. Stein, and G. Stein. 1990. Multiple types of mRNA-cytoskeleton interactions. *J. Cell. Biochem.* 44:177-187.

Zambetti, G., W. Schmidt, G. Stein, and J. Stein. 1985. Subcellular localization of histone messenger RNAs on cytoskeleton-associated free polysomes in $HeLa_3$ cells. *J. Cell. Phys.* 125:345-353.

Zambetti, G., J. Stein, and G. Stein. 1990. Role of messenger RNA subcellular localization in the posttranscriptional regulation of human histone gene expression. *J. Cell. Phys.* 144:175-182.

Zambetti, G., L. Wilming, E.G. Fey, S. Penman, J. Stein, and G. Stein. 1990. Differential association of membrane-bound and non-membrane-bound polysomes with the cytoskeleton. *Exp. Cell Res.* 191:246-255.

Zamore, P.D., M.L. Zapp, and M.R. Green. 1990. RNA binding: Bs and Basics. *Nature* 348:485-487.

Zumbe, A., C. Stahli, and H. Trachsel. 1982. Association of a M_r 50,000 cap-binding protein with the cytoskeleton in baby hamster kidney cells. *Proc. Natl. Acad. Sci. USA* 79:2927-2931.

CHAPTER V

VISUALIZATION OF SINGLE mRNA MOLECULES AT CYTOSKELETAL INTERSECTIONS

INTRODUCTION

There is now considerable biochemical evidence which indicates that mRNA is translated on the cytoskeleton (reviewed in Nielson et al, 1983; Hesketh and Pryme, 1991). In the original work (Lenk et al, 1977), greater than 97% of cellular polysomes were bound to an insoluble cytoskeletal fraction, whereas monomeric ribosomes were contained in the soluble fraction. These observations have been extended by studies showing that mRNAs are concentrated in cytoskeletal fractions using probes for total polyadenylated mRNA (Cervera et al, 1981; Ben-Ze'ev et al, 1981; Ornelles et al, 1986), and numerous mRNA species (Bonneau et al, 1985; Singer et al, 1989; Zambetti et al, 1985). The use of viral model systems has demonstrated that mRNA is translated only when bound to the cytoskeleton; therefore, this association may be obligatory for protein synthesis (Cervera et al, 1981; vanVenrooij et al, 1981; Ben-Ze'ev et al, 1981; Bonneau et al, 1985).

The mechanisms involved in the attachment of mRNA to the cytoskeleton are only poorly understood. There is considerable evidence which indicates that attachment of mRNA to the

cytoskeleton is independent of the polysome and can occur in the presence of protein synthesis inhibitors (Lenk et al, 1977). The poly(A) sequence has been shown to be involved in the attachment of mRNA to the cytoskeleton (Taneja et al, submitted). Cytoskeletal interactions with both ribosomes (Howe and Hershey, 1984; Suprenant et al, 1989) and nascent peptides (Zambetti et al, 1985) have also been demonstrated, which is independent of the mRNA. Other biochemical reports have indicated an association of translational factors with the cytoskeleton, independent of mRNA (Howe and Hershey, 1984; Dang et al, 1983; Mirande et al, 1985). Recently, an actin binding protein in Dictyostelium was shown by sequence analysis to be EF-1a (Yang et al, 1990), suggesting a direct relationship between the cytoskeleton and translational machinery. All of the above data suggest that multiple sites exist on an mRNP which control both the attachment and translation of mRNA on the cytoskeleton.

The association of mRNA with the cytoskeleton is also involved in influencing the intracellular location of protein synthesis. In Drosophila oocytes, the localization of bicoid RNA to the anterior pole is microtubule dependent (Pokrywka and Stephenson,1991) and requires a 625-nt 3'UTR sequence (Macdonald and Struhl,1988). In Xenopus oocytes, the localization of veg-1 RNA to the posterior pole requires both microfilaments and microtubules (Yisraeli et al 1990) and is mediated by a 360-nt 3' UTR sequence (Mowry and Melton,

1992). In somatic cells, the targetting of actin mRNA to fibroblast lamella is dependent on microfilaments (Sundell and Singer, 1991) and requires a 120-nt 3'UTR sequence (Kislauskis and Singer, in preparation). In summary, the interaction of mRNP with the cytoskeleton is a highly complex process and involves multiple components which mediate attachment, translation and intracellular location.

A basic biological question concerning the interaction of mRNP with the cytoskeleton can be answered through the direct visualization of mRNA molecules in situ. It is not understood what cytoskeletal components are involved in the attachment of mRNP to the cytoskeleton or functionally involved in the spatial control of protein synthesis. The use of in situ hybridization techniques for electron microscopy could potentially provide the resolution to localize single mRNA transcripts and study their direct interaction with cytoskeletal filaments. The high resolution provided by the electron microscope (0.3 nm) permits visualization of mRNA at the level of a single cytoskeletal filament and is ideally suited for this analysis. This technology would specifically reveal the cytoskeletal location involved in the attachment and translation of mRNA and provide information concerning the mechanism of attachment between mRNA and the cytoskeleton.

Localization of single mRNA molecules would also demonstrate how close mRNA molecules are positioned with respect to one another within the cytoskleton. This work is likely

to have further implications toward understanding if functionally related proteins can be synthesized at the same site to promote assembly of macromolecular complexes? Previous light microscopic reports have indicated that nonuniform intracellular distributions of mRNA may correlate with the synthesis of proteins at their sites of assembly. For example, actin mRNA was localized to the fibroblast leading edge where actin is actively polymerizing (Lawrence and Singer, 1986). Myelin basic protein mRNA was localized to oligodendrocyte processes, where MBP is involved in compaction of the myelin sheath (Trapp et al, 1987). However, it is not possible with the light microscope to study how the mRNA-cytoskeletal association could be involved in the synthesis of proteins near specific cell structures. The ultrastructural detection of single mRNA molecules would be an essential technology in determining whether and how the mRNA-cytoskeletal interaction is involved in the synthesis of macromolecular complexes at their site of function.

We have been developing high resolution in situ hybridization techniques for electron microscopy (Singer et al, 1989; Silva et al, 1991; Bassell and Singer, 1991). Using colloidal gold conjugated antibodies for the detection of biotinated probes, the ultrastructural appearance of hybridization to actin mRNA was in the form of tightly linked clusters of gold particles present in spiral or circular conformations (Singer et al, 1989). Hybridization to myosin heavy chain mRNA, which is considerably larger than

actin mRNA, was characterized by the presence of comparatively longer clusters of gold particles (Pomeroy et al, 1991). Therefore, the data suggested that the gold particle clusters were consistent with biotinated probe molecules hybridizing to a template, but it was impossible to distinguish between one or perhaps several mRNA molecules. Recent data in our laboratory however indicated that the length of gold particle clusters is not always proportional to the size of the target mRNA. For example, histone mRNA gold particle clusters were as large as those observed for considerably larger mRNAs (Chapter II), suggesting the clustering of multiple mRNA molecules (in preparation). The identification of a single mRNA molecule, and analysis of its cytoskeletal localization requires detection methods with superior resolution.

In this study, the development of novel high resolution in situ hybridization techniques to visualize single polyadenylated mRNA molecules is described. Since the majority of mRNAs possess poly (A) tails at their 3' ends (Sheiness and Darnell, 1973; Brawerman, 1981), this provided a convenient sequence to probe and permitted conclusions of general significance to cellular mRNA. The technology developed to visualize single mRNA molecules was threefold: (1) Chemically labelled oligonucleotide probes with one single biotin moiety per probe molecule and primary reagents directly conjugated to one gold particle. This results in a single probe molecule detected by a single gold particle. (2) Double label detection of two nucleic acid sequences

using biotin and digoxigenin labeled oligonucleotide probes. Two oligonucleotide probes having an identical sequence, but labelled with different haptens, could be hybridized in competition to the same mRNA sequence. Characterization of immunogold detection signal permitted unequivocal identification of a single mRNA molecule. The hybridization of oligonucleotide probes to nonoverlapping sequences of an individual mRNA permitted the visualization of different portions of an mRNA molecule with extremely high resolution. (3) Reverse transcriptase in the presence of labelled nucleotides to extend hybridized primers in situ. This methodology also permitted visualization of the conformation of a single mRNA molecule.

These high resolution methods not only permitted unequivocal identification of single mRNAs, but also the precise cytoskeletal location(s) where single mRNA molecules are translated. It was found that poly(A) mRNA is not uniformly distributed along cytoskeletal filaments, but localized to their intersections. Single mRNA molecules were detected at intersections and this localization was shown not to require polysome binding. The specific use of oligonucleotide probes targetted to actin mRNA suggested that the intersection may be the domain of only 1-2 mRNA molecules. In a parallel study, it is demonstrated that these can be intersections of microfilaments or intermediate filaments (Chapter IV). The implications of these

findings for cytoskeletal roles in protein synthesis and sorting are discussed.

RESULTS

Intracellular Distribution of Poly(A) mRNA- Correlative Light and Electron Microscopy

We have recently described the utilization of a silver enhancement detection method to correlate light and electron microscopic in situ hybridization (Bassell and Singer, 1991). Previous methods for ultrastructural analysis with colloidal gold labelled antibodies did not permit observations at low magnifications with the electron microscope, nor could they be used for light microscopy. This prevented visualization of the overall hybridization signal i.e. signal to noise analysis of cell populations. By precipitating silver onto colloidal gold, the particles become large enough to be visible by light microscopy. These samples can also be evaluated by electron microscopy at lower magnifications than possible with unenhanced colloidal gold antibodies. This technology proved valuable in this study for the development of single mRNA molecule detection methodology.

Hybridization to poly (A) in Triton-extracted and glutaraldehyde fixed fibroblasts is detected using silver enhancement (Figure 29). We have previously shown using quantitative biochemical and microscopic methods that >90% of

FIGURE 29. Light Microscopic Detection of Biotinated Oligo-dT Probes using Silver Enhancement.

A. Hybridization of biotin-labelled oligo-dT to Triton-extracted glutaraldehyde fixed fibroblast culture. Detection using antibiotin and 10-nm gold labelled secondary antibody followed by silver enhancement.

B. Control oligo-dA (biotin) hybridization.

C. Biotin-labelled oligo-dT hybridization competed with excess unlabelled oligo-dT.

All silver enhancement reactions terminated at 7.5 minutes.

Bar, 50μm.

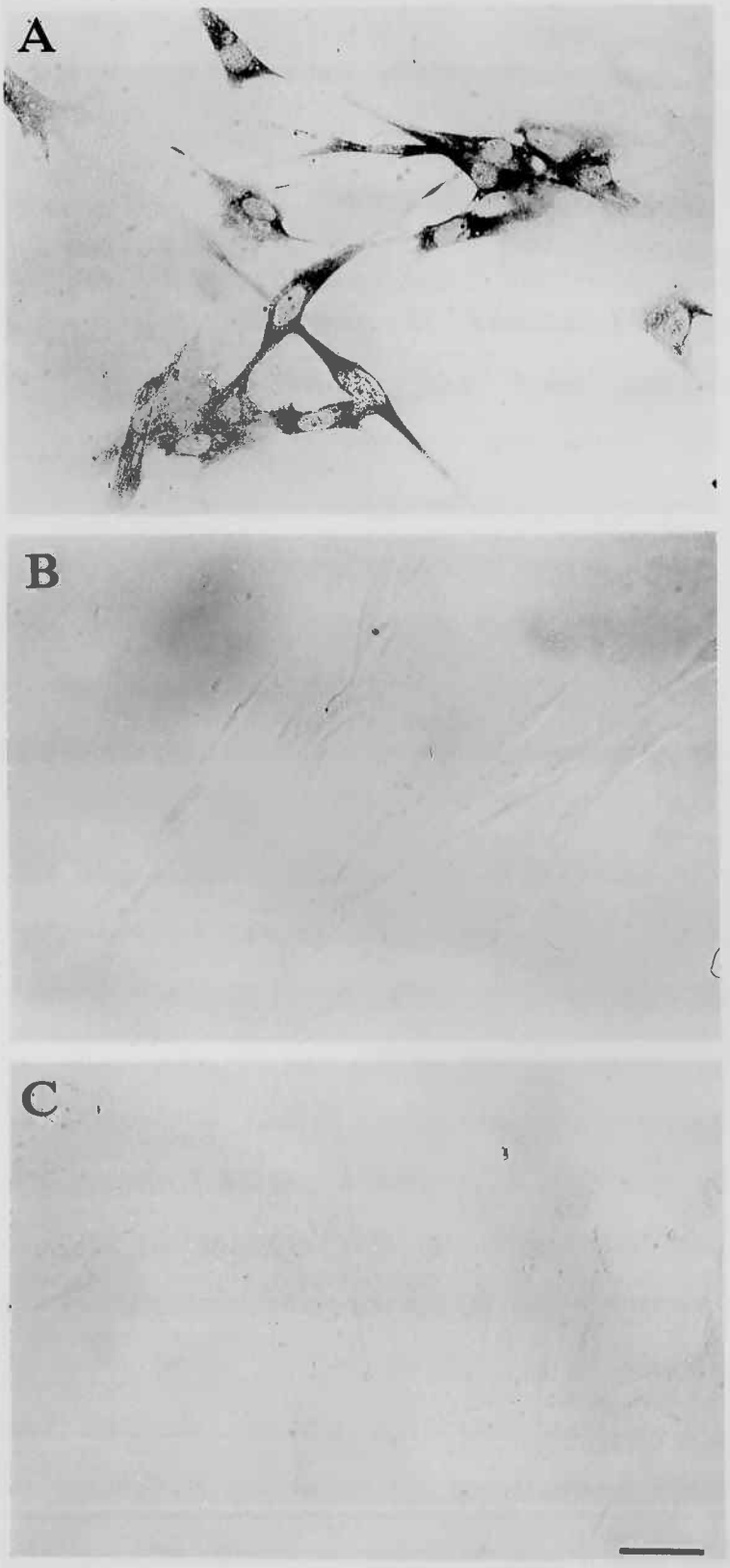
A
B
C

poly (A) mRNA is retained following this extraction procedure. Only minimal background was observed using biotinated oligo-dA probe or by competition of the biotinated oligo-dT probe with unlabeled oligo-dT (Fig. 29B-C).

Electron microscopic detection of biotinated oligo-dT hybridization by silver enhancement has been previously described (Chapter IV) in both thin sections and whole mounts. Thin section analysis revealed that >84% of the silver particles could be localized within 5nm of polysomes (Chapter IV, Figure 22). This indicated that the hybridization conditions had not adversely affected the translational apparatus and permitted ultrastructural analysis of the relationship of translated poly (A) mRNA with the cytoskeleton.

In thin sections and whole mounts, the distribution of poly (A) was not homogeneous along filaments, but appeared concentrated at or near filament intersections (Chapter IV, Figure 24). However, the large size of the silver particle (100-200nm) obscured fine structural analysis and it could not be determined if poly (A) was directly localized to the vertex. The objective of the silver enhancement was to provide low magnification electron microscpic and light microscopic analysis which were essential in evaluating signal to noise levels as well as the overall distribution of mRNA. Further analysis of the mRNA-vertex localization required the higher resolution provided by unenhanced colloidal gold labeled antibodies for electron microscopy. The silver

enhancement of colloidal gold labelled antibodies will be further utilized in this study at the light microscope level to evaluate new reagents and methods.

Localization of Poly(A) mRNA to Intersections

We used 10nm colloidal gold labelled antibodies to detect hybridized poly(A) in situ with high resolution. The electron microscopic appearance of oligo-dT(biotin)hybridization was in the form of individual gold particles and tightly linked gold particle clusters. The quantitative relationship between the number of particles per unit area and the number of particles per cluster is shown in Figure 30. A signal to noise ratio of 7.6:1 is obtained for single gold particles (oligo-dT/oligo-dA) and increased to 17.8:1 when three or more particles were present within a cluster. This qualitative and quantitative distinction between hybridization and nonspecific binding has been previously observed when biotinated probe molecules are hybridized to mRNA templates which are significantly larger than the probe (Singer et al, 1989; Pomeroy et al,1991). For example, for detection of 2Kb actin mRNAs, a signal to noise ratio of 3:1 was observed for single particles and increased to 30:1 for > 7 gold particles per cluster. The GPC's observed here for oligo-dT

FIGURE 30: Ultrastructural Detection of Biotin Labeled Oligo-dT Probes- Immunogold Quantitation

Analysis of fifty EM micrograph (over $1000\mu^2$ total cellular area). Photographs were taken at perinuclear, central and peripheral regions from ten cells in oligo-dT (biotin) samples and six cells in control oligo-dA (biotin) samples. Data from three independent hybridizations to Triton-extracted glutaraldehyde (4%) fixed fibroblasts. Signal-to-noise ratios for each size GPC are indicated between bars.

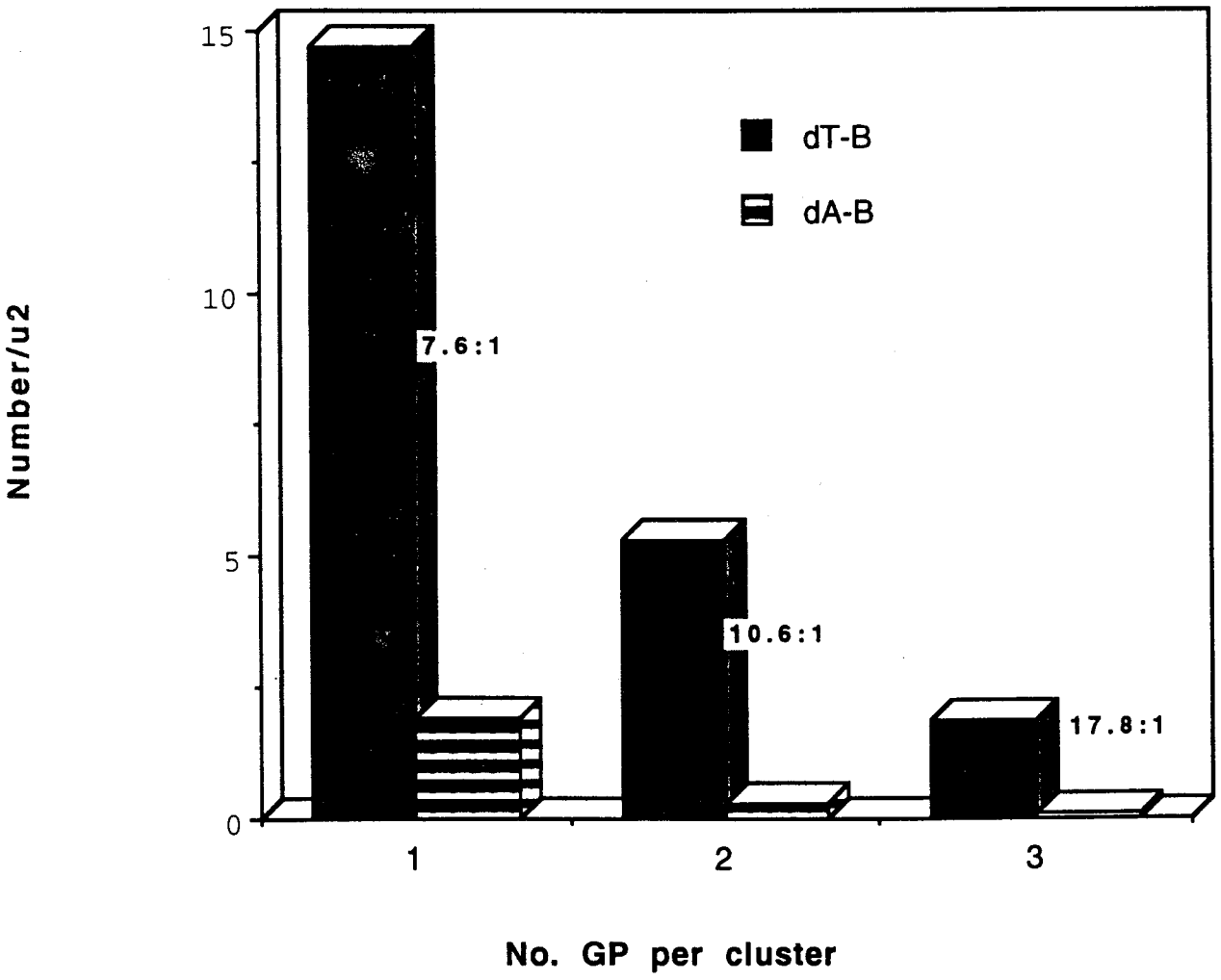

probes are significantly smaller, i.e. only rarely larger than five particles. However, it was unclear why detection of poly (A) tails, a template comparable in size to the probe (50nts), would result in an increase in signal to noise ratios as the size of GPC increased. Steady state poly(A) tail measurements indicate a range from 50-70 bases (Sheiness and Darnell, 1973). The oligo-dT probe molecule consists of a chemically synthesized fifty-five nucleotide deoxythymidine sequence which is 3'-end labeled with approximately 10-25 biotinated deoxyuridine residues (determined by gel electrophoresis). Therefore the majority of poly (A) tails will be hybridized by a single probe molecule.

What then accounts for the increase in cluster size? Amplification of the immunogold detection procedure might occur through the binding of >1 primary antibody to a terminal transferse tail and/or >1 secondary antibody to the primary antibody. However, this amplification cannot explain why larger GPC's are statistically more likely to represent hybridization to poly (A). One explanation, is that these large GPC's (size>3) represent the hybridization of >1 probe molecule to larger poly(A) tails. Newly synthesized poly(A) tails range from 200-300 adenylate residues and represent approximately ten percent of total poly(A) mRNA (Sheiness and Darnell,1973). This is consistent with the data in Fig.30, which indicates that 8.4% of the GPC's contain three or more particles. However, an alternative explanation is that these large GPC's contain >1 poly(A) mRNA

molecule. This might occur because poly(A) binding protein has four binding sites for poly(A), although it is not known whether this protein actually binds more than one mRNA molecule (Sachs and Kornberg, 1985). Both of these possibilities would be expected to produce clustering of gold particles.

The colloidal gold detection has also permitted an estimation of the hybridization and detection efficiency. From the data in Fig.30, if each gold particle clusters is assumed to be a single mRNA and the amounts per μ^2 for each size category are totaled (14.7+5.3+1.8=27) and corrected by removing background, there are an average of 25 mRNA molecules/μ2. Multiplication by an average cell area of 1000 μ^2 estimates that approximately 25,000 poly(A) mRNA molecules per cell are detected by this methodology. This is actually an underestimaton of the actual hybridization efficiency since most of the micrographs analyzed were not from thick cellular regions i.e. perinuclear, which contain the largest fraction of mRNA. Using biochemical analysis, the number of poly (A) mRNA molecules has been estimated at 200,000 in cultured myoblasts (Schwartz and Rothblum, 1981).

The majority of gold particle clusters (>72%) were localized to cytoskeletal intersections and not uniformly distributed along individual filaments. Figure 31 is a sampler of some of the types of intersections containing poly(A) mRNA. The labelled intersections exhibited complex branching patterns and were composed of between 2-5 filaments. In order to verify that the

FIGURE 31: Localization of Poly(A) to Cytoskeletal Filament Intersections.

(A) Highly branched vertex (arrow). Bar, 100nm.

(B) Poly(A) associated with an intersection of two filaments (large arrow), and along an individual filament (within 10nm of intersection).

(C) Thin section of an intersection containing poly(A) mRNA.

(D) Poly(A) mRNA localized to points along individual filaments.

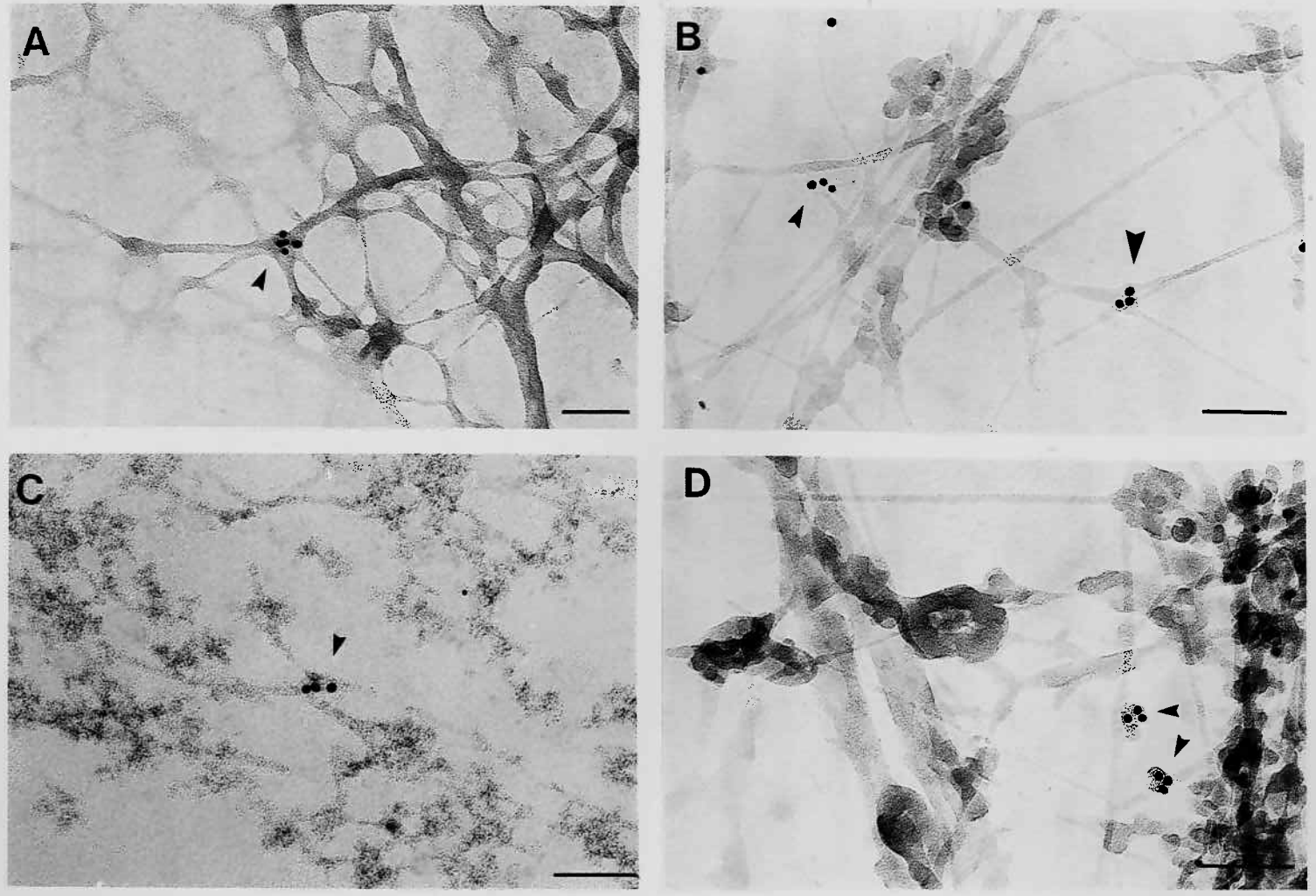
A
B
C
D

gold particles were directly attached to the intersection, the localization of poly(A) to intersections was confirmed in thin sections (Fig.31C). Poly(A) mRNA was less frequently localized to sites along the length of single filaments (Fig.31D). The localization of poly(A) to cytoskeletal intersections is quantitated from three hybridizations (Table 4), and demonstrates a strong correlation with these structures.

Resolution of Single mRNA Molecules -Stoichiometric Reduction

The next series of experiments involved the development of ultrastructural methods to permit the unequivocal visualization of a single poly(A) mRNA molecule. This technology is critical to identify how individual mRNA molecules are positioned and spaced within the cytoskeleton. One approach was to develop a sensitive colloidal gold detection method which possessed a stoichiometry of one gold particle for one probe molecule. This method would eliminate the ambiguity of the previous method which resulted from amplification in the number of gold particles due to the antibodies. The first step toward this goal was to synthesize an oligo-dT probe which had only a single biotin molecule. Through the use of a nucleotide modified with an amino group on a linker arm in the 2' position, biotin groups can be attached at precise locations within the chemically synthesized oligonucleotide. The light microscopic detection of this probe

TABLE 4: Ultrastructural Localization of Poly(A) mRNA

Localization of poly(A) mRNA
to Cytoskeletal Intersections

Hybridization	Intersection (%)
1	72
2	82
3	76

The gold particles included in this analysis required visual distinction between a single filament or intersection of two or more filaments. The large depth of field in a whole mount preparation therefore limits the number of scorable molecules. Two hundred gold particles (GPC) of size >3 particles were selected from micrographs of three oligo-dT (biotin) hybridizations. Prior quantitation of signal-to-noise ratios (Fig. 30) indicated that the probability is 95% that these signals represent hybridization to poly(A) mRNA. GPCs were scored as localized to single filament if they were >10nm from the intersection. The percent of GPCs which are associated with intersections is indicated above.

using the two step silver enhancement procedure resulted in excellent signal to noise ratios. The next goal was the development of a method for direct detection of single probe molecules. To this end we screened colloidal gold labelled reagents which would bind the biotin molecule at a ratio of 1:1. Reagents using avidin labelled to gold were tested from several sources, but only weak signals were observed. Antibodies to biotin which were directly labelled to gold produced acceptable binding; the silver enhancement reaction times were a few minutes longer than using gold labelled secondary antibodies. The most sensitive method employed an antibody to biotin followed by Protein A labeled gold, an F_C receptor which binds to immunoglobulins at a 1:1 ratio. The detection of the oligo-dT probe with a single biotin group using Protein-A(10nm gold) and silver enhancement is shown in Figure 32. A decrease in sensitivity was observed compared to the probe with multiple biotins on the 3' end. This suggested that more than one antibody to biotin can bind a hybridized probe molecule labeled with multiple biotins.

The ultrastructural detection of oligo-dT probes with a single biotin using an antibody to biotin and Protein-A labelled revealed that >90% of the hybridization signal was in the form of individual gold particles (Figure 33, Table 5). The number of single gold particles was significantly above background (signal to

FIGURE 32. Light Microscopic Detection of Poly (A) mRNA using Silver Enhancement: Methodological Development for High Resolution Immunogold.

A. Hybridization of chemically biotinated oligo-dT probe (one biotin group) to triton-extracted paraformaldehyde fixed fibroblast culture. Detection using antibiotin and 10-nm gold labelled protein-A followed by silver enhancement.

B. Hybridization of chemically biotinated oligo-dA probe. Detection using Protein-A.

C. Detection of digoxigenin labelled oligo-dT using a monoclonal antidigoxigenin antibody and 5-nm gold labelled secondary antibody followed by silver enhancement.

D. Hybridization of oligo-dA (digoxigenin) Detection using antidigoxigenin monoclonal antibody.

E. Detection of oligo-dT (digoxigenin) using directly conjugated antidigoxigenin polyclonal antibody (5nm gold).

F. Hybridization of oligo-dA (digoxigenin). Detection using directly conjugated antibody.

Bar, 50μ

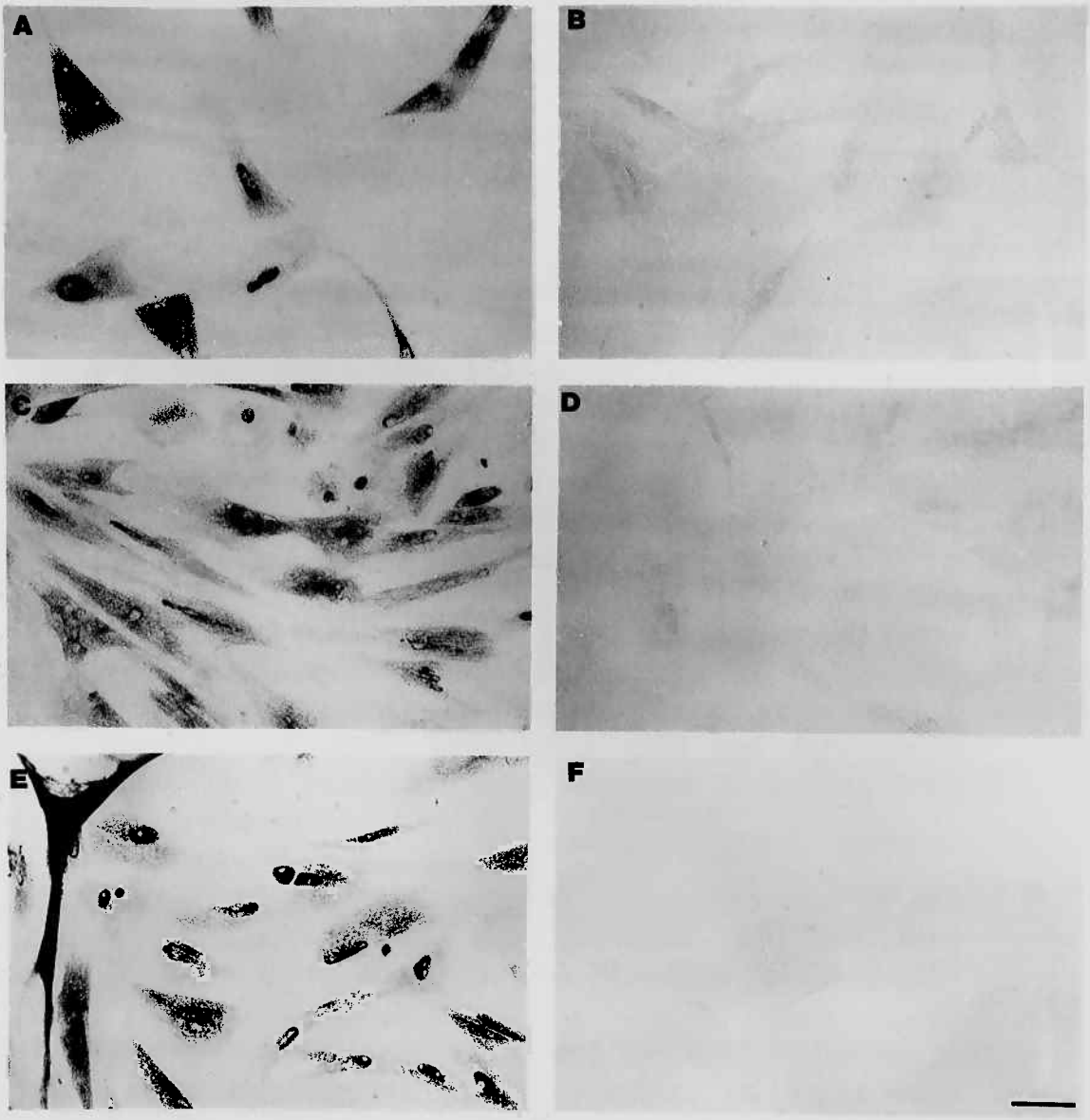
A
B
C
D
E
F

FIGURE 33. Ultrastructural Visualization of Single mRNA Molecules using High Resolution Detection Methods.

A. Hybridization of chemically biotinated oligo-dT is detected using antibiotin and Protein-A (10nm gold) whole mount preparation. Single gold particles correspond to detection of single oligonucleotide probe molecules.

B. Same as (A) except cells were treated with puromycin (100ug/ml for 45 minutes) prior to Triton-extraction and fixation.

C. Simultaneous hybridization of biotinated oligo-dT and digoxigenin labelled oligo-dT, detection of biotin using rabbit antibiotin and goat anti-rabbit (15nm gold). Detection of digoxigenin using mouse antidigoxigenin and goat anti-mouse (5 nm gold). Detection of digoxigenin using mouse antidigoxigenin and goat anti-mouse (5nm gold). The majority of gold particle clusters (85%) contain one size of gold. Example of a cluster containing both 5nm and 10nm gold particles (arrowhead).

D-E. Hybridization of one biotinated actin oligonucleotide probe and four digoxigenin labelled actin oligonucleotides to specific nucleic acid sequences along the length of an actin mRNA molecule. Detection of biotin with 10nm gold and digoxigenin with 5nm gold. Gold particle cluster observed containing both sizes of gold (arrowhead).

F-G. Hybridization of unlabelled oligo-dT primer extended in situ using reverse transciptase in the presence of biotinated nucleotide. Detection using antibiotin and Protein-A (10nm gold).

H. Hybridization of chemically biotinated oligo-dT extended in situ using reverse transcriptase in the presence of digoxigenin labelled nucleotide. Detection of biotin using Protein-A (10nm gold) and directly conjugated antidigoxigenin antibody (5nm gold). Orientation of the poly(A) tail (10nm particle) and 5' sequences (5nm particles) at cytoskeletal intersection.

Bar, 100nm.

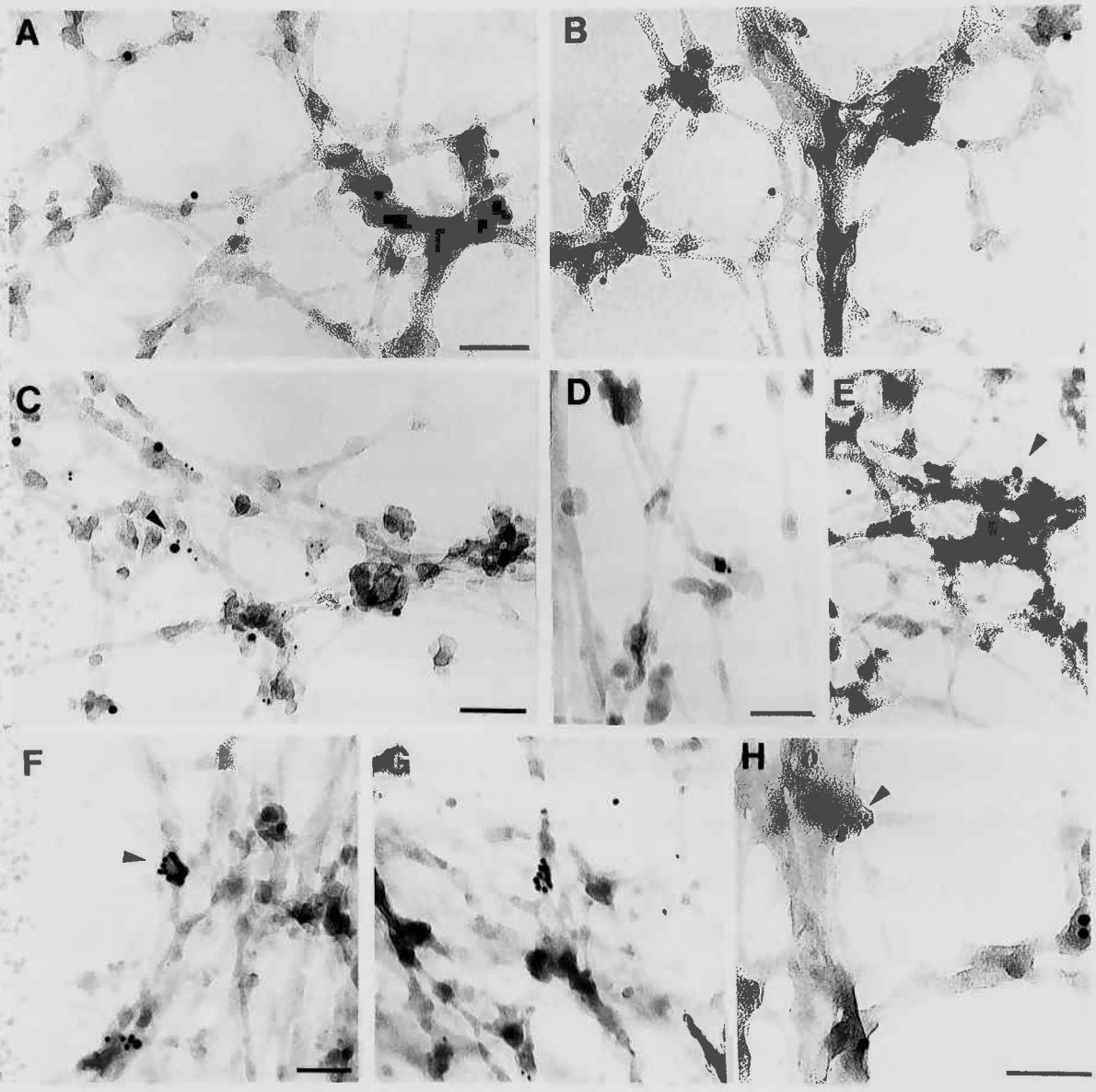
A
B
C
D
E
F
G
H

TABLE 5. Ultrastructural Localization of Poly(A) mRNA: Correspondence of Single Gold Particles to Single Oligonucleotide Probe Molecules.

	Untreated	Puromycin
Single Particles	91%	87%
Vertex Localization	77%	72%
Signal/Noise Ratio (dT-B/ dA-B)	9:1	8.5:1

Fibroblasts grown on grid assembles were untreated or treated in puromycin (100ug/ml for 45 minutes). Cells were Triton-extracted (2 minutes) and fixed in glutaraldehyde (4%). Grids were hybridized with either chemically biotinated oligo-dT or oligo-dA probes and detected with antibiotin and Protein-A (10nm gold). Cells were photographed at 28,000X magnification. 4-5 micrographs were taken per cell, and 3-4 cells evealuated per probe. Above analysis compiled form over 400 individual gold particles in two oligo-dT hybridizations.

noise ratio of 9:1) and indicated that single poly(A) mRNA molecules were identified. As observed with the previous method which allowed amplification of gold particles, poly (A) mRNA was localized to cytoskeletal intersections (Fig.33) .

In order to identify the molecular components involved in the localization of poly(A) to the intersection, the effects of polysome dissociation were evaluated. Prior treatment of cells with puromycin had no significant effect on the localization of poly(A) to cytoskeletal vertices (Table 5). This treatment has previously been shown to release >90% of rRNA and only 10% of mRNA from the cytoskeleton (Taneja et al, submitted). These data indicate that the mechanism of localizing poly(A) mRNA to intersections does not involve the polysome or translational apparatus and is probably mediated by the mRNA and its associated proteins.

Double Label In Situ Hybridization Using Biotin and Digoxigenin Labelled Probes

To develop an additional approach to identify single mRNA molecules, a method was devised using two oligo-dT probes each labelled with a different hapten. Oligo-dT probes were enzymatically end labelled with either biotin or digoxigenin and then hybridized simultaneously. A monoclonal antibody to digoxigenin (BMB) and a polyclonal antibody to biotin were

incubated with the hybridized cells. Different sized colloidal gold labelled secondary antibodies were used to detect the mouse or goat antibodies. The light microscopic detection of these probes is shown in parallel samples in Figure 32. This demonstrated that each probe hybridized independently. At the ultrastructural level, >85% of the individual or clustered gold particles were of only one size of gold. In 15% of the scored events, both size particles occured together (<5nm apart). A sampler of the double label competition experiment is shown in Figure 33. The quantitation of the different types of signal is shown in Fig. 34.

What hybridization events in the above experiment would lead to both sized gold particles occurring together at a frequency of 15%? In the previous section, individual poly(A) mRNA molecules were identified by a single gold particle using a chemically biotinated probe and Protein-A labelled gold. This analysis also revealed that a minor component of the signal (10%) was in the form of clusters. One explanation for these data is that >1 mRNA molecule could be localized to a cytoskeletal intersection. However, since we do not have precise measurements on the efficiency of poly(A) detection by these methods (see above), it is not possible to resolve how many poly(A) mRNA molecules are localized at an intersection. An additional caveat is that the gold particle clusters with >1 particle in the previous section (Table 5), or the heteroclusters observed

FIGURE 34. Oligo-dT (biotin) and Oligo-dT (digoxigenin) probes were hybridized simultaneously to whole mount preparations. Biotin detection using antibiotin and 15-nm gold labelled secondary antibody. Digoxigenin detection using monoclonal antidoxigenin antibody and 5-nm gold labelled secondary antibody. Cytoskeletons were photographed at 28,000X magnification. Between 3-6 micrographs were taken per cell and 2-3 cells were evaluated per sample. Gold particles were grouped into three categories: Biotin (15 nm particles occuring individually or in a cluster), Digoxigenin (5nm particles, individual or clustered), and Hetero (cluster of 5 and 15 nm particles.) A cluster is defined as having >1 gold particle with < 3 nm spacing between particles. As a control, biotinated oligo-dA and digoxigenin labelled-oligo were evaluated similarly. Signal to noise ratios appear between dT and dA bars.

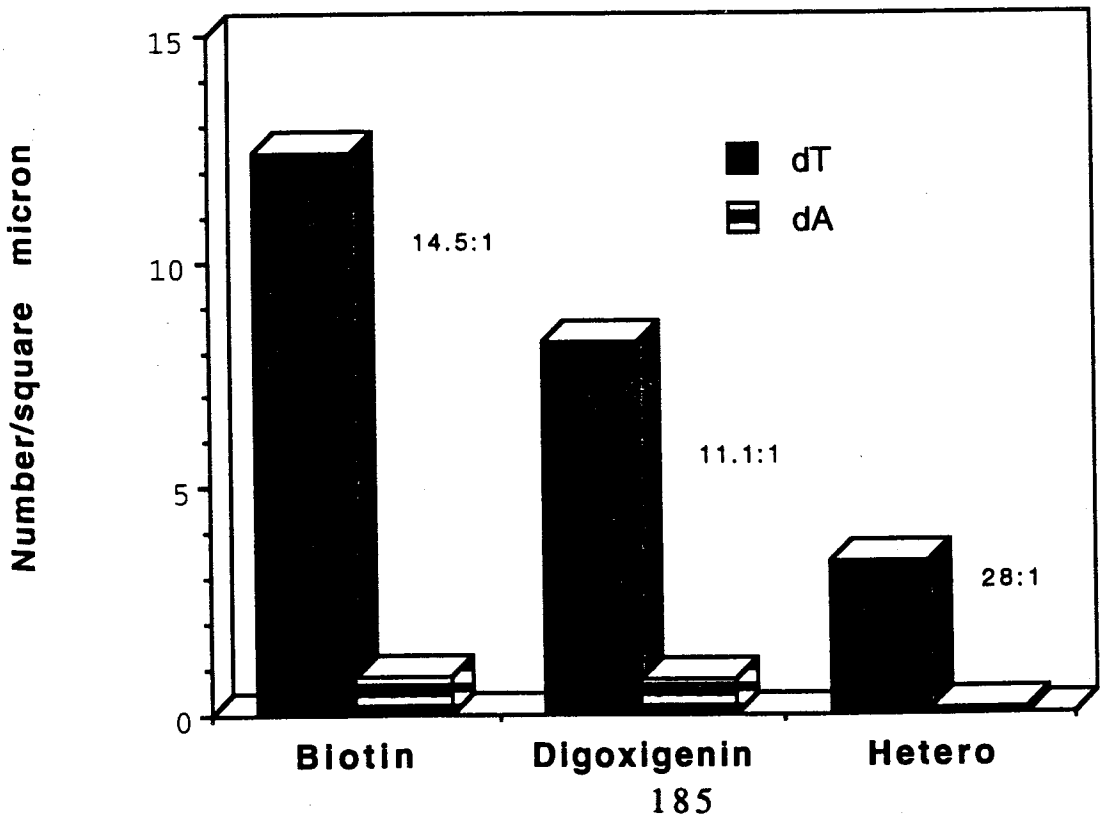

here (Figure 34) might be attributed to the hybridization of >1 oligo-dT probe molecule to a poly(A) tail.

In order to address these issues, the above double labelling approach was performed on a nonrepetitive sequence from a specific mRNA (actin) which presented less ambiguity as to whether each of the hybridized probe molecules localized intramolecularly (>1 oligo-dT probe per single mRNA) or intermolecularly (group of poly(A) mRNAs each hybridized with one oligo-dT probe). Oligonucleotide probes targeted to various coding and untranslated nucleic acid sequences along the length of β-actin mRNA (Taneja and Singer, 1987; Taneja and Singer, 1990) have been previously shown to hybridize at high efficiency. This provided a model system to apply the double label method for electron microscopy.

Figure 33D-E is an example of a gold particle cluster obtained when one oligonucleotide probe, labelled with biotin was hybridized to a 45 base coding sequence and detected by a 10nm particle. This particle is flanked by 5nm particles which occur from the hybridization of four digoxigenin labelled oligonucleotides to other non-overlapping nucleic acid sequences. Do clusters which contain both size gold particles correspond to individual mRNA molecules? To address this issue we devised an approach to quantitatively distinguish heteroclusters which were attributed to single or clustered mRNA molecules. In Figure 35A an oligonucleotide probe (#23) was labelled with either biotin or

digoxigenin and hybridized simultaneously to a 53nt coding sequence. Following immunogold detection, the majority of gold particle clusters (94%) contained only one size gold (homocluster). This signal is attributed to single and clustered mRNA molecules. The frequency of heteroclusters was 6% and shown to be quantitatively significant by comparison to control hybridizations. This signal can only be attributed to clustered mRNA molecules, since the two probes cannot hybridize to a single mRNA molecule. Similar results (2% heteroclusters) were observed in an analogous experiment with an oligonucleotide probe to a 3' UTR sequence (Figure 35B). By contrast, the simultaneous hybridization of oligo-19 (biotin) and oligo-23 (digoxigenin) to separate actin mRNA sequences resulted in 41% heteroclusters. This signal can be attributed to single and clustered mRNA molecules, compared to <6% heteroclusters (Figure 35A-B) which are attributed to only clustered mRNAs. This data suggests that both oligonucleotide probes can be detected along a single mRNA molecule. A complication to this analysis arises form the fact that the probability of obtaining heteroclusters is 2X higher in hybridizations of two oligonucleotide probes (Figure 35C) compared to hybridization with a single probe (Figure 35A-B). After this correction, which is based on a hybridization efficiency of 50%, the frequency of heteroclusters is still higher when two probes are targeted to separate sites.

The frequency of heteroclusters observed in the above experiment provides additional information on how many mRNA molecules might be clustered together i.e. single vertex. As the number of mRNAs within a cluster increase, the percentage of heteroclusters derived from clustered mRNAs increases at a faster rate than heteroclusters derived from a single mRNA. Therefore, at high mRNA copy numbers it will be impossible to distinguish single mRNAs from clustered mRNAs using the above approach. Since we were able to demonstrate an increase in the percentage of heteroclusters when single mRNA molecules are included in the signal (Figure 35C), compared to when they are not (Fig. 35A-B), this suggests that the clustered mRNA/single mRNA ratio must be low. This conclusion is further supported by statistical analysis of the heterocluster signal which is attributed to only clustered mRNAs (Figure 35A-B). If only one mRNA molecule is localized to a vertex, then no heteroclusters would be observed. Based on a 50% hybridization efficiency, the clustering of two mRNA molecules would result in 12% heteroclusters (0.5 X 0.5/ 2). If four mRNAs are colocalized, the probability of observing heteroclusters increases to 22% ($0.5^4 + 0.5^3 + 0.5^2$ /2). Since the observed frequency is less than 6% (Figure 35A-B), this suggests that intersections containing actin mRNAs have between 1 to 2 mRNA molecules. Further work is needed to extrapolate this data to poly(A) mRNA, which will involve additional quantitation of hybridization efficiency.

FIGURE 35. Two actin oligonucleotide probes were synthesized from non-overlapping actin mRNA sequences (oligo-19, oligo-23). Probes were labelled with biotin and digoxigenin in separate terminal transferase reactions.

(Panel 1) Hybridization of 23-B and 23-DG in competition to the same actin mRNA sequence. Following immunogold detection of biotin (10nm gold) and digoxigenin (5nm gold), signal was grouped into three categories: 5 nm gold particle cluster, 10nm gold particle cluster, 5 and 10 nm particle clusters.
(Panel 2). Similar competition experiment with oligo-19.
(Panel 3). Hybridization of oligo-19 (Biotin) and oligo-23 (Digoxigenin) to separate sequences along actin mRNA.

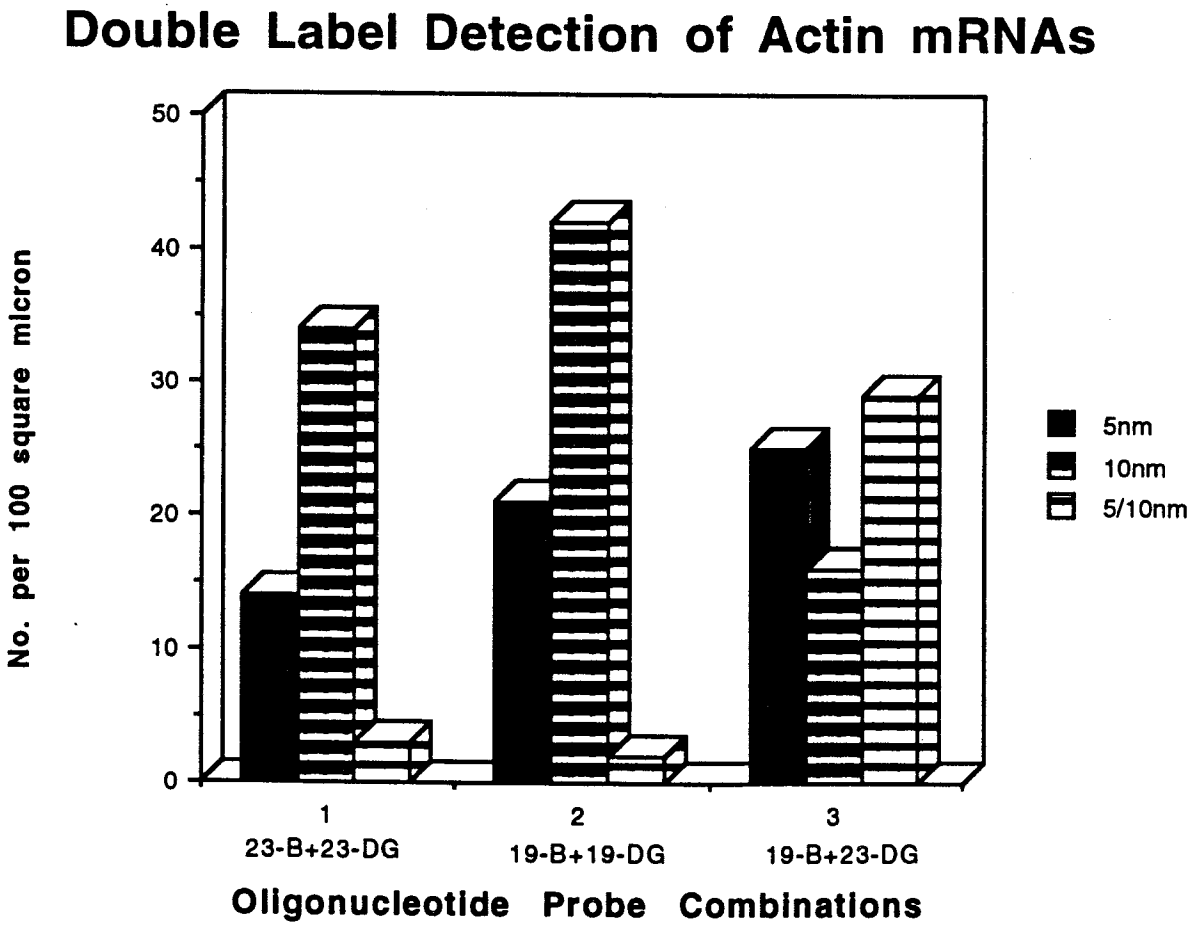

An additional caveat to these experiments is that due to the utilization of the amplified immunogold method (probes with multiple haptens, gold labelled secondary antibodies) most of the gold particle clusters did not exhibit the predicted arrangement of the 5 and 10nm gold particles. The further development of a 1:1 double label detection system should allow direct correlation of individual gold particles with intermolecular distances between hybridized probe molecules. The ultimate potential of this technology is to develop a "morse code" allowing one mRNA to be detected by a 10nm particle flanked at both ends by 5nm particles, and another mRNA detected by 5nm particles flanked by 10nm particles.

In Situ Transcription

The use of oligonucleotide probes modified with a single hapten moiety has permitted the detection of single mRNA molecules with ultrastructural resolution. The direct visualization of a single oligonucleotide probe molecule hybridized to a considerably larger mRNA molecule does not allow visualization of the the orientation or conformation of the mRNA molecule with respect to the cytoskeleton. Recent biochemical data has demonstrated that selective RNAase digestion of mRNA excluding the poly(A) tail does not release poly(A) from the cytoskeleton (Taneja et al, submitted). The ultrastructural analysis which

demonstrated that poly(A) is localized within 5nm of a vertex. This proximity suggested that the poly(A) tail may be the mRNP anchor for the vertex. The ability to directly visualize the poly(A) tail concomitant with the rest of the mRNA molecule could be a powerful tool to address this question. This technology would also be valuable for studying mRNA conformation in situ. Previous morphologic evidence has suggested the possibility that the mRNA is circular having 3'-5' interactions (Christenson et al, 1989).

In order to investigate the orientation and conformation of mRNA molecules, we describe here the use of reverse transcriptase to extend hybridized oligonucleotide primers in situ. The technique of in situ transcription (IST) was originally described (Tecott et al, 1988) utilizing ^{32}P labelled nucleotides and autoradiographic light microscopic detection. In situ transcription has not been reported for use with nonisotopic detection. Using the previously published method, no evidence of primer dependent signal could be obtained using an oligo-dT primer and biotinated nucleotides. A major difference between the published method and our preliminary experiment was the substitution of biotinated nucleotide for radiolabelled nucleotide. The following parameters needed to be evaluated in order to optimize in situ transcription for use with oligo-dT primers and biotinated nucleotides in fixed cell cultures: (1) fixation (2) primer size (3) choice of labelled nucleotide (4) unlabelled/labelled nucleotide ratio (5) post cDNA synthesis

TABLE 6: LIGHT MICROSCOPIC OPTIMIZATION OF IN SITU TRANSCRIPTION USING SILVER ENHANCEMENT

PRIMER	NUCLEOTIDES	WASH	PRETREATMENT	FIXATION	RESULT
dT55	*dA TG 250µM biotin-11-dCTP, 50nM no unlabelled dCTP	*2XSSC	Triton Extraction	Glutaraldehyde	No dT signal
dT55	dACG 250µM biotin-16-dUTP, 50µM no unlabelled dTTP	2XSSC	Triton Extraction	Glutaraldehyde	No dT signal
dT55	dACG 250µM biotin-16-dUTP, 50µM dTTP, 50µM	2XSSC	Triton Extraction	Glutaraldehyde	Fair dT signal
dT55	dACG 250µM biotin-16-dUTP, 50µM dTTP, 250µM	2XSSC	Triton Extraction	Glutaraldehyde	Strong dT signal primer independent cell specific staining
dT55	dATG 250µM bio-11-dCTP, 50µM dCTP, 250µM	2XSSC	Triton Extraction	Glutaraldehyde	Good dT signal primer independent background
dT32, dT23	dACG 250µM bio-16-dUTP, 50µM dTTP, 250µM	2XSSC	Triton Extraction	Glutaraldehyde	Good dT signal primer independent background
dT55	dACG 250µM bio-16-dUTP, 50µM dTTP, 250µM	15% formamide 2XSSC	Triton Extraction	Glutaraldehyde	primer indep. cyto. background removed
dT55	dACG 250µM bio-16-dUTP, 50µM dTTP, 250µM	15% formamide 2XSSC	None	Paraformaldehyde	weak dT signal
dT23, dT32 dT55	dACG 250µM bio-16-dUTP, 50µM dTTP, 250µM	15% formamide	+Puromycin Triton Extraction	Glutaraldehyde	dT^{55} stronger signal w/puromycin

*Based on original IST method (Tecott et al. 1988).

washes (6) polysome dissociation before extension. The specific details and rationale for these optmization are discussed in Material and Methods. The results of this optimization are summarized in Table 6, and are described below.

A major increase in signal was observed by increasing the biotinated nucleotide concentration (bio-16-dUTP) and providing diluted unlabelled nucleotide (dUTP). The signal to noise ratio was maximal at a ratio of 5:1 unlabelled/labelled nucleotide. At this ratio, biotinated dUTP produced a stronger signal than biotin-dCTP. Oligo-dT primers of size 23, 32 and 55 bases produced comparable results. In comparison to in situ hybridization with biotinated oligo-dT probes, the in situ transcription signal was of similar intensity, but the controls exhibited higher background levels. This background occurred in the absence of control primers and was not observed when the reverse transcriptase was omitted from the reaction buffer. This suggested that there may be endogenous priming sites for reverse transcription. Primer independent reverse transcription was also observed in the original report and contributed the major source of background.

Fortunately, this endogenous priming could be largely eliminated by washing in 15% formamide 2XSSC following the reverse transcriptase reaction. This is an improvement over the original IST method which was less stringent, utilizing only 2XSSC washes. One explanation for the lower stringency of primer

independent hybrids could be that the endogenous priming sites promoted synthesis of shorter sequences than with oligo-dT primers. Primer independent transcripts would therefore have a lower melting temperature and could be selectively removed by increasing the stringency.

Another important parameter which was considered is the accessibility of the poly(A) mRNA molecule to reverse transcription in fixed cells. The extraction and fixation conditions were shown to have a major effect on the in situ transcription signal. In paraformaldehyde fixed cells only weak IST signals were evident, in contrast to the ease of detection of biotinated oligo-dT probes by in situ hybridization. By contrast, Triton-extracted cells exhibited strong IST signals. It is likely that fixation of proteins onto the mRNA might inhibit the synthesis of full length cDNA. If nucleic acid sequences which are immediately 5' to the primer are blocked, then the enzyme is prevented from incorporating label. Similarly, in situ transcription will not occur if the 3' end of the primer is sterically prevented from hybridizing. With in situ hybridization, the fixation of proteins along the length of mRNA may decrease the number of probe molecules which can hybridize, but detection is still possible because each probe molecule hybridizes independently. Also, the formation of imperfect hybrids will not prevent detection with in situ hybridization.

It was possible that the efficiency of reverse transcription in fixed cells could be improved by prior dissociation of polysomes from mRNA. Cells were treated with puromycin and Triton-extracted to remove the released ribosomes. Increased IST signals were consistently observed when using a large oligo-dT primer (55nts). Silver enhancement reaction times were 1-2 minutes shorter, in order to produce equivalent signal intensity when compared to non-puromycin treated cells. However, the effects of puromycin on IST signals for the shorter oligo-dT primers (23, 32 bases) were variable. Only in half of the experiments were stronger IST signals observed after puromycin treatment. It is not clear why ribosome removal from mRNA would promote the more efficient reverse transcription off longer primers than shorter ones. Possibly, the extension or hybridization of longer primers is sterically affected by bound ribosomes.

A comparison of the optimized in situ transcription method to in situ hybridization is shown in Figure 36. Strong cellular staining is observed in both in situ hybridization (Figure 36A) and in situ transcription (Figure 36C). The silver enhancement reaction times for IST were 30-60 seconds shorter, producing comparable visual intensity to ISH. The distribution of the IST signal was indistinguishable from ISH. The cytoplasmic staining was concentrated in perinuclear regions, and did not resemble the distribution of any of the individual filament systems. Figure

FIGURE 36. Light Microscopic Detection of Poly (A) mRNA using In Situ Transcription.

A. In situ hybridization with biotinated oligo-dT to Triton-extracted paraformaldehyde (2%) and glutaraldehyde (0.2%) fixed fibroblast culture. Silver enhancement detection of antibiotin and 1nm-gold labelled secondary antibody.

B. In situ hybridization with biotinated oligo-dA probe.

C. In situ transcription with unlabelled oligo-dT primer and biotin-dUTP.

D. In situ transcription with unlabelled oligo-dA primer and biotin-dUTP.

E. In situ hybridization with oligo-dT (biotin) to Triton-extracted glutaraldehyde (4%) fixed fibroblast.

F. In situ transcription with oligo-dT and biotin-dUTP in Triton-extracted glutaradehyde fixed fibroblasts.

All samples were washed in 15% formamide 2XSSC following hybridization and reverse transcription. Silver enhancement reaction times in (A,B) 9 minutes (C,D) 8 minutes (E) 7 minutes (F) 6.5 minutes.

Bar, 50 μm

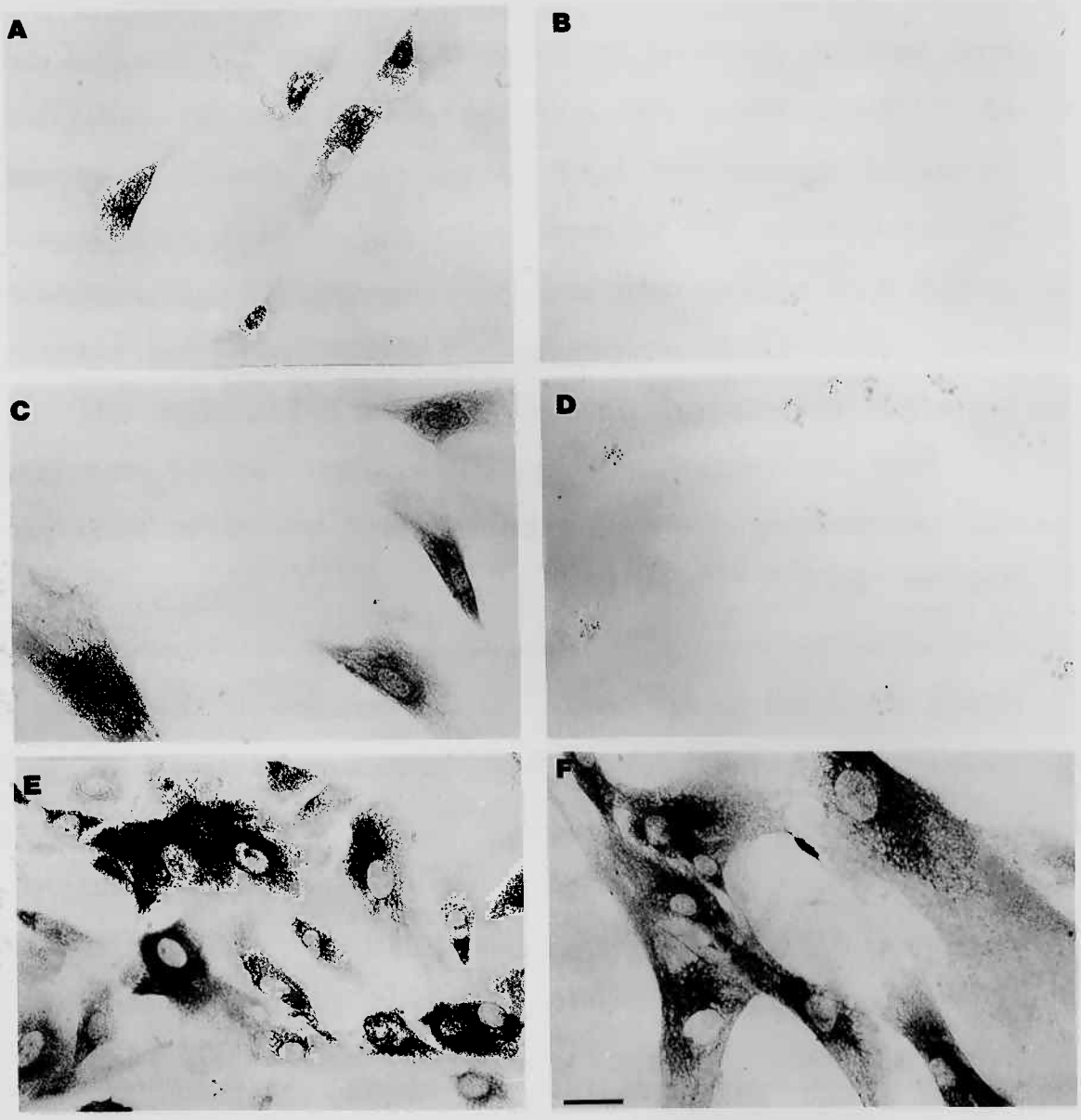
A
B
C
D
E
F

36B,D shows that the nuclear background is considerably higher with IST than ISH. This noise was attributed to endogeneous priming which could not be melted off with formamide washes. Both ISH and IST were able to detect the previously reported focal localization of nuclear poly(A) RNA (Carter et al,1992). As observed in Chapter 4, the nuclear label was stronger in Triton-extracted cells fixed in paraformaldehyde or low concentrations of glutaraldehyde. Cytoplasmic label was most intense with Triton-extraction and glutaraldehyde fixation (Figure 36 E,F).

The optimized nonisotopic in situ transcription technique could now be specifically applied at the ultrastructural level. A comparison of in situ hybridization and in situ transcription with oligo-dT primers is shown in Figure 37. With in situ hybridization, biotin labelled oligo-dT probes are hybridized only to the poly(A) sequence of mRNA. Detection of the biotin groups from the primer was accomplished by the binding of antibiotin primary antibodies and Protein-A labelled colloidal gold. With in situ transcription, the oligo-dT primer was unlabeled and extended using reverse transcriptase in the presence of biotinated nucleotides. Antibody binding is therefore possible at multiple sites along the length of an mRNA and only the incorporated transcript was detected. At the ultrastructural level, it was expected that larger gold particle clusters would be observed with the in situ transcription method. Because of their length and composition, the IST hybrids should have a higher melting

A. IN SITU HYBRIDIZATION

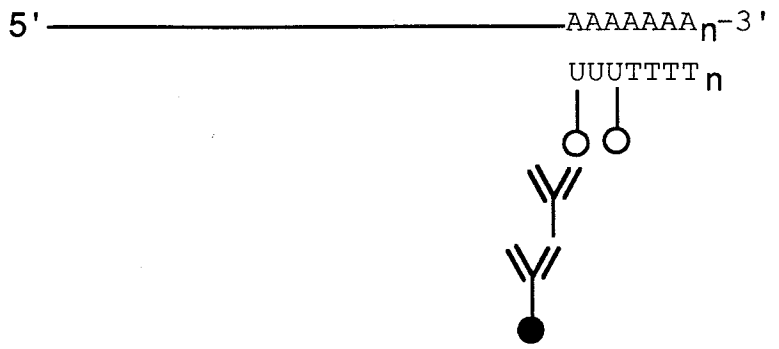

B. IN SITU TRANSCRIPTION

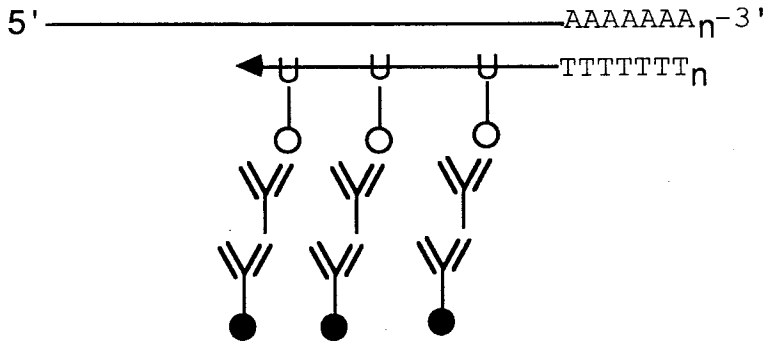

TABLE 7. Quantitation of In Situ Transciption Signal using Immunogold.

	Method				
Probe	ISH	IST	ISH	IST	IST(Double Label)
	15%	Formamide	50%	Formamide	50% Formamide
dT	18	256	5	204	68
dA	4	28	3	12	2

Number of large gold particle clusters (>5 particles) observed per $130\mu^2$. Micrographs taken at 28,000X magnification from critical point dried whole mounts. In situ hybridization with oligo-dT (biotin) or oligo-dA (biotin) followed by either 15% formamide 2XSSC or 50% formamide 2XSSC washes. Detection with antibiotin and protein-A (10nm). For in situ transcription, primer hybridization is followed by 15% formamide 2XSSC wash and reverse transcriptase incubation followed by 15% formamide 2XSSC or 50% formamide 2XSSC wash (indicated above). For double label in situ transciption, oligo-dT (biotin) primers were extended in presence of digoxigenin-dUTP. Immunogold detection using different size gold particles. Number of large gold particle clusters containing both size particles is shown above.

temperature than those detected using in situ hybridization. The quantitative results of these relationships are summarized in Table 7. Oligo-dT primers were hybridized in 15% formamide 2XSSC for ISH and IST. Following reverse transcription, all samples were washed in 15% formamide 2XSSC. For gold particle clusters (size>5 particles), a 14 fold increase in frequency was observed with the in situ transcription signal compared to in situ hybridization. After a 50% formamide 2XSSC wash, the ISH signal was decreased by 72%, compared to 20% for IST. The large gold particle clusters observed with IST were qualitatively and quantitatively similar to those observed from the hybridization of biotinated probe molecules along the length of actin, vimentin and tubulin mRNA (Singer et al, 1989). The gold particle clusters were frequently observed in circular conformations containing >10 particles. A sampler of reverse transcribed poly(A) mRNA molecules detected by colloidal gold particles is presented in Figure 33 F-G.

Are these long gold particle clusters single mRNA molecules? The visualization of circular gold particle conformations is consistent with published observations of circular mRNA using other approaches (Hsu and Coco-Prados, 1979; Ladhoff et al, 1981; Christensen et al, 1987). However, a single label IST technique does not provide unequivocal evidence that the observed conformations are attributed to the transcription of a single mRNA molecule. Based on the high resolution ISH data presented

earlier, it is unlikely that these conformations could be attributed to parallel arrangements of associated mRNA molecules.

In order to confirm the single transcript hypothesis as well as provide information on the orientation of the mRNA we developed a double labelling techniques to permit the simultaneous visualization of the hybridized primer and synthesized cDNA. The approach was to hybridize a biotin labelled oligo-dT primer and reverse transcribe in the presence of digoxigenin labelled nucleotides. Biotinated oligo-dT primers which were labelled at the 3' end using terminal transferase could not be reverse transcribed, indicating that the terminal transferase tail did not hybrize at its 3' end. A primer was synthesized with a single 5' biotin group. This then served as an effective substrate for reverse transcriptase, at the light microscope level using antidigoxigenin antibodies and silver enhancement detection. There was no detectable difference in IST signals between unlabelled and biotinated oligo-dT primers.

For detection of the two labels using electron microscopy, biotin was detected using antibiotin followed by Protein-A(10nm); and a directly labelled antidigoxigenin antibody (5nm). At the ultrastructural level, signals were frequently observed in the form of clusters containing both sizes of gold (heteroclusters). A signal to noise ratio of 34:1 (Table 7) was obtained from the quantitative analysis of heteroclusters observed with oligo-dT and control oligo-dA primers (both labelled with a single biotin group). The

number of 5 and 10nm particles within a cluster was indicative of single mRNA molecule detection. The 5nm particles within a heterocluster exceded 10nm particles, with most heteroclusters containing a single 10nm particle (96%). The rare heteroclusters observed with a control oligo-dA primer did not exhibit this relationship. This data would indicate that the cDNA signal resulted from a single primer. Therefore, this supplies additional evidence that a single mRNA molecule is detected. Figure 33H is an example of a double label gold particle conformation using reverse transcriptase. The heteroclusters were observed positioned within the intersection. Because the clusters tended to form circular or spiral conformations it was not possible to conclude that the poly(A) tail was more directly associated with vertex than the transcribed signal.

DISCUSSION

Individual mRNA molecules have never been visualized in situ. In this work we have identified single mRNA molecules at the intersection of cytoskeletal filaments. The identification of single mRNA molecules was accomplished through the development of the following novel high resolution in situ methods: (1) Establishment of a direct correspondence between the number of probe molecules and the number of detector colloidal gold particles. No previous detection methodology has

established such a precise stoichiometric association between hybridized probe and detector reagents. (2) Use of double labelling to establish that only one site exists for a hybridized probe molecule. (3) Use of reverse trancriptase to extend the hybridized probe and thus enhance its signal, and permit direct visualization of the conformation of mRNA. This ability to use two independent events: hybridization and primer extension provide a high degree of certainty for single molecule identification.

The localization of mRNA to cytoskeletal intersections indicates that components of the intersection, rather than the core filament, are involved in the mechanism of mRNA attachment to the cytoskeleton. The cytoskeletal intersections which contain poly(A) mRNA exhibited distinct structural features. These intersections often contained several highly branched filaments (Figure 31). Double label mRNA and protein experiments (Chapter IV) showed that both microfilament and intermediate filament intersections are involved in the attachment of mRNA to the cytoskeleton. Within the actin cytoskeleton, these intersections are assembled by the actin binding proteins, filamin and α-actinin (Figure 25). These high molecular weight homodimers possess actin binding sequences at their amino termini, and hence crosslink adjacent microfilaments. The presence of central rod domains within these polypeptides confer flexibility and high angle branching to these microfilament intersections. By contrast, tightly packed microfilaments i.e. stress

fibers were not observed to contain mRNA (Figure 23). The tight parallel packing of microfilaments is controlled by bundling proteins e.g. fimbrin, which lack central rod domains.

It is possible that proteins which bind mRNA to the branched intersections might also bind actin. This would require that they have both mRNA binding and actin binding motifs. A database was searched for such dual motifs which found only the actin binding protein, villin, to have both sequences (Anthony Ross, personal communication). The proteins filamin and α-actinin do not have obvious mRNA binding motifs. Possibly other proteins, as yet undetermined, are involved in binding mRNA to actin at the vertex.

Recent evidence has demonstrated that elongation factor-1A is an actin crosslinking protein (Yang et al, 1990). Elongation factors are involved in the positioning and translocation of amino-acyl tRNA molecules within the ribosome. Previous work has convincingly demonstrated that the attachment of mRNA to the cytoskeleton is independent of the translation apparatus (Lenk et al, 1977). However, it was possible that the localization of mRNA to cytoskeletal intersections might require translational components. In this study, it was determined that the association of poly(A) mRNA with the cytoskeletal intersection is independent of the translational apparatus, because prior treatment of cells with puromycin did not alter this localization (Table V). Therefore the association of poly(A) mRNA

with the vertex is not mediated solely by translational factors which bridge the ribosome to the cytoskeleton.

The localization of mRNA to intersections has been previously implied from the visualization of whole cells by high voltage electron microscopy (Wolosewick and Porter, 1979), where polysomes were seen at junctions of microtrabeculae. This data is not in conflict with the work presented here if one believes that microtrabeluae are actually a different image of cytoskeletal filaments, obtained after fixation of cytosolic proteins onto the cytoskeleton (Heuser and Kirschner, 1980). The data presented here supports this argument by demonstrating that the localization of poly(A) mRNA to intersections is present after removal of soluble protein. It is therefore unlikely that microtrabecular junctions contain any additional structural components which are lost during cytoskeletal preparation. The work presented here extends these original observations to include the localization of mRNA within the cytoskeleton.

What is the biological function to the localization of poly(A) at intersections? One possibility is that the association of mRNA with the vertex is obligatory for translation. The cytoskeletal vertex may serve as a translational compartment providing for the efficient accounting and sequestration of mRNA, ribosomes and translational factors. While it has long been observed that mRNA can be translated in cell free systems, protein synthesis is considerably more efficient in vivo. Secondly, this mechanism

could allow proteins to be synthesized at precise intracellular locations. The cell is a complex structural entity requiring mechanisms to account for the syntheisis, sorting and degradation of its millions of protein molecules. It is possible that the mRNA-vertex interaction is involved in controlling both of these features.

What mechanisms would be involved to promote the synthesis of proteins at common locations? This process could be achieved by the targetting of multiple mRNA molecules to a single vertex, or to vertices which are close enough to facilitate interactions of the newly synthesized proteins. mRNA molecules can be positioned close together i.e. <50nm (Figure 33) by the localization of single mRNA molecules to adjacent intersections. Therefore, the targetting of mRNA molecules to adjacent vertices may facilitate structural or functional relationships of their cognate proteins. Since the average mRNA is about 1.5Kb or an extended length of 450nm, the distance between vertices is smaller than the size of an mRNA. It is possible that the nascent chains of adjacent mRNA molecules could interact or even assemble cotranslationally. However, the intersection could serve as a single specific compartment for the targetting of mRNA molecules coding for functionally related proteins. Histone mRNAs may be an example of this case (Chapter II).

We suggest that the mRNA-vertex interaction represents a fundamental structure from which to generate heterogenous intracellular distributions of mRNA (Figure 38). A particular

intracellular location would be specified by the interaction of a specific nucleic acid sequence with a specific filament associated protein. Numerous locations could be achieved by different nucleic acid sequence-cytoskeletal protein combinations. In this model, multiple sites on an mRNA have affinity for the intersection. The poly(A) sequence is depicted as the anchor for the vertex (Taneja et al, submitted). The 3'UTR sequence would then specify location within the cell (Macdonald and Struhl,1988; Mowry and Melton,1992). Nascent peptide sequences may play an accessory role in attachment of distinct classes of mRNA. Membrane associated mRNAs were attached to the cytoskeleton through the nascent peptide (Zambetti et al, 1990). Some cytoskeletal proteins i.e. myosin are cotranslationally assembled onto the cytoskeleton (Isaacs and Fulton, 1987). In our proposed model, the cellular receptors for the above sequence information are cytoskeletal intersections. Numerous receptors could be specified by interactions with different microfilament or intermediate filament associated proteins. Although this model is speculative, this discussion has direct bearing for future work on how a cell controls the spatial location of protein synthesis.

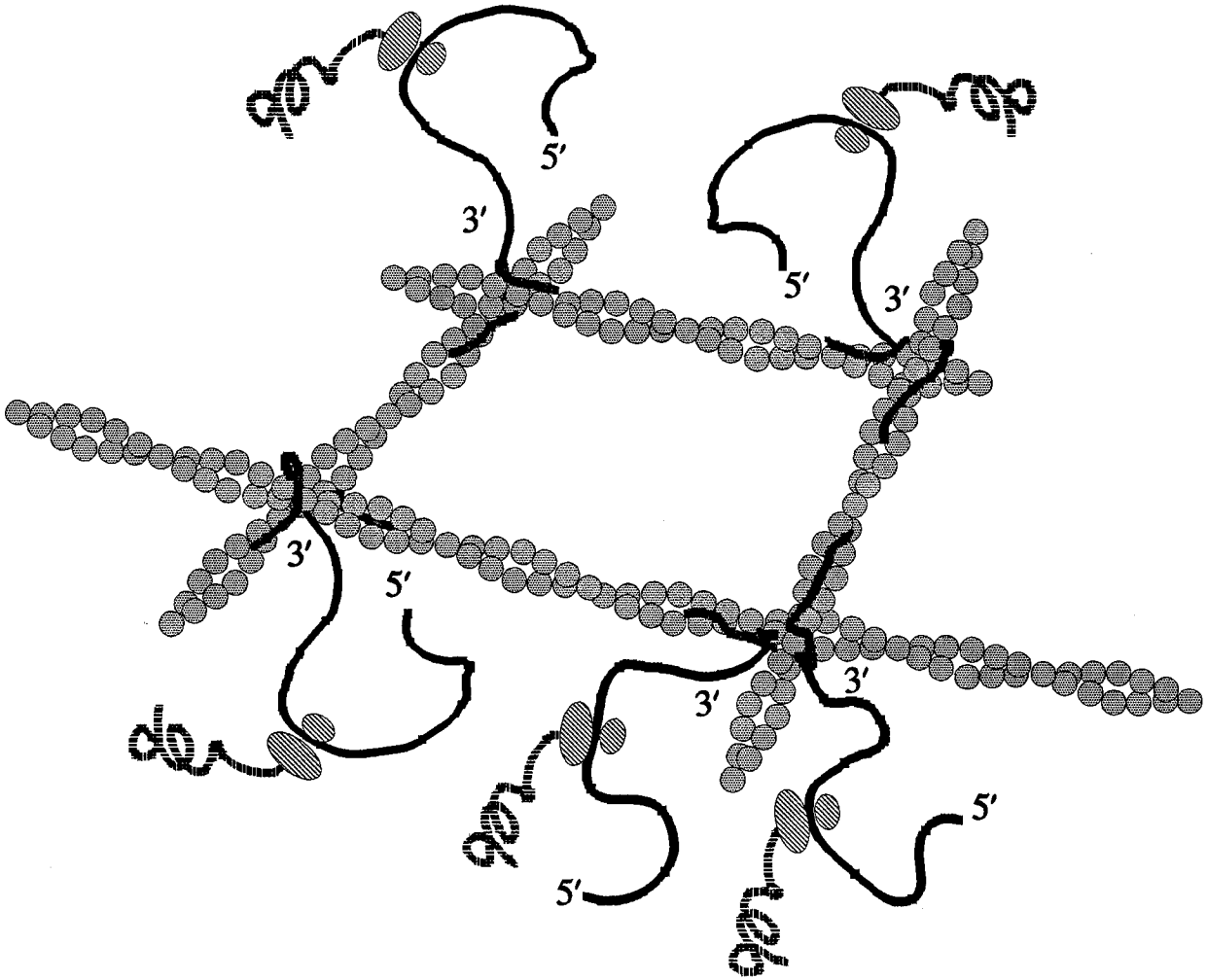
5′
3′
5′
3′
3′
5′
3′
3′
5′
5′

MATERIALS AND METHODS

Cell Culture- The details of the culture system and the Triton-extraction and fixation methods are discussed in the Materials and Methods section to Chapter 4. For polysome dissociation experiments, cells were incubated with 100μg/ml of puromycin (Sigma Chemical Co.) for 45 minutes in culture media prior to extraction and fixation. This treatment was sufficient to inhibit protein synthesis by 90-96% as determined by ^{35}S methionine incorporation into protein (Sundell and Singer, 1990).

Probe Preparation- Synthetic oligo-dT (23,32,55nts) probes were labelled at the 3' end with either biotin-16-dUTP or digoxigenin-11-dUTP (Boehringer Mannheim) using terminal transferase. Synthetic oligo-dT (32nts) was 5' end labelled using biotin succinamide ester to react with a single nucleotide modified with an amino group on at the 5' terminus. Oligonucleotide probes to β-actin mRNA were synthesized to specific coding (nts1442-1495 designated as KLT23) and 3'UTR (nts 3061-3111 designated as KLT19) sequences (Taneja and Singer,1990). Probes were 3' end labelled with either biotin-16-dUTP or digoxigenin-11-dUTP using terminal transferase. All probes were purified by Sephadex G-50 chromatography.

Hybridization- Specific details of the hybridization conditions for oligo-dT probes are discussed in the Materials and

Methods section to Chapter 4. Hybridization with actin oligonucleotide probes was performed under similar conditions but at a higher stringency (50% formamide 2XSSC). Post-hybridization washes were also at this stringency.

Immunocytochemistry- Detection of biotinated probes was accomplished using a rabbit antibody to biotin (Enzo Biochemicals) and either colloidal gold (10nm) labelled goat anti-rabbit secondary antibody or Protein-A (Amersham Inc.). Detection of digoxigenin labelled probes was accomplished with a monoclonal to digoxigenin (Boehringer Mannheim) and a colloidal gold (5nm) labelled goat anti-rabbit secondary antibody (Amersham). Alternatively, a directly labelled sheep polyclonal antibody to digoxigenin (5nm) was used (Biocell Laboratories,Cardiff). Antibodies were diluted 1:10 in 1% BSA, 0.1% Triton (TBS) for 1-2hrs. at 37°C. Details of silver enhancement detection are described in Chapter 4.

In Situ Transcription- Following posthybridization washes, samples are incubated at 37°C for 60' with the following: reverse transcriptase (avian myoblastosis virus, Boehringer Mannheim, 600U/ml); ribonuclease inhibitor (RNAsin, Boehringer, 0.12U/µl); unlabelled nucleotides (TTP,dCTP,dATP,dGTP at 250µM); biotin-16-dUTP or digoxigenin-11-dUTP (50µM, Boehringer Mannheim); in a 50mM tris-HCl buffer (pH 8.3) with 6mM $MgCl_2$, 40mM KCl, 7.5mM dithiothreitol. Samples were twice washed in 15% or 50% formamide in 2XSSC for 30' at 37°C.

The original method (Tecott et al, 1988) used ^{35}-S labelled dCTP at 50nM and did not include unlabelled dCTP. Reverse transcription however did not occur using biotinated nucleotide under these conditions. In consideration that the K_m for biotinated nucleotides might be higher, it was possible that the low concentration of labelled nucleotide might be limiting the enzyme. We optimized the signal by increasing the concentration of the labelled nucleotides, and by diluting the labelled nucleotide could with unlabelled nucleotide in the reaction mixture i.e. 5:1 dCTP/biotin-dCTP. Another component to this optimization was that the biotinated dCTP analog used in preliminary experiments (Enzo Biochemicals) has a shorter carbon allyl arm (utilized as a spacer between the nucleotide and the biotin moiety) than optimal for antibody binding. The longer allyl spacer, available on dUTP (Boehringer Mannheim), resulted in stronger signal.

Other parameters which were optimized to increase the IST signal included: fixation conditions and polysome dissociation prior to cDNA synthesis, and stringency of post cDNA synthesis washes. The rationale for this optimization is discussed in the text to Table VI.

Controls and Quantitation- To control for in situ hybridization of labelled oligo-dT probes, parallel samples were hybridized with oligo-dA probes which were hapten labelled. Alternatively, oligo-dT labelled with hapten was competed with 1000 fold excess oligo-dT probe which was unlabelled with

hapten. To control for in situ transcription with unlabelled oligo-dT primers; parallel samples were hybridized without primer, or with oligo-dA primers. Also, samples were hybridized with oligo-dT and reverse transcribed with heat inactivated enzyme. Signal to noise ratios of all reagents were first evaluated at the light microscopic level using silver enhancement detection and then followed by ultrastructural analysis.

At the electron microscopic level using colloidal gold labelled antibodies, quantitation was performed by counting individual gold particles. At a magnification of 28,000X each cell was photographed in 3-9 nonoverlapping fields. Between 5-10 cells were evaluated for each sample. Signal to noise ratios were obtained by comparing the number of gold particles in oligo-dT and oligo-dA samples.

Electron Microscopy- See Methods section for Chapter 4.

REFERENCES

1. Cervera, M., Dreyfuss, G., Penman, S. 1981. Messenger RNA is translated when associated with the cytoskeletal framework in normal and VSV-infected HeLa cells. Cell 23, 113-120.
2. van Venrooij, W.J., Sillekens, P.T., van Eekelen, C.A., Reinders, R.J. 1981. On the association of mRNA with the cytoskeleton in uninfected and adenovirus-infectd human KB cells. Exper. Cell Res. 135, 79-91.
3. Ben-Ze'ev, A., Horowitz, M., Skolnik, H., Abulafia, R., Laub, O., Aloni, Y. 1981. The metabolism of SV40 RNA is associated with the cytoskeletal framework. Virology 111, 475-487.
4. Bonneau, A., Darveau, A., Sonenberg, N. 1985. Effect of viral infection on host protein synthesis and mRNA association with the cytoplasmic cytoskeletal structure. J. Cell Biol. 100, 1209-1218.
5. Lawrence, J.B. Singer, R.H. 1986. Intracellular localization of messenger RNAs for cytoskeletal proteins. Cell 45, 407-415.
6. Sundell, C.L., Singer, R.H. 1991. Requirement of microfilaments in sorting of actin messenger RNA. Science 253, 1275-1277.
7. Nielson, P., Goelz, S., Trachsel, H. 1983. The role of the cytoskeleton in eukaryotic protein synthesis. Cell Biol. Inter. Reports 7, 245-254.

8. Hesketh, J.W., Pryme, I.F. 1991. Interaction of mRNA, polyribosomes and cytoskeleton. Biochem. J. 277, 1-10.

9. Lenk, R., Ransom, L., Kaufmann, Y., Penman, S. 1977. A cytoskeletal structure with associated polyribosomes obtained from HeLa cells. Cell 10, 67-78.

10. Ornelles, D.A., Fey, E.G., Penman, S. 1986. Cytochalasin releases mRNA from the cytoskeletal framework and inhibits protein synthesis. Mol. Cell. Biol. 6, 1650-1662.

11. Singer, R.H., Langevin, G.L., Lawrence, J.B. 1989. Ultrastructural visualization of cytoskeletal mRNAs and their associated proteins using double-label in situ hybridization. 108, 2343-2353.

12. Zambetti, G., Schmidt, W., Stein, G., Stein, J. 1985. Subcellular localization of histone messenger RNAs on cytoskeleton-associated free polysomes in HeLa$_3$ cells. J. Cell. Phys. 125, 345-353.

13. Howe, J.G., Hershey, J.W.B. 1984. Translational initiation factor and ribosome association with the cytoskeletal framework fraction from HeLa cells. Cell 37, 85-93.

14. Suprenant, K.A., Tempero, L.B., Hammer, L.E. 1989. Association of ribosomes with in vitro assembled microtubules. Cell Mot. Cytoskel. 14, 401-415.

15. Zambetti, G., Wilming, L., Fey, E.G., Penman, S., Stein, J., Stein, G. 1990. Differential association of membrane-bound and

nonmembrane-bound polysomes with the cytoskeleton. Exp. Cell Res. 191, 246-255.

16. Dang, C.V., Yang, D.C.H., Pollard, T.D. 1983. J. Cell Biol. 96, 1138

17. Mirande, M., Corre, L.L., Louvard, D., Reggio, H., Pailliez, J., Waller, J. 1985. Association of an aminoacyl-tRNA synthetase complex and of phenylalanyl-tRNA synthetase with the cytoskeletal framework fraction from mammaalian cells. Exp. Cell Res. 156, 91-102.

18. Yang, F., Demma, M., Warren, V., Dharmawardhane, S., Condeelis, J. 1990. Identification of an actin-binding protein from Dictyostelium as elongation factor 1a. Nature 347, 494-496.

19. Trapp, B.D., Moench, T., Pulley, M., Barbosa, E., Tennekoon, G., Griffin, J. 1987. Spatial segregatin of mRNA encoding myelin-specific proteins. Proc. Natl. Acad. Sci. 84, 7773-7777.

20. Singer, R.H., Lawrence, J.B., Silva, F., Langevin, G.L., Pomeroy, M., Billings-Gagliardi, S. 1989. Strategies for ultrastructural visualization of biotinated probes hybridized to messenger RNA in situ. In Current Topics in Microbiology and Immunology. A.T. Haase (eds.) Springer-Verlag, Berlin-Heidelberg. 55-69.

21. Silva, F.G., Lawrence, J.B., Singer, R.H. 1991. Progress toward ultrastructural identification of individual mRNAs in thin

section: myosin heavy-chain mRNA in developing myotubes. Tech. Immunocytochem. 143, 58-67.

22. Bassell, G.J., Singer, R.H. 1991. Ultrastructural in situ hybridization using immunogold. In Electron Microscopy in Diagnosis and Research. M.A. Hyatt (ed.), CRC Crit. Rev. Biochem., in press.

23. Pomeroy, M.E., Lawrence, J.B., Singer, R.H., Billings-Gagliardi, S. 1991. Distribution of myosin heavy chain mRNA in embryonic muscle tissue visualized by ultrastructural in situ hybridization. Develop. Biol. 143, 58-67.

24. Sheiness, D., Darnell, J.E. 1973. Polyadenylic acid segment in the mRNA becomes shorter with age. Nature 241, 265-268.

25. Brawerman, G. 1981. The role of the poly(A) sequence in mammalian messenger RNA. CRC Crit. Rev. Biochem. 10, 1-38.

26. Sachs, A.B., Kornberg, R.D. 1985. Nuclear polyadenylate-binding protein. Molecul. Cell. Biol. 5, 1993-1996.

27. Lawrence, J.B., Singer, R.H. 1985. Quantitative analysis of in situ hybridization methods for the detection of actin gene expression. Nucl. Acids Res. 13, 1777-1799.

28. Taneja, K. L., Singer, R.H. 1990. Detection and localization of actin mRNA isoforms in chicken muscle cells by in situ hybridization using biotinated oligonucleotide probes. J. Cell Biochem. 44, 1-12.

29. Taneja, K.L., Singer, R.H. 1989. Quantitative in situ hybridization to actin mRNA isoforms. J. Anal. Biochem.

30. Tecott, L.H., Barchas, J.D., Eberwine, J.H. 1988. In situ transcription: specific synthesis of complementary DNA in fixed tissue sections. 17, 1661.

31. Hsu, M., Coco-Prados, M. 1979. Electron microscopic evidence for the circular form of RNA in the cytoplasm of eukaryotic cells. Nature 280, 339-340.

32. Ladhoff, A.M., Uerlings, I., Rosenthal, S. 1981. Electron microscopic evidence of circular molecules in 9-S globin mRNA from rabbit reticulocytes. Cell Biol. Int. Rep. 7, 101-106.

33. Christensen, A.K., Kahn, L.E., Bourne, C.M. 1987. Circular polysomes predominate on the rough endoplasmic reticulum of somatotropes and mammotropes in the rat anterior pituitary. Am. J. Anat. 178, 1-10.

34. Schwartz, R.J. and Rothblum, K.N. 1981. Biochem. 20: 4122-4129.

35. Taneja, K., Singer, R.H. 1987. Use of oligodeoxynucleotide probes for quantitative in situ hybridization to actin mRNA. Analytical Biochem. 166, 389-398.

36. Wolosewick, J.J., Porter, K.R. 1979. Microtrabecular lattice of the cytoplasmic ground substance. J. Cell Biol. 82, 114-139.

37. Heuser, J.E., Kirschner, M.W. 1980. Filament organization revealed in platinum replicas of freeze-dried cytoskeletons. J. Cell Biol. 86, 212-234.

CHAPTER VI

CONCLUSIONS-Summary

It has been well documented that certain mRNAs can be localized intracellularly to different topographical regions (reviewed in Singer, 1991). The ability of a cell to localize mRNA requires the presence of internal cellular structures which would anchor mRNAs at specific locations. Considerable work has shown that mRNA, and specifically translatable mRNA, is associated with the cytoskeleton (reviewed in Hesketh, 1991). Therefore, the interaction between mRNA and the cytoskeleton may result in the synthesis of proteins at specific locations. The objective of the work presented in this thesis was to characterize this interaction with resolution sufficient to determine how mRNA is spatially organized within the cell. The most direct approach for this study was to visualize mRNA at the ultrastructural level. The high resolution provided by the electron microscope (0.3nm) would allow mRNA molecules to be unequivocally proximated to individual filaments. This thesis contains work showing development of novel in situ hybridization methods for electron microscopy which have permitted the morphological characterization of the mRNA-cytoskeletal interaction within a spatial context.

At the light microscope level, the intracellular distribution of poly(A) mRNA has often been described as homogeneous and utilized as a control for the localized distribution of some specific mRNA species. This may have erroneously suggested that most mRNA is not localized and hence plays no role in influencing where proteins are synthesized. However, it is entirely possible that most mRNAs have some specific cellular destination or address. Therefore, the observed homogeneous distribution of poly(A) mRNA may reflect the sum total of localized and nonlocalized mRNAs. Additionally, the apparent homogeneity of poly(A) mRNA may belie a spatial and functional organization which is unresolved at the light microscope.

The contention of this thesis is that previous light microscopic analysis lacked sufficient resolution to observe the actual compartments within a cell which are involved in mRNA localization. Therefore, ultrastructural methods were developed to visualize the spatial organization of poly(A) mRNA simultaneous with its association with the cytoskeleton. This thesis postulated that the visualization of poly(A) mRNA with ultrastructural resolution would reveal a nonhomogeneous distribution with respect to the cytoskeleton. Using the developed ultrastructural in situ hybridization methods, this thesis demonstrates that poly(A) mRNA is compartmentalized within the cytoskeleton exhibiting heterogeneous interactions with each filament system and their

substructures. The results are discussed below in context with the experimental methods developed to test specific hypotheses.

A shortcoming of any ultrastructural analysis after in situ hybridization is the inability to visualize the colloidal gold at low enough magnification to view the entire cell. This prevents analysis of the overall intracellular mRNA distribution simultaneous with high magnification observation of cellular structures. This inability makes it impossible to directly correlate light and electron microscopic observations. This problem is further compounded by the fact that light microscopic methods have often been applied to whole cells, while the high resolution EM studies use thin sections. The most common criticism of immunogold detection using electron microscopy has been that one can see the "tree but not the forest".

These problems are exemplified by the light and electron microscopic observations on the intracellular distribution of histone mRNA (Chapter II). At the light microscopic level, the distribution of histone was characterized as "clustered" when using autoradiography (Figure 1) or alkaline phosphatase to detect the hybridized probe (Figure 3). At the electron microscopic level using colloidal gold labeled antibodies, the histone signal was characterized by clusters of gold particles (Figures 5-7). Does a cluster of gold correspond to a cluster of silver grains or alkaline phosphatase precipitate? Alternatively, does the gold signal represent a subset of the light microscopic signal? It is not

possible to resolve this issue using one set of detection methods for light microscopy and another detection method for high magnification electron microscopy.

The development of a silver enhancement methodology for both the light and electron microscopic detection of biotinated probes is presented here in Chapter II, Figures 16-20. This is the first application of silver enhancement for correlative light and electron microscopic in situ hybridization. This technology has permitted a synoptic view of the spatial organization of poly(A) mRNA within the cell and served as the methodological foundation for the thesis. Through a continuum of magnification and resolution, samples are evaluated first by light microscopy and then processed for electron microscopy.

An early application of the silver enhancement methodology was to evaluate the spatial relationship of polysomes with respect to labelled cytoskeletal filaments. The association of polysomes with labelled cytoskeletal filaments has not been previously studied. This work first required the optimization of Triton-extraction and fixation conditions which would simultaneously permit the labelling of cytoskeletal proteins and the preservation of polysomal and cytoskeletal morphology. Using these optimized conditions, the light microscopic detection of antibodies to actin, vimentin and tubulin exhibited the characteristic fibrillar patterns of each filament system (Figure 21). These samples were

then processed for thin section ultrastructural analysis (Figure 23). **Polysomes were observed attached to both microfilaments and intermediate filaments.** The application of the silver enhancement detection method permitted the first morphologic evidence for mRNP interactions with multiple filament systems.

The intracellular distribution of poly(A) mRNA was also studied using silver enhancement detection for correlative light and electron microscopic in situ hybridization. At the light microscope, the distribution of poly(A) mRNA did not exhibit an obvious fibrillar appearance or resemble the individual filament distribution patterns of microfilaments, intermediate filaments or microtubules (Figure 21). Ultrastructural examination in thin sections (Figures 22-23) and whole mounts (Figure 24) revealed that **poly(A) mRNA was not uniformly distributed along filaments, but clustered at cytoskeletal intersections.**

It had not been feasible to detect hybridized probes in cells unless the cell had been extracted with Triton before fixation. The inefficiency of detection in unextracted cells has been attributed to the poor penetrability characteristics of these high molecular weight complexes (10nm gold particle coated with 3-4 antibodies). However, the characterization of poly(A) as non-fibrillar may be an artifact of extraction and it was important to observe the poly(A) mRNA distribution without cellular pretreatment. **To permit detection of mRNA in unextracted cells, this**

thesis presents the first use of one-nanometer colloidal gold labelled antibodies (1-2 particles per antibody). **The intracellular distribution of poly(A) mRNA was not affected by the Triton-extraction procedure** (Figure 21-22).

It was important to show that the detected mRNA was functional i.e. associated with polysomes. Therefore, it was necessary to visualize polysomes simultaneous with the in situ hybridization signal. Previous electron microscopic in situ hybridization studies have not been able to visualize polysomes. It could therefore be suggested that the ultrastructural signal could be due to untranslated mRNA. In addition, visualization of polysomes indicates that the hybridization conditions have not disrupted the morphology of the translational apparatus. This demonstration is required before any conclusions can be made concerning the functional relationship of the mRNA to the cytoskeleton. The use of silver enhancement to develop the detection signal directly at the site of hybridization makes possible this correlation, and is in contrast to enzymatic amplification which permits the detection signal to diffuse from the hybridized probe. **Thin section analysis of poly(A) detection using silver enhancement demonstrated strong colocalization of signal with morphologically identifiable polysomes.** 84% of the silver particles localized within 5nm of a polysome (Figure 22). This demonstrates that the detected mRNA molecules are being translated.

The association of poly(A) mRNA with specific cytoskeletal proteins was evaluated in Triton-extracted whole mounts using an optimized double label immunogold method. Biotin labelled oligo-dT probes were hybridized and detected using an antibody to biotin and a colloidal gold labelled secondary antibody. Monoclonal antibody to a cytoskeletal protein was detected using a different size colloidal gold labelled secondary antibody. The silver enhancement detection method was first used to optimize the extraction, fixation and hybridization conditions such that hybridization to poly(A) could be visualized simultaneous with well labelled and preserved cytoskeletal filaments. **The majority of poly(A) mRNA was associated with the actin cytoskeleton**, with 72% of the hybridization localized within 5nm of a labelled microfilament. Previous methodology did not permit visualization of filaments labelled along their length, therefore it was only possible to conclude that mRNA was near actin (Singer et al,1989). Moreover, the previous study was an evaluation of three mRNA species: actin, vimentin and tubulin. The evaluation of poly(A) in this study therefore serves to generalize these observations, while the added preservation and labelling of microfilaments permits analysis of how mRNA is assembled onto the actin cytoskeleton.

Poly(A) mRNA was not uniformly distributed within the actin cytoskeleton, and localized to the

intersections of orthogonal networks (Figure 25). Greater than 50% of poly(A) mRNA colocalized with the actin binding proteins, filamin and α–actinin (Table III). This class of actin binding proteins produces flexible crosslinks between microfilaments and promotes the assembly of orthogonal networks. Poly(A) mRNA did not localize to the extreme periphery of these branched actin networks i.e. lamellipodia, where the small cytoplasmic volume appears to exclude protein synthesis. Poly(A) mRNA did not distribute to compartments of the actin cytoskeleton outside orthogonal networks. For example, poly(A) mRNA was not observed within stress fibers (Figure 23) or at attachment sites to the plasma membrane (Table III, vinculin/poly-A).

A substantial amount of poly(A) mRNA was also associated with intermediate filaments, as the double label analysis revealed that 33% of the hybridization signal localized within 5nm of labelled vimentin filaments. This result was confirmed using a different monoclonal antibody. Prior disorganization of the actin cytoskeleton using cytochalasin provided additional support for the presence of an mRNA-intermediate filament association (Figs. 26-27). This observation is consistent with the morphologic data obtained earlier (Figure 23) indicating polysome associations with both microfilaments and intermediate filaments. This is the first direct demonstration that intermediate filaments are involved in the attachment of mRNA to

the cytoskeleton. Moreover, this is the first direct evidence from a single study which indicates that poly(A) is not solely attached to one filament system.

Microtubules were observed to play a minor role in the attachment of poly(A) mRNA to the cytoskeleton at steady state. Double label detection in Triton-extracted cells showed that only 12% of the poly(A) signal by in situ hybridization was observed associated with microtubules. This was determined to represent bonafide hybridization to poly(A) by the comparison of oligo-dT(biotin) and control oligo-dA(biotin) detection on microtubules. The majority of poly(A) signal (88%) was clearly associated with cytoskeletal filaments not labelled by tubulin antibody. From thin section analysis, polysomes were not observed associated with microtubules. Since we are observing the steady state attachment of poly(A) mRNA, this data is not inconsistent with the reported role for microtubules in mRNA transport.

The ultrastructural in situ hybridization methods thus far has demonstrated that poly(A) mRNA is nonhomogeneously distributed within the cytoskeleton, being associated with specific filament systems and their substructures. However, it was not possible with the existing methodology to know how individual mRNA molecules are positioned and spaced within the cytoskeleton. This description is a critical step in identifying the microenvironment in which functionally related proteins could be

synthesized at the same location. To address these objectives requires the abilty to unequivocally visualize individual mRNA molecules. **Novel ultrastructural in situ hybridization methods were developed to directly visualize single mRNA molecules. The development a single mRNA molecule detection technology required the stoichiometry of hybridization and detection to be quantitatively controlled such that one probe molecule would correspond to one gold particle.** This was accomplished by the direct chemical labelling of oligonucleotide probes with a single biotin group. Detection of the biotin molecule utilized an antibody to biotin and Protein-A labelled with a colloidal gold particle. Ultrastructural quantitation demonstrated that 90% of the hybridization signal was in the form of single particles which were localized to cytoskeletal intersections (Figure 33, Table V). **This demonstrated that single mRNA molecules can be unequivocally identified at intersections.** This localization was not affected by prior dissociation of the polysome (Figure 33, Table V). **The positioning of mRNA at the intersection is therefore not mediated by translational factors which bridge ribosomes to the cytoskeleton.**

The detection of single mRNA molecules was independently confirmed through the development of a double label detection method for biotin and digoxigenin labelled oligonucleotide probes. Detection of both haptens is accomplished with antibodies labelled

to different size colloidal gold particles. **The development of a double label probe detection methodology permitted the simultaneous visualization of two oligonucleotide sequences on a single mRNA molecule with high resolution.** The hybridization of biotinated oligo-dT and digoxigenin labelled oligo-dT probes to poly(A) served as a model system to develop this technology (Figure 33-34). This methodology was then applied to the identification of individual actin mRNA molecules. The competitive hybridization of a biotinated and a digoxigenin labelled actin oligonucleotide probe to the same actin mRNA sequence did not result in significant signal of both probes observed close together i.e. within a cluster of gold particles. Conversely, the noncompetitive hybridization of biotinated and digoxigenin labelled actin oligonucleotide probes to separate actin mRNA sequences resulted in significant colocalization of both probes. This demonstrated that a major component of this signal is attributed to detection of the two probe sequences within a single actin mRNA molecule. These data indicate that most of the actin mRNA detected are in the form of 1-2 mRNA molecules. This technology offers enormous potential by being able to simultaneously visualize multiple oligonucleotide sequences and permit study of intermolecular or intramolecular spatial relationships.

These in situ hybridization methods using oligonucleotide probes have permitted the detection of single mRNA molecules.

This was accomplished through the direct visualization of single oligonucleotide probe molecules. However, these high resolution methods do not permit visualization of the complete mRNA molecule, which could provide important information on the conformation and orientation of an mRNA molecule with respect to the cytoskeletal intersection. Previous attempts to visualize the conformation of an mRNA molecule involved the hybridization of biotin labelled nick translated probe fragments along the length of specific mRNAs (Singer et al, 1989). Detection of these probes using colloidal gold labelled antibodies revealed the presence of circular templates and suggested that the 5' and 3' ends of the mRNA molecule interact. However, this method lacked the resolution to conclude that these conformations were attributed to a single mRNA template. Combining the high resolution of the developed single oligonucleotide molecule detection method with the visualization of 5' sequences would permit the unequivocal visualization of the mRNA conformation.

This thesis presents the development of an in situ transcription methodology to visualize the conformation and orientation of an individual mRNA molecule. This technique involves the use of reverse transcriptase to extend hybridized primers in the presence of labelled nucleotide(Table VI). The detection of oligo-dT primed transcripts using colloidal gold labelled antibody revealed the presence of circular templates (Figure 33). However, there was no single mRNA conformation

which was universally representative of all mRNA. For example, many mRNA molecules exhibited spiral conformations and did not demonstrate 3'-5' associations. A double label application of in situ transcription was developed which permitted visualization of the poly(A) tail concomitant with the synthesized cDNA sequence. This methodology should ultimately prove valuable toward evaluation of the orientation of the mRNA molecule with respect to the intersection. Thin section analysis indicated that the majority of the polysome did not contact the intersection (Figure 25). However, the orientation of mRNA molecules using double label in situ transcription suggested the presence of interactions at multiple sites along the mRNA molecule (Figure 33). Future applications of this novel methodology combined with biochemical manipulation would be valuable toward identifying the specific nucleic acid sequences which confer attachment to the intersection.

CONCLUSIONS-Perspectives

To study the interaction of mRNA with the cytoskeleton by direct visualization is a novel approach started by my thesis advisor, Robert Singer. However, the study of spatial cellular relationships by visualization is by no means novel. The field of cell biology began with the tools of microscopy. The work of

Porter showed that finely granular particles were observed in the cytoplasm (Porter et al,1945). From the work of Palade, small particulate cytoplasmic components were observed free and attached to membranes (Palade, 1954). These historic observations contradicted the current view that a cell lacks internal structure. Therefore, it is somewhat surprising that the original report of Penman (Lenk et al,1977) which demonstrated that mRNA is attached to the cytoskeleton would not be immediately followed by more visual observation. Was there nothing more to see? The biochemical studies which followed over the next decade played an important role, leaving little doubt that the majority of protein synthesis is associated with the cytoskeleton (reviewed in Hesketh,1991). However, the interaction of mRNA with the cytoskeleton is a spatial interaction. It is impossible to understand spatial interactions through the exclusive use of biochemical manipulation.

This thesis is a continuation of the work started in the Singer laboratory which seeks to characterize the mRNA-cytoskeletal interaction within a spatial context. This work has required the development of ultrastructural in situ hybridization methodology. In the original report (Singer et al,1989), the mRNAs for actin, vimentin and tubulin were closely associated with the actin cytoskeleton. In collaboration with the Billings-Gagliardi laboratory, the mRNA for myosin heavy chain was observed near developing myofibrils, but attached to the non-

myofibrillar cytoskeleton (Pomeroy et al, 1991). In this thesis, the majority of poly(A) mRNA was directly visualized at the intersections of microfilaments. A substantial component of poly(A) was also observed associated with intermediate filaments. The cytoskeletal vertex may contain one, or perhaps a few mRNA molecules. These observations could not have been made by any other approach.

The above descriptive observations can now lead to directed biochemical and molecular inquiry. For example, the nucleic acid sequence which confers attachment to the vertex can be identified. The actin binding protein which bridges mRNA to the actin cytoskeleton can be isolated and cloned. These experiments will complement our observations and promote a complete mechanistic understanding of the proposed models (Figures 28,38), as the ultrastructural methodology provides a means to study the spatial organization of any identified proteins. It is hoped that this thesis has also provided the motive, method and rationale for future ultrastructural observation.

Further work is needed to understand why poly(A) mRNA is attached to either microfilaments or intermediate filaments. The proposed model for mRNA compartmentalization predicts that these interactions can determine the particular intracellular location of specific mRNAs. For example, in neurons, the synthesis of microtubule associated protein-2, a dendritic protein, is localized to dendrites. The mRNA for tau, an axonal protein, is

localized to the cell body. **Is the intracellular segregation of proteins regulated by the attachment of their mRNAs to separate filament systems? Is the attachment of specific mRNAs to separate filament systems used by a cell to influence its shape?** In the above example, what would happen to dendritic architecture if MAP-2 mRNA could not be localized to dendrites? These fundamental questions would undoubtedly benefit from ultrastructural in situ hybridization methods.

Can functionally related proteins be synthesized at common locations? Is this mechanism used by the cell to influence its own spatial organization? This thesis has developed methodology to permit the unequivocal identification of a single mRNA molecule. The proposed model suggests that individual or groups of intersections might be functionally selective allowing attachment of specific mRNAs. As a model to evaluate this hypothesis, consider the localization of actin mRNA to microfilament intersections within the lamella. Are adjacent intersections or single intersections occupied by mRNAs coding for motility related proteins? The study of myofibril assembly could serve as another model system to evaluate whether intersections serve as compartments for the synthesis of functionally related proteins. For example, the mRNA for myosin heavy chain was localized to cytoskeletal elements near myofibrils (0.1-0.5μ). Do these cytoskeletal sites promote the attachment of only mRNA

coding for myosin, and exclude non-myosin coding mRNA? The utilization of the ultrastructural in situ hybridization methodology in these model systems would be ideally suited to address the above hypotheses.

A major challenge of future research on mRNA localization will be to determine whether this phenomenon functions to influence where most proteins are synthesized within a cell. An alternative perspective, is that the nonuniform localization of mRNA plays a basic role in controlling only where structural proteins i.e. cytoskeletal are synthesized. This view follows from light microscopic data which has demonstrated nonuniform mRNA localization in somatic cells for mRNAs coding for structural proteins i.e. actin, vimentin, MAP-2, myelin basic protein. However, it is important to appreciate that mRNAs which code for structural proteins are abundant, and therefore more amenable to most in situ hybridization analysis. To resolve these fundamentally distinct functions (cellular vs. structural), it would be useful to study the intracelluar distribution of mRNA coding for nonstructural proteins using the high resolution provided by these ultrastructural in situ hybridization methods. The possibility was raised that histone mRNAs might not follow the one mRNA molecule, one intersection rule (Chapter 2). The colocalization of H3 and H4 mRNAs at a single vertex might serve as a mechanism to promote the assembly of histone oligomeric

complexes. Alternatively, these sites could be the subcellular component involved in histone mRNA stability. It is known from a biochemical approach, that the posttranscriptional regulation of histone mRNA stability involves a subcellular component (Zambetti et al, 1988). Further work with the ultrastructural in situ hybridization technology would permit evaluation of whether mRNAs coding for noncytoskeletal proteins are localized to specific cytoskeletal domains.

Rough endoplasmic reticulum associated mRNAs are another class of mRNA which need to be evaluated by ultrastructural in situ hybridization methods. **Are mRNAs which code for membrane and secretory proteins compartmentalized within the RER membrane?** The polarized epithelial cell provides a good model for asking some of these questions. For example, are the signal peptides of secretory proteins inserted at separate RER sites than nonsecretory proteins? Are mRNAs coding for brush border membrane proteins localized in different regions than mRNAs coding for basolateral membrane proteins? Are mRNAs which code for polypeptides of an oligomeric complex bound to adjacent sites on the RER membrane? **This investigation would have direct bearing on understanding whether the nonuniform localization of mRNA plays a general role in controlling where noncytoskeletal proteins are synthesized.**

In summary, this thesis has utilized descriptive and quantitative visual observation to characterize the cytoskeletal components involved in the spatial organization of mRNA. This work was made possible through the development of ultrastructural in situ hybridization methods. It is hoped that this work will provide a foundation for future ultrastructural and molecular studies to address how and why a cell controls the location of mRNA molecules.